# Metamodel-based Product Family Design Optimization for Plug-In Hybrid Electric Vehicles

**by**

**Zhila Pirmoradi**

M.Sc., University of Tehran, 2009
B.Sc., Isfahan University of Technology, 2006

Thesis Submitted in Partial Fulfillment of the
Requirements for the Degree of
Doctor of Philosophy

in the

School of Mechatronic Systems Engineering
Faculty of Applied Sciences



**SIMON FRASER UNIVERSITY**

**Fall 2015**

# Approval

| | |
|---|---|
| **Name:** | **Zhila Pirmoradi** |
| **Degree:** | **Doctor of Philosophy** |
| **Title:** | **Metamodel-based Product Family Design and Application to Plug-In Hybrid Electric Vehicles Family Design Optimization** |
| **Examining Committee:** | **Chair:** Dr. Jason Wang<br>Assistant Professor |

Dr. G. Gary Wang
Senior Supervisor
Professor _____

Dr. Siamak Arzanpour
Supervisor
Associate Professor _____

Dr. Krishna Vijayaraghavan
Supervisor
Assistant Professor _____

Dr. Erik Kjeang
Internal Examiner
Associate Professor
School of Mechatronic Systems Engineering _____

Dr. Shaahin Filizadeh
External Examiner
Associate Professor
Department of Electrical and Computer Engineering
University of Manitoba _____

**Date Defended/Approved:** November 24th, 2015

## Abstract

Plug-in Hybrid Electric Vehicles (PHEVs) have been recognized as a solution to mitigate the green-house emission for transportation. A factor to succeed in the marketplace is to provide products that can meet customer expectations and satisfy various functional requirements. As such, the design of PHEVs for diverse market segments requires sufficient differentiation in this product to maximize customer satisfaction with the new technology. However, there are challenges coupled with diversity in production of such a complex product for various customers. This dissertation attempts to address the challenges.

This thesis proposed the use of product family design to ensure both the manufacturing efficiency and the customer satisfaction for PHEVs in various market segments. A thorough review of the developments in product family design is first performed, and directions for developing an efficient family design methodology are identified. In order to select the desired or the most preferred variants for the family design purposes, a review of the market studies and fleet data for PHEVs has been performed and summarized as well, based on which a set of five PHEVs- known as variants- are selected for family design assessments. Thirdly, a methodology is proposed for PHEV product family design to enable scale-based design of the selected PHEV variants. The proposed method is verified through a test problem from the literature, and its application to the PHEVs design provides design solutions for the PHEV product family under study. Since the vehicle performance is assessed through expensive simulations, it is shown that the selected optimization algorithm, along with the commonalization strategy and the decision criteria for commonalizing specific design variables make an efficient methodology in terms of the computational costs, and the overall performance of the obtained family solutions. The proposed methodology can also find applications in other product designs that involve expensive simulations and unknown design equations.



**Keywords**: Plug-in Hybrid Electric Vehicles (PHEV); Scalable Product Family Design (PFD); Platform Configuration; Meta-model based Design; Sensitivity Analysis; Radial Basis Function-High Dimensional Model Representation (RBF-HDMR)

*To my best friend and my love Mehran, my beloved Dad & Mom, & my wonderful sisters Leila & Sima*

*whose happiness is my happiness*

## Acknowledgements

I would like to appreciate the kindness and support of several people during my PhD, a long but also a short journey. I sincerely thank Professor Gary Wang, my kind and insightful supervisor for his advice and wisdom, and for entrusting me with this position in the Product Design and Optimization Lab (PDOL). The creation and completion of this thesis would have not been possible, if it wasn't for his supportive directions and mentorship. I would also like to thank my supervisory committee, Dr. Siamak Arzanpour and Dr. Krishna Vijayaraghavan for their assistance. I am also thankful to my examiners committee, Dr. Eric Kjeang and Dr. Shaahin Filizadeh for their kindness in reviewing this dissertation and for providing me with insightful feedback. Thanks to my lab mates for their friendship and willingness to help, and thanks to the Auto21 research foundation of Canada for sponsoring the work for this thesis in part. Special thanks to Guanchen Zhang for his assistance, opinions, and extreme help (especially with SimDriveline).

Eternal thanks to my parents and my sisters for their dedicated partnership in my success, and for their endless supports and encouragements. Most of all, thanks to Mehran for his love and tremendous support, his infinite wisdom and kindness, and for always believing in me. More of this is his than he'll ever know.

# Table of Contents

# List of Tables

# List of Figures

# Chapter 1. Introduction

## 1.1. Background

The urgent need to replace non-renewable energies with new energy types that are sustainable, less expensive, and more environment-friendly has resulted in development of Hybrid Electric Vehicles (HEV) and the more advanced version – Plug-in Hybrid Electric Vehicles (PHEV). These vehicles benefit from electrical energy as a supplementary source of propulsion, and are powered through the combination of an internal combustion engine (ICE) and an electric motor with a battery pack. PHEVs are differentiated from HEVs based on the ability of their battery pack to be charged through plugging the vehicle into the grid. The PHEV allows for operation in both a pure electric mode, and a conventional hybrid electric vehicle mode on longer trips.

The mileage that PHEVs can drive in the electric mode without using any fuel is referred to as All Electric Range (AER). *PHEVx* is a widely-known way of characterizing these vehicles, where *x* shows the range that the vehicle can drive purely on battery power [1]. A PHEV allows for operation in pure electric mode for limited distances, while possesses the operation and range of a conventional hybrid electric vehicle on longer trips. While AER can be one of the design factors, other requirements for the performance can be of equal importance, including the acceleration time, maximum speed, and gradeability. As such, the combination of three component sizes including the ICE, battery, and electric motor ─ together known as the powertrain ─ is of remarkable importance in PHEV design. Another important factor is the defined strategy to leverage the propulsion resources, referred to as the control strategy.

Since the design requirements for PHEVs depend on the driving conditions and patterns (i.e., mileage per day, average distance travelled between two charges, maximum speed and acceleration requests), the optimality of a vehicle design will not be the same for different users.

As such, developing specific powertrains is required for meeting needs of different customer groups. However, while variety in the design can increase the marketability of such product and attract more market segments, it can in turn result in increased effort and cost for manufacturing. Therefore, in order to maximize the benefits of diversity in the design of this complex product, product family design can be an efficient solution to meet both targets (i.e., satisfying more customers, and obtaining manufacturing efficiency).

Product family design (PFD) is a strategy to increase the manufacturing cost savings through commonalizing components/variables or functions in different products, and increasing the product diversity for a larger share of the market. Product family is a group of related products, known as variants, which are differentiated from a set of common components, modules, functions, or sub-systems known as platforms. Product family design (PFD) can be challenging due to the increased complexity from finding which components to be shared, and assigning common values to those components to increase commonality without sacrificing the performance of individual variants [2]. The platform configuration deals with determining the best variables to be in the platform, and the best variants to be included in each platform/sub-platform, while losing as little as possible on the performance of individuals, and obtaining as much as possible on commonality [3]. The platform and the individual variants should be selected such that the individual performance targets are not compromised, or of the least allowable performance loss. There is an inherent trade-off between benefits and losses from family design, imposing difficulties to the product family design strategies. In this study, we address the product platform design based on quantitative analyses, as compared to qualitative approaches that can be found in many of the business-oriented research studies [4]

## 1.2. Motivation

Though remarkable improvements are obtained toward PHEV design and technology advancements over the past few decades, most of the existing research studies have focused on performance requirements for the powertrain without coupling them to the manufacturing concerns or market integration. In addition, most of these studies have focused on optimization of single designs, where the manufacturing cost might be an issue due to the needed setup and added efforts for meeting needs of customers in various market segments. PHEV family design not only can assure satisfaction of more customer segments, but also allows efficient mass

customization. This study is motivated to fill this gap, i.e., to develop an efficient methodology (i.e., computationally non-expensive) for PHEV powertrain family design beneficial to both the manufacturer and the customers.

Design of complex products such as PHEVs highly relies on well-customized design methodologies for the requirements and conditions of the problem under study. In the case of the research in this dissertation, the simulation-based design optimization puts significant load on the run time for objective function assessments, and therefore determining the best practice for its optimization as well as family design is an important part of the research and can risk the efficiency of outcomes, if not well tailored to the needs and hurdles of such a design problem. Through a thorough review of the literature on the available product family design methodologies for scale-based families, it was determined that a number of family design methodologies called two-stage approaches would be fitting this problem better as compared to the integrated approaches, due to the reduced complexity of their exploration process for platform configuration, and for the entire family optimization. More details on these approaches and advantage/disadvantages of each will be discussed in later chapters. Multi-objective optimization is the fitting approach leveraged in this research for reduced production costs, complexity, technological requirements, and reduced time to market, and of an optimal level of commonality versus uniqueness.

In addition, the design process for a product like PHEV is highly dependent on the availability of valid platforms such as simulation models that allow for modeling the governing relations among all the components. It is of significant importance to develop or utilize simulation models that can meet the needs and purposes of the research. Among the required aspects to be modelled, the expected drive profile which is known as drive cycle, the powertrain, control strategy application to the model, connection of the powertrain to the transmission, and driver settings are a few to name. While there are a number of software tools available in the market for simulating the performance of the non-conventional vehicles, there are advantages and limitations to each, reducing their utility for the researchers. As such, a fundamental part of research for the design optimization of these vehicles is to develop a generic simulation model that allows users modeling the desired parameters, customizing the output, and applying modifications to the codes to facilitate connection of the simulation model to desired optimization algorithms. In this research, a generic model is developed for the aforementioned

purposes, which is validated through test data from Argonne National Laboratory (ANL), Electric Power Research Institute (EPRI), National Household Travel Survey (NHTS), and other studies in the literature.

Since PHEVs are shown to serve as a solution for reducing emissions and dependency on non-renewable energy resources, they will attract more attention in future as a substitute for conventional ICE vehicles. For instance, first Prius PHEV was planned to join the market in late 2011 and the production version was unveiled at the International Motor Show Germany in September 2011 [5]. While four major automakers including General Motors, DaimlerChrysler, Ford, and Volkswagen have manufactured prototypes of PHEVs, mass production of this vehicle has not yet been started in a large-scale [6]. Most of the PHEV design studies focused on prototyping and testing hundreds of design parameters for improving the performance of PHEVs, recently the emphasis of research has shifted to simulation-based optimization algorithms that work together in a loop with a computer simulation model to reach optimal design solutions [7]. To this point, no attention has been paid to the manufacturing efficiency aspect of PHEVs as a product family. Moreover, the PHEV product family design will be challenging due to the large run-time and costly computational efforts for running complex simulation models each time the objective function and the performance constraints need to be evaluated toward the optimization.

## 1.3. Objectives of research

To address the needs for PHEV family design and to develop methods supporting family design based on simulations, the main objectives pursued in this thesis are as follows:

1. Developing a PHEV powertrain design optimization problem formulation, which is derived from the market, manufacturing, and environmental consideration studies in the literature
2. Expanding the developed problem into the family design domain
3. Configuring a product platform for the obtained powertrain family, in order to maximize the manufacturing efficiency and to obtain optimal level of commonality
4. Developing a generic methodology for platform configuration which is applicable to similar design problems, where expensive and black-box simulations can exponentially increase the design costs

## 1.4. Scope of the proposed work

The research objectives are to be achieved through the following actions:

- Identification of the PHEV market segments as references for family design
- Modeling of the PHEV based on the selected specifications such as powertrain configurations, and validation of the developed model
- Development of a generally applicable methodology for simulation-based PHEV family design.

Ideally, the market segmentation for a family of products is identified through marketing research and close study of customer preferences. There are several methodologies developed for integrating preferences and analyzing them toward identification of the required product specifications for gaining the desired market share. As for the PHEV design, there are emerging studies and research performed by well-known research laboratories and universities across North America, Europe, and Japan to establish a platform for market identification for these vehicles. The findings of such research are used in this study as a basis for deciding the appropriate variants in a PHEV family. The details of the market studies review is discussed in Chapter 6.

Product family design consists of scale-based or module-based approaches. Scale-based families include variants that all possess the same variables/functions, and some of those variables can take common values, while other variables take unique values in each variant. The module-based family includes variants that share some functions, while each variant has some unique functions or modules. Each variant or product in the chosen family has design specifications, which are usually different from the specifications of the rest of the variants. The first stage in a typical family design study is to obtain optimal designs for each individual or variant, based on the market needs and customer expectations within the specific segment for which the variant has to be designed. The next stage is to decide and find the best components/variables/functions to be shared among some or all of the products in a family. Also, for an existing set of products, an objective of interest might be to identify opportunities for cost saving through modifying the existing designs. In such case, the product family design problem would be called a redesign problem which is a bottom-up approach that provides component sharing solutions –known as commonalization strategies- for modifying the existing

product designs in future production generations. The second strategy is a top-down approach which can be the basis for design of the products in the early stages before the actual product realization.

The next step after deciding on the specifications and performance expectations from each variant is called the product platform configuration, which refers to the strategy that enables identification of the best candidates for sharing and commonalization among the entire family, as well as the best common value/specification for each of the commonalized variables/components.

By obtaining an optimal platform configuration, the family design problem reduces to optimization of the non-shared or scalable variables, which results in obtaining the design solution for the entire family members. The sharing or commonalization of some variables increases the chance of losing optimality in performance for the individual products, as compared to when there was no commonalization and each variant would take its optimal specification values. The objective of the last stage in the family design process is to re-optimize non-shared variables in a new design problem with some fixed values on the commonalized components/variables, so that the resulting family members can stay as much within the desired performance range as possible.

For modelling the performance of non-conventional vehicles, there are a number of commercial and customizable software applications available, each with advantages and disadvantages. PSAT, Advisor, PEV-CIM, and SimDriveline are some of such tools, with different approaches to assist the design. Advisor uses the backward looking approach, while PSAT uses the forward looking approach. SimDriveline is a toolbox of Matlab which allows modelling of a vehicle in either way and provides more freedom in the modelling and parameters setting. PSAT- upgraded and renamed to Autonomie- is a commercialized software platform developed by the Argonne National Laboratory, which allows assembling of all the components of the vehicle and changing the values for some of the parameters toward performance assessment. The ready library of component files makes it a convenient tool. However, depending on the optimization problem, it might be required to model the effect of more parameters than what are available in PSAT. As such, SimDriveline is used for developing and validating the desired PHEV model in this study.

The validated model can be connected to the efficient optimization algorithms which suit the challenging conditions of the simulation-based problem, i.e., the computational complexity resulting from expensive function calls for obtaining the objective function value. The selected algorithm in this study includes the Sequential Quadratic Programming (SQP) for the test problem, and the Trust Region Mode Pursuing Sampling (TRMPS2) algorithm applied to the PHEV optimizations. These algorithms will be explained in detail, in Chapters 5 and 6.

## 1.5. Structure of the thesis

This research has focused on developing a family design optimization problem which simultaneously takes the customer needs, manufacturing efficiency concerns, and environmental considerations into account. Furthermore, for efficiently solving the developed problem, appropriate algorithms are developed and their performances are studied over the course of family design for this product.

The structure of the dissertation is as follows:

Chapter 2 provides the review of literature for the two areas of interest, i.e., PHEV design optimization, and the product family design. The specific focus is then given to the platform configuration and family design optimization methodologies developed in the literature. A review of the current methods and their advantages as well as shortages in addressing the specific needs of our design problem is discussed afterwards.

Chapter 3 will provide details on the PHEV simulation model developed for our study, along with the mathematical equations governing the relations of various components in the PHEV powertrain. Parametric modeling has been embedded into the developed simulation model, so that for various PHEVs the scaling of components is enabled for optimization.

In Chapter 4 the proposed family design methodology will be presented and the steps are explained toward developing a platform configuration which can serve as the basis for the entire family design of the product variants. Chapter 5 provides a case study, or the performance assessment of the proposed method through applying it to the well-known problem of designing a family of ten universal electric motors. Further adjustments and improvements to

the methodology is then made toward increasing the commonality level, while keeping the performance loss within the allowed range. The methodology is further verified through designing test cases and evaluating the effect of various numerical values on the decision points for the platform configuration.

In Chapter 6, the market review of PHEVs will be given, through which a list of selected variants will be obtained. The design problem is then presented in detail, and the selected five variants are optimized, each aiming at minimizing the CO2 emissions and the powertrain costs, and maximization of the fuel efficiency for each variant. Target values for each objective function are adapted from the literature. The improved PFD methodology will then be applied to the selected optimal variants in order to develop a platform configuration for the power-split PHEV powertrains, so that the maximum level of commonality among the powertrain components can be achieved while the gap between the optimal performance of each variant and its optimal design as a family member will be at the minimum possible level. Through comparing the performance loss on the three objectives of interest for the two cases (individual designs vs. family design), conclusion is made about the fitness of the proposed methodology to handle the simulation-based PHEV family design problem.

Finally, Chapter 7 summarizes the contributions and addresses the questions answered through the dissertation. Open questions and potential ideas for further research are also provided at the end of the chapter, along with a list of limitations and assumptions made through the research in the dissertation.

# Chapter 2. Theory and Literature Review

Hybrid Electric Vehicles (HEV) and Plug-in Hybrid Electric Vehicles (PHEV) can be assessed from various aspects such as their charging infrastructure requirements, their impact on the grid and electricity demand, their drivability in different driving conditions, and their design requirements for meeting the road and driver requests.

HEVs leverages from an electric moto, a battery and an IC engine. More attention has been paid to the flow control in the past two decades due to existence of two degrees of freedom in their energy or propulsion source. In HEVs, the battery is charged through the engine and by regenerative braking during the deceleration. But as the engine is used to charge the battery and then the battery is used to drive the vehicle, there are large losses in this loop while using the fuel. The electric drive mode is very limited for an HEV due to limited battery power. Therefore having a more powerful battery will increase the electric drive range of the vehicle, thus improving fuel economy. Since such a large battery cannot be charged solely by regenerative braking and charging via the engine would not be efficient, it needs to be charged externally by a domestic electric outlet. These HEVs, having an external charging facility for the large battery pack and having a significantly larger EV range, are called plug-in hybrid electric vehicles (PHEVs) [8].

## 2.1. PHEV design

As the global demand for automobiles continuously rises, the influence of fossil-fuel-based automobiles on global warming increases accordingly as an important contributor to the environmental crisis. With promising technologies, many automobile companies have released their new generation PHEVs which incorporate electric machines with the conventional

combustion engine to improve the fuel economy and to reduce the gas emission, and these vehicles can be a dominating force in the future automobile market [9].

Compared with HEVs, PHEVs have the plug-in ability which further reduces the reliance on gasoline and extends the usage of the cleaner electricity. The extension on electricity usage also improves the overall efficiency of the vehicle, especially the efficiency of the engine, to reduce the undesirable emissions.

PHEVs include an electric drivetrain and internal combustion drivetrain that can be coupled to each other and to the road. These drivetrains allow the energy paths to the road to be in parallel, in series or in combination, through a configuration known as power-split [10]. The trade-off among these configurations can be quite complex to balance the efficiency, cost, manufacturability, and driveability, and there is no clear globally optimal configuration accordingly. PHEVs can be constructed through optimizing the desired configuration for its component sizes [11].

Another issue of importance coupled to the powertrain design is selection of a proper control strategy. The power management strategy ─the algorithm that determines the split of power request between the combustion engine and electric drive─ is a vital factor for the efficiency of a PHEV. Different control strategies result in different performance profiles due to imposing specific strategies for choosing operation modes. The operation modes of a PHEV include the Charge Depleting mode (CD), in which the battery is the only source of propulsion, and the Charge Sustaining (CS) mode in which the engine is leveraged as an auxiliary power source in order to keep the battery State of Charge (SOC) remaining in a specific range (In this case, PHEVs operate similar to HEVs [12]).

The CD mode can also be either All Electric CD or blended CD; in All Electric CD mode, the engine is not allowed to turn on until the SOC reaches a pre-determined lower bound, while in CD blended mode the battery is the main source of power supply but not the only source. However in blended CD mode, the SOC will reduce on average, similar to All Electric CD mode and the engine turns on, only in cases that the power requirement exceeds the electric motor ability [13]. Typically, PHEVs provide greater amounts of on-board energy storage than HEVs by incorporating more onboard electricity storage, e.g., larger batteries. According to the literature, PHEV usually fall in the range of 10-60 miles of AER [14].

PHEV market penetration started from a few years ago, and the mass production is not released as much as conventional vehicles. General Motors introduced the first Chevrolet Volt off the assembly line on November 30, 2010. Sales and deliveries began in December 2010. GM planned production for 2011 for only 10,000 units. F3DM became the world's first mass produced plug-in hybrid compact sedan as it went on sale in China to government agencies and corporations on December 15, 2008. A global demonstration program involving 600 pre-production test cars began in late 2009 and took place in Japan, Europe, Canada, China, Australia, New Zealand, and the United States. The production version was unveiled at the September 2011 Frankfurt Motor Show, and sales were scheduled to begin in Japan, the United States and Europe by early 2012 [15]. The production of this vehicle was terminated in late 2012 after selling 3760 units, and as of December 2015, more than 25 models of highway-capable PHEVs have been manufactured with various volumes of production [16]

Research on the optimization of the powertrains has been of significant interest, and several studies have addressed this issue based on different objectives such as achievement of maximum fuel economy, minimum Greenhouse Gas Emissions, minimum operating cost and/or life cycle cost, etc. The main issues that need to be decided are configuration selection, power management strategy, the design variables for the powertrain, objective functions, and the performance constraints applied by the standards, the market, or both. The past research works about each of these issues are briefly reviewed.

## 2.2. Product Family Design and Optimization

A product family can be considered as a set of products that share a number of common components and functions, while each product has its unique specifications to meet demands of certain customers [17]. The common parts are usually defined as the product platform [18]. A successful product family depends on how well the trade-offs between the economic benefits and performance losses incurred from having a platform are managed [19]. Two literature review studies by Jiao et al. [20] and Pirmoradi et al. [21] show the advancements and developments in the product family design, which serves as a reliable solution for meeting the increased variety of customers' expectations. It is a strategy that enables companies to offer products with more design varieties with less lead times. While offering more variety in products can satisfy the increasing customers' demands and helps companies gain more of market

share; but in turn such increased variety can lead to higher design and production costs as well as longer lead times for new variants. As a result, a trade-off arises between cost-effectiveness and satisfying demand diversity [22]. Such a trade-off can be properly managed by exploiting product family design (PFD) and platform-based product development.

Platforms provide the core of product families. They can be defined as sets of components, technologies, sub-systems, processes, and interfaces that form a structure to develop a number of products [23]. Platform design attempts to maximize commonality and minimize individual performance deviations. Deviation of performance is considered as the difference of a variant design from ideal design—a design that satisfies a specific range of customer needs [18]. Three types of platforms exist: *scalable platforms*, in which variants can be produced through shrinkage or extension of scalable variables; *modular platforms*, which enable product differentiation through adding/removing/substituting different modules; and *generational platforms*, in which possible requirements for changing the design over a period of time are considered to allow variation of next generations [20].

Market segmentation is vital to determine the appropriate platform leveraging strategy, developed in response to the competitive nature of the market in the recent decades. There are several data-driven techniques developed for this purpose, namely conjoint analysis, clustering, and use of neural networks [24]. Another well-known approach is called Market Segmentation Grid (MSG), which is a qualitative approach used for differentiation of the products developed by Mayer and Lehnerd [25]. A matrix approach that determines the user groups and tiers to the product performance/price is used in the MSG approach to determine the total market for a given product family. A typical grid is shown in Figure 2-1, where the segments are horizontally plotted and the performance tiers are vertically plotted to show unique market niche at the intersections. There are three leveraging strategies; 1) the horizontal leveraging strategy, where there are various products for the same given performance tier, spanning across different market segments. An example is the Gillette razors for male and female segments, flooding the market with derivatives of its Mach 3 product. 2) the vertical strategy is when the products are differentiated from low performance to high performance, for a given market segment. 3) the beachhead approach leverages both horizontal and vertical strategies, and most of the automotive platforms such as Toyota follow this combined strategy. These strategies are illustrated in Figure 2-1.

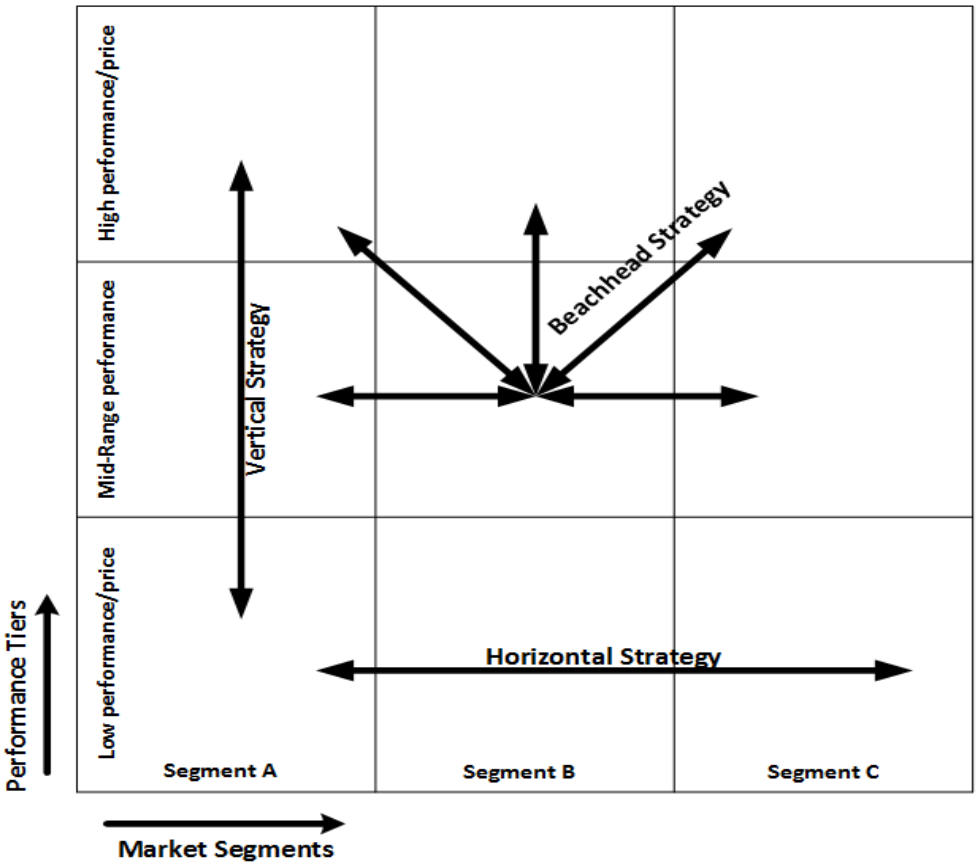


Figure 2-1: Market segments grid according to Mayer and Lehnerd [17]

Not only does the platform configuration or architecture need to be determined in the early design stages (i.e., selection of the platform variables and the variant members for each platform/sub-platform), but also the design for the platform and the individual variants derived from that platform should be determined in a way that would not compromise the individual performance targets for each variant [26]. Since the benefits increase when sharing is increased and more variables and variants are added to the platform, the commonality maximization is a desired target from the manufacturing aspect. However, when more variables take the same value, there is more performance change in each variant performance, as compared to its optimal performance with unique variables/components. This inherent trade-off imposes difficulties to the product family design, and necessitates leveraging efficient optimization methods to find the best combination of values and variables for the platform. Product platform design research can be categorized into two approaches; a more qualitative approach that can be found in the business-oriented research studies [27], and quantitative methods, similar to the

proposed method of this dissertation, which attempt to make platform configuration decisions based on quantitative analyses.

## 2.3. Scalable Family Design

The scale-based design refers to design for a family of products that all possess the same variables, and some of those variables can take common values among some or all of the products in that family, while other variables will take unique values for each product. The other type is called module-based family in which the variants share some modules while each has its unique modules that are absent in other variants. The scale-based design includes three stages. The first stage is called platform configuration, where the platform architecture is identified and the platform variables as well as the variants which share those variables are identified. The second stage is determination of the values to be shared for each variable in each platform/sub-platform, and the third stage relates to finding optimal values for the non-shared variables so that the family performance targets are achieved and performance requirements can be met, or the resulting performance loss is within acceptable limits.

Several approaches for design optimization of product families have been developed over the past decades. An extensive review and categorization for forty of such optimization approaches was implemented by Simpson [28]. While the scale-based and modular family design problems have been widely studied, they have been mainly addressed by assumptions such as pre-determined platform architecture, and restricted commonality where either the sharing shall be among all the variants, or there would be no sharing. Also, another categorization is made by Fujita [29], in which three different classes of design optimization problems have been defined: 1) The platform is known a priori and has a fixed configuration 2) Optimal module selection from a set of pre-determined values and 3) Simultaneous optimization of both attributes and the platform configuration.

For the scale-based design, a number of methods have been developed, which either assume a fixed platform, or allow optimization of the architecture as a stage of the design. One development for the pre-selected platform cases is the Product Platform Concept Exploration Method (PPCEM) by Simpson et al. [30], which leverages robust design principles to minimize the performance sensitivity to the variation of the scale factors. Other developments for the fixed

platform case include integrating PPCEM and physical programming for product family design by Messac et al. [31], and treating commonality as a constraint to the design problem by Fellini et al. [32]. In regard to the case of unknown platform architecture, which involves the platform configuration task, the developments include integrating the configuration problem with the commonality-performance trade-off problem by Nayak et al. [33], known as Variation-Based Platform Design Methodology (VBPDM). This approach attempts to maximize commonality within the family, while achieving the performance requirements through variation of the smallest number of design variables.

The Product Family Penalty Function (PFPF) method developed by Messac et al. [34] is another work to find the best set of platform and scale variables, based on the performance losses resulting from commonalization. Since the identification and optimization for the platform and the scaling variables are correlated and dependent on each other, the case of solving a joint problem for addressing both of these subtasks at the same time is challenging and combinatorial in nature with computational complexities. A number of studies have tackled such a challenge. For example, a non-gradient based design optimization algorithm was developed by Chowdhury et al. [35] to increase the computational efficiency of the Mixed-Discrete Non-Linear joint PFD problem. Also, the same authors [36] developed a Comprehensive Product Platform Planning (CP3) framework to formulate the platform planning problem, independent from the optimization process. In later developments, Messac et al. [37] compared two of such one-step methodologies that enable converting the combinatorial PFD problems into continuous optimization problems. Another study in this area is a methodology which enables decomposed single-stage and gradient-based optimization of the PFD problems to efficiently solve the joint problem ([38]).

The CP3 framework [36] is a performance-oriented method that attempts to find the commonalities which can result in the optimum cost and performance objectives for the family. In contrary, the proposed method here is a commonality-oriented approach which attempts to increase commonality within acceptable computational cost, while not sacrificing the family performance more than the allowed tolerance. The target of CP3 method is to provide a generic structure for the design problem to be solvable through any continuous optimization method (which needs gradients) or evolutionary algorithms (which are too expensive for black-box type problems). This is not a target of interest in this dissertation, as the selection of the optimization

algorithm would depend on the problem type under study. Instead, the current method can be applied to any problem with any variables to provide information on the objective function and the design problem structure, and to allow making decisions toward platform configuration based on parsimonious assessments.

Sensitivity analysis was first used by Fellini et al. [39] to calculate the performance losses resulting from sharing, and to use such information for identification of the appropriate variables that can serve as scale variables in a family of automotive body structures. Similarly, Wei et al. [40] used a multi-objective optimization-based platform design methodology (TMOPDM), which attempts to identify the platform variables based on their level of impact on the family performance, and uses the coefficient of variation as a decision parameter for identifying such variables.

In a later study by Dai and Scott [27], the sensitivity analysis was performed to find the performance violations per change of each variable for each variant, and based on calculation of a global sensitivity index (i.e., the average of SI values for each variable over the entire family) the platform candidate set was selected for sharing assessments. In their study, the sharing decisions are made based on step by step performance evaluations for each pair-wise sharing through an agglomerative clustering analysis, and the best platform configuration is selected based on the minimum of accumulative performance losses from all the sharing steps. Our study has similarities to their method; however, we will discuss that our approach is different and more efficient in that the extensive function evaluations are not needed due to relying on insightful parameters when selecting the platform candidates, the preferred platform value(s), and the members of each platform/sub-platform. Among the other developments in the same area, Ninan and Siddique [41] leverage the platform cascading strategy to optimize the family based on a single-platform strategy, and then to cascade new platforms from the previous step so that allowable performance loss can be obtained through the minimum possible deviation from the previous platform configuration.

## 2.4. Optimization of families and platforms

While design optimization is widely applied to single products, its application for product families requires more caution due to expansion of the problem size, and necessity of additional

considerations. For example, the general formulation of a constrained optimization problem should expand to include the values of the design variables for each product in the family, so that a new set of constraints are satisfied while a set of objectives for the family optimization are achieved [42]. Therefore in the context of family design optimization and platform optimization, the trade-off between individual product performance and the commonality level among family members becomes a challenge. Identification of the Pareto frontier sets for resolving this trade-off is one potential solution to this challenge [43]. Minimizing performance loss and maximizing commonality is another approach developed for product platform optimization [30]. The platform and family optimization problems can be classified into two problem types; in the first category, the platform is determined first and their values are optimized, and then family members are instantiated based on that platform through optimization of non-common variables. In the second class the platform variables as well as family design variables are optimized simultaneously, and decisions about which variables to be common among the family is made at the same time while deciding about best values for all variables. While determination of the common variables among a family of products can result in significant reduction of the problem size, selection of which variables to be common and which ones to be unique is a challenge and strongly affects the efficiency of the resulting problem. Since it might not be obvious that which variables affect the product performance more than the others, it might be quite risky to determine the platform variables prior to go through the family optimization problem. On the other hand, consideration of all possible variables for deciding about their commonality or uniqueness also adds significantly to the problem computational costs, because all different combinations of variables shall be separately examined in that case [42]. Forty approaches for optimizing product platforms and families of products are classified and reviewed by Simpson et al. in [42]. This classification is listed in Table 2-1.

In the automotive industry, Volkswagen, Skoda, Seat and Audi, produce the Beetle, Golf, Bora, Octavia, Toledo and A3 from a single platform, sharing common components such as engine, transmission, brakes, seat, axles, etc. [44]. Another example of leveraging platforms is Honda, developing an automobile platform that can be scaled along its width and length to realize a ‘‘world car’’ [31]. Fellini et al., [45] applied a multi-objective optimization formulation to a family of three automotive powertrains. Their applied approach was developed by Nelson et al. [46] to quantify the trade-offs involved in designing product platforms. They made a comparison on efficiency of derivative-free global optimization algorithms, decomposition

methods, coordination strategies, and surrogate models for such a large dimensional problem. Though the aforementioned study is the only powertrain family design study, it is a conceptual design for seeking efficient ways to decompose a platform design problem, more than offering design solutions for the powertrain family. Their main focus has been on quantifying the encountered trade-offs in sharing components among the powertrains.

**Table 2-1: Categorization of product family and platform design optimization approaches [42]**

| Category | Possible options |
|---|---|
| **Product family type** | Module-based/ Scale-based |
| **Optimization objective** | Single objective/ Multiple objectives |
| **Market demand** | Modeled/ Not considered |
| **Manufacturing Costs** | Modeled/ Not considered |
| **Uncertainty** | Modeled/ Not considered |
| **Platform specification** | Priori/ Posteriori |
| **Number of stages** | Single-staged/ Two stages/ More than two stages |
| **Optimization algorithm** | GA/ SA/ Branch and Bound/ Exhaustive Search/ Patent Search/ Non-linear Programming/ Sequential Linear Programming/ Sequential Quadratic Programming/ Dynamic Programming/ Generalized Reduced Gradient/ etc. |
| **Optimization framework** | Decision-Based Design/ Target Cascading/ 0-1 integer programming/ Physical Programming / Compromise Decision Support Problem |

In regard with application of Product Family Design Optimization approaches to the vehicles and automotive components, a number of studies have been done, listed as follows:

- Optimizing the number of platforms, applied to an automotive family for finding the optimal number of vehicle platforms that maximize the overall family profit [44]
- Comparing product variety design concepts (standardization, modularity, mutability, etc.) for the automotive platforms design (product variety design tries to enable production of several related products for different market segments, from a common base) [47]
- Developing an analytic model of component sharing among automotive braking systems [48]
- Presenting a comprehensive view of modularity in design, production, and application for the global automotive industry [49]
- Applying the Target Cascading methodology for evaluating the trade-off between family and individual design targets, and implementing it for a family of vehicles [50]

- Developing a platform selection approach based on information from individual optimization of the variants, applied to a family of automotive body structures [39]
- Optimizing a family of automotive body side frames and selecting the component sharing without exceeding user-specified performance bounds [51]

In summary, up to this moment no research study is available about PHEVs design with simultaneous attention to the marketing, manufacturing, and environmental aspects. Objectives such as the fuel economy, and emissions (and very few cost considerations) are the only included items in design studies for these vehicles. As a result, this study is motivated to develop market-oriented as well as manufacturing- oriented objectives into design of PHEVs, for obtaining increased customer acceptance, and production efficiency. The production efficiency is suited through developing a product family of PHEV powertrains. Platform optimization is the solution for assuring market coverage and minimizing loss of performance in the developed family (commonality sacrifices performance of individual products). It should be noted that all the subjects and tools mentioned in this literature review are required for pursuing the objectives mentioned above. In the following section, the proposed work and the objectives will be presented.

In the next chapter, the modeling of a power-split PHEV will be presented with details on governing equations and the parameters affecting performance of each component in the power train.

# Chapter 3. PHEV Modeling

Since this dissertation aims at providing a family design solution for PHEVs, we need a reliable model of the vehicle performance to use at various stages of the PFD. For this purpose, this chapter will provide details of the model developed for the specific needs of this dissertation, which is a replication of well-known simulation models developed by Argonne National Laboratory (ANL), but is different from the existing models in that it is fully parametric and generic to enable optimization efforts based on any desired selection of design variables.

A PHEV typically has an internal combustion engine (ICE), one or two electric motors, and a rechargeable battery. Depending on different power train configurations, different transmission systems are required to adjust the power flow. Since PHEVs are mainly designed to optimize the fuel efficiency, the power from the ICE and motors has to be delicately controlled for different operation modes. As a result, the powertrain design and power management are complicated.

To study the PHEV technology and to make a model for simulation and optimization purposes, this chapter demonstrates a Toyota Hybrid System (THS) power train model and the associated control strategies for Toyota Prius 2004. The validation of the model is done by comparing the simulation results with the real-vehicle test data. The performance constraints are also examined to ensure the validity of this model. After the validation processes, the model is necessarily adjusted to be compatible with an existing optimization algorithm to find the optimized sizes of different components.

As a preliminary work, we used Toyota Prius model in PSAT, for performing component sizing optimization. We connected the PSAT model to an optimization algorithm called Pareto Set Pursuing (PSP) multi-objective optimization approach for finding the best

components that enable $PHEV_{20}$ and $PHEV_{40}$ to meet driving conditions imposed by two drive cycles (UDDS and the Winnipeg Weekly Drive Cycle WWDC), and meeting the performance constraints. The chosen optimization targets are fuel economy, operating cost, and emissions minimization. This algorithm helped to reduce computational cost of design space exploration for such high-dimensional problem (containing 4880 feasible points as combinations of 20 batteries, 14 motors, and 16 engines), and showed that optimization of design problems of discrete variables can be facilitated in tractable order of time, compared to approaches such as exhaustive search or evolutionary algorithms. The result of our study offered optimal hybridization degree of the powertrain components for PHEV20 and 40, under UDDS and WWDC cycles, and the summary of findings and conclusions are as follows [52]:

- The proposed simulation and optimization model automated with PSAT simulator is an effective and efficient method in finding the best hybridization combination for PHEVs drivetrain components with respect to a given drive cycle.
- Multi-objective optimization applied for PHEV drivetrain components hybridization design is a novel approach to achieve sustainable mobility.
- The proposed approach can efficiently search for the optimal hybridization for PHEV's considering multiple objectives.
- In comparison to the exhaustive search approach which takes around 560 days of running simulations for 4480 combinations, this approach takes only 17 days and is a remarkable improvement for such expensive optimization problem.
- Simulation results demonstrate that battery, motor, and engine work collectively in defining a hybridization scheme for optimum performance of PHEVs. In this regard, the integrated formulation of the powertrain design problem will be the next step, as mentioned in the research objectives.
- The optimal design varies with several factors such as drive cycles, AER, configuration, etc.

This chapter describes the components of a PHEV, including the powertrain, driver, external parameters such as resistant forces in the move of the car, etc. Also, the decision

triggers for switching the operation modes (from engine-only to battery-only or to both propulsion sources) are explained to clarify the control strategies applied to this model.

## 3.1. Powertrain configurations

Hybrid vehicles can be classified according to their powertrain configurations. Three configurations in use for HEV/PHEVs are as follows, and their benefits and limitations are briefly explained:

### 3.1.1. Series configuration

This configuration for an HEV/PHEV is equivalent to having an EV with an extended electric range. This configuration decouples the engine from the wheels so that the engine can be operating independently to charge the battery with the help of the generator. The motor supplies the power to the wheels and it takes its power from the battery [53]. It can be seen in Figure 3-1.

The advantage of this configuration is that the engine can operate at its highest efficiency points for obtaining the best fuel economy. The power always follows the electrical path, which is of lower efficiency in comparison to the mechanical path, because of additional magnetic electric field transformation and the heat loss of the electric accessories. Therefore, it becomes relatively inefficient when the vehicle reaches the driving range that could be more efficiently driven by an engine directly. Such inefficiency increases when the vehicle runs on the highway [54]. Therefore, the overall powertrain efficiency might fall down due to the lower efficiency of the electric machine(s) [55].

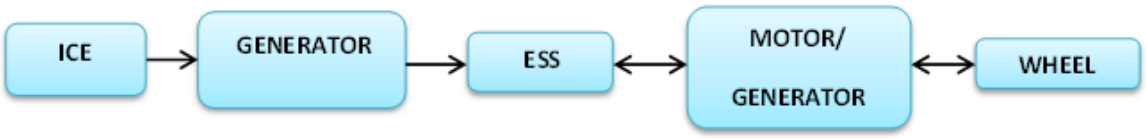


**Figure 3-1: Series powertrain configuration, ESS: Energy Storage System**

### 3.1.2. Parallel configuration

In this configuration, the power is added from the engine to the wheels, and engine and motor are both directly connected to the wheel. Depending on the power split between the two actuators, the vehicle is propelled by both simultaneously [53]. The engine is not connected to the generator, but is coupled directly to the transmission. In this configuration, the mechanical coupling can be either pre-transmission or post-transmission, shown in Figure 3-2 and Figure 3-3 respectively. The drawback of this configuration is that a single electric machine is used both as a generator and as a motor. The electric power assistance must be constrained to avoid draining the battery and frequent role-reversal may be necessary [55].

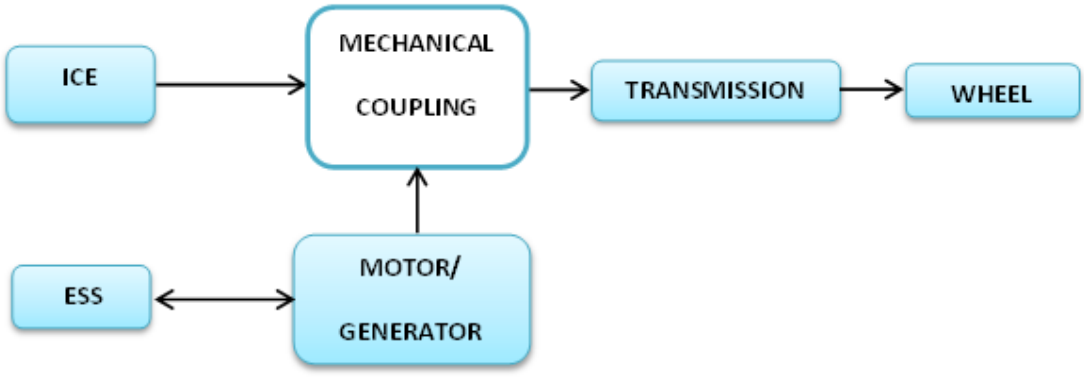


**Figure 3-2: Parallel powertrain configuration with pre-transmission mechanical coupling**

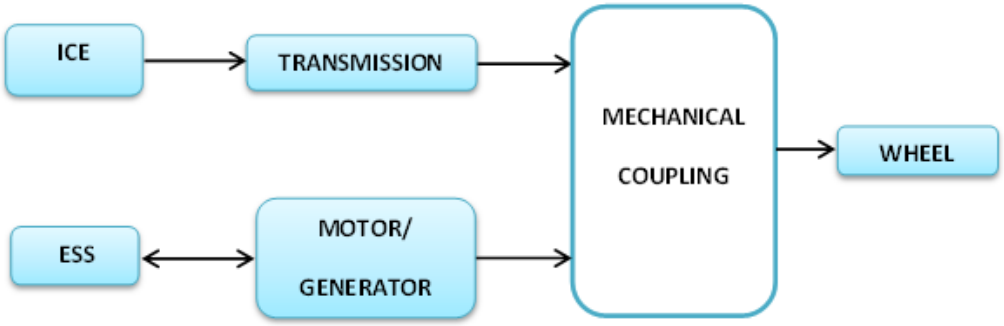


**Figure 3-3: Parallel powertrain configuration with post-transmission mechanical coupling**

### 3.1.3. Power-split configuration

This configuration allows for operation in both series and parallel configurations. The configuration is illustrated in Figure 3-4 [56]. In this configuration, the power split depends on the power split device, referred to as planetary gear set. The advantage of this configuration is that in this configuration the engine speed is decoupled from the vehicle speed, and therefore the engine can be operated at maximum efficiency [53]. This advantage helps reducing emissions, and improving the fuel economy. Therefore, if proper control strategy is applied to this configuration, it is capable of taking advantages of previous configurations, while preventing their disadvantages [55].

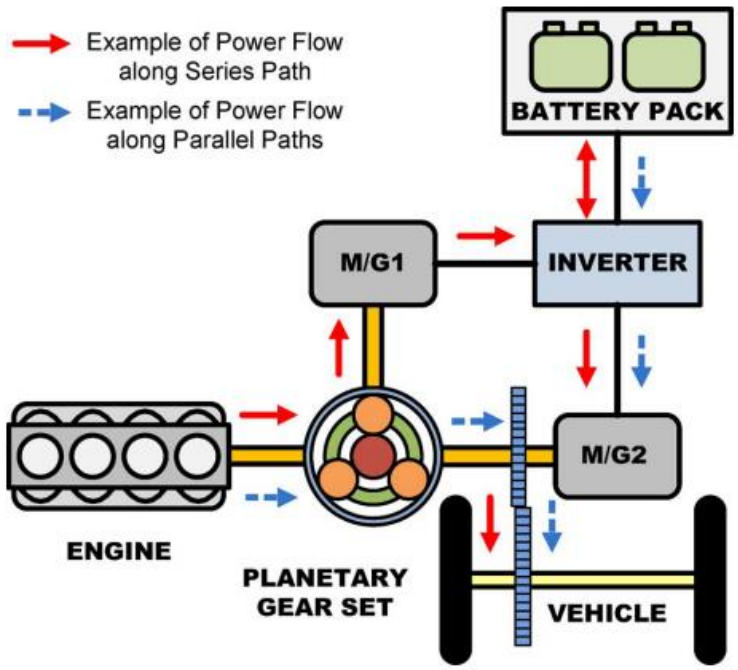


**Figure 3-4: Power split configuration for PHEV [56]**

The single-mode power split configuration combines the ICE with two electric motor/generators (identified as MG1 and MG2) through a planetary gear set. The planetary gear set creates both series and parallel paths for power flow to the wheels. The parallel flow paths (dashed arrows) include a path from the engine to the wheels and a path from the battery, through the motors, to the wheels. The series flow path, on the other hand, takes power from the engine to the battery first, and then back through the electrical system to the wheels (solid arrows). This redundancy of power flow paths, together with battery storage capacity, increases the degree to which powertrain control for performance and efficiency can be adjusted, while meeting overall vehicle power demand [56]. Many dual-mode hybrid vehicles are planned for production over the next several years from GM, Chrysler and BMW. It seems that power-split hybrids will remain dominant in the commercial hybrid market for the foreseeable future [55]. While in parallel and series configurations, the transmission connects the engine and final drive, in the power-split, this transmission is replaced by a power split device or the planetary gear system. Thus, a power-split configuration can operate in series when the speed is low, to avoid drawbacks

of the parallel, and switching to the parallel in highway driving and high speeds to avoid drawbacks of the series [54].

## 3.2. Power-split Powertrain

Having been developed for over ten years, Toyota Prius has a popular hybrid system referred to as Toyota Hybrid System (THS), which features a planetary gear set to split the power from the engine. With such power-split configuration, the engine could propel the vehicle alone, or charge the battery through a generator. A traction motor provides another source of power to either assist the engine or independently drive the vehicle [54]. The flexibility of power management makes the power-split configuration more attractive upon improving the overall efficiency of the vehicle. The powertrain configuration and the operational modes of this THS are illustrated in is shown in Figure 3-5.

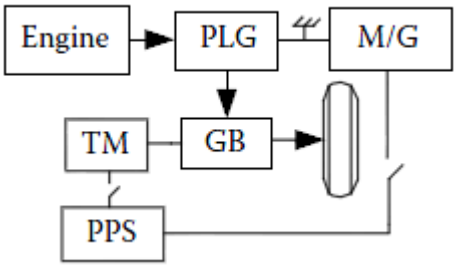


PLG- Planetary Gear Unit

PPS- Peak Power Source

M/G- Motor/Generator

TM- Traction Motor

GB- Gear Box

**Figure 3-5 Engine alone (adapted from [57])**

### Power-split device

According to the advantages and drawbacks mentioned in the earlier section of this chapter, the power-split configuration is chosen as the desired configuration for our powertrain design problem. The required performance equations and design considerations related to this configuration are explained in the next section.

As mentioned earlier, the main component for power split in this configuration is the power-split device, which determines the dynamics of the power split [53]. This system is shown in Figure 3-6. The flywheel-transmission-internal-combustion hybrid vehicle - a HEV leveraging from Flywheel energy storage as a secondary energy storage system which stores the energy in form of mechanical kinetic energy- and the planetary gear train with Continuously Variable Transmission (CVT) mechanism were the early power-split devices designed and studied at 1980 and 1993 respectively, though they were not applied to any passenger vehicles until late 1990s [54]. THS was the first power-split passenger vehicle introduced in 1997. Prius and most of the hybrid fleet from Toyota mainly leverage this system in their powertrain configuration. Another major power-split system design is the Allison Hybrid System known as AHSII, invented by GM as a dual-mode power-split system, and applied to several mid-sized SUV and pickup trucks and has become a major competitor in recent years [54].

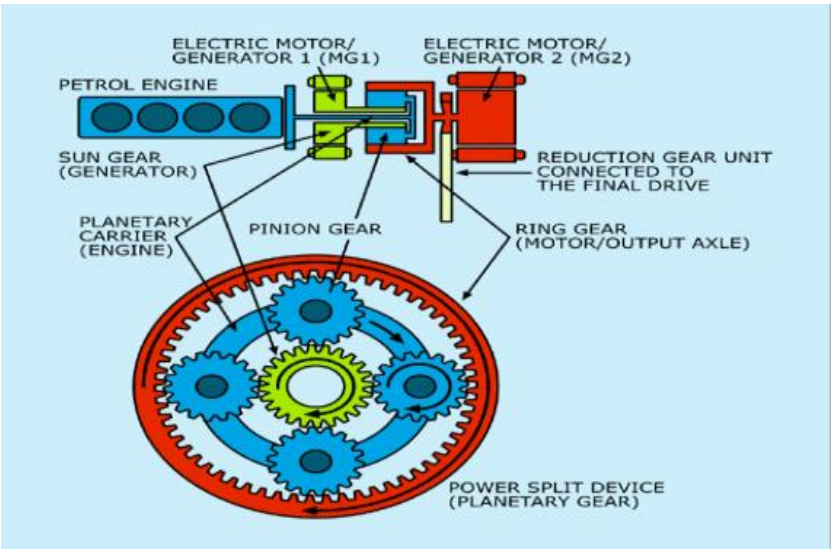


**Figure 3-6: The planetary gear system for power split ([53])**

The gear in the center is called sun gear. The gear surrounding the sun gear is the planet gear. The planetary gear set has three sets of gears moving on the carrier, and the shaft of the planet is connected to the carrier. In a power split hybrid vehicle, the ICE is connected to the carrier, Motor/generator (MG2) is connected to the ring gear, and

Motor/generator (MG1) is connected to the sun gear [53]. MG1 is predominantly used as a generator, while MG2 is used as a motor. In mathematical computations of the vehicle dynamics, wherever MG1 serves as a generator, its power value will take positive sign, while for MG2 in case of operating as a motor its value will be positive. Otherwise, the power for these components will take negative values. The fundamental equation for planetary gearing derived by the Willis' formula is that the gear must rotate so as to maintain a fixed ratio of angular speeds relative to the carrier body [58]. The speed relationships between the planetary gears set components can be written as:

$$\omega_{MG1}.S + \omega_{MG2}.R = \omega_{ice}.(R + S) \quad (3\text{-}1)$$

Where:

*S*: number of teeth of the sun gear

$\omega_{MG1}$: Angular velocity of $MG_1$

*R*: number of teeth of the ring gear

$\omega_{MG2}$: Angular velocity of $MG_2$

It shall be noted that the angular velocity of the powertrain components is equal to the speed of the gear connected to them:

$\omega_{MG1} = \omega_s$, the speed of sun gear

$\omega_{MG2} = \omega_r$, the speed of ring gear

$\omega_{Ice} = \omega_c$, the speed of carrier gear

The gear ratio of engine/motor is the ratio of number of the teeth of the ring gear to that of the sun gear:

$$GR = \frac{maximum\ engine\ or\ motor\ speed\ (\frac{km}{h})}{maximum\ vehicle\ speed\ (\frac{km}{h})} = \frac{v_{PS,max}}{v_{v,max}} = \frac{2.\pi.r_{wh}\omega_{PS,max}.3.6}{v_{v,max}} \quad (3\text{-}2)$$

$\omega_{PS,max}$ is the angular velocity of the propulsion source (engine or motor), $v_{v,max}$ is the maximum speed of the vehicle (km/h), and $r_{wh}$ is the wheel radius. The max speed of the vehicle is in m/s which has to be converted to km/h, resulting in 3.6 showing on the numerator.

The basic power balance equation for all possible operation modes of this configuration is as follows:

$$P_{req}(t) = P_{fc} + P_{el} \quad (3\text{-}3)$$

Where

$P_{fc}$: Power supplied through the fuel converter

$P_{el}$: Power supplied by the electric accumulator

$P_{req}$: Power request from the driver

The electrical power is the sum of the powers supplied through $MG_1$ and $MG_2$:

$$P_{el} = P_{el1} + P_{el2} = P_{MG2} - P_{MG1} \quad (3\text{-}4)$$

where $P_{MG1}$ is the power of the electric motor number 1 (generally the generator), and $P_{MG2}$ is the power of the electric motor number 2 (generally the electric motor).

## 3.3. Performance requirements for the vehicle

The governing forces during propulsion of the vehicle in general are shown in Figure 3-7. Three major parameters come into effect for modeling the vehicle forces: grade, aerodynamic drag, and rolling resistance [59].

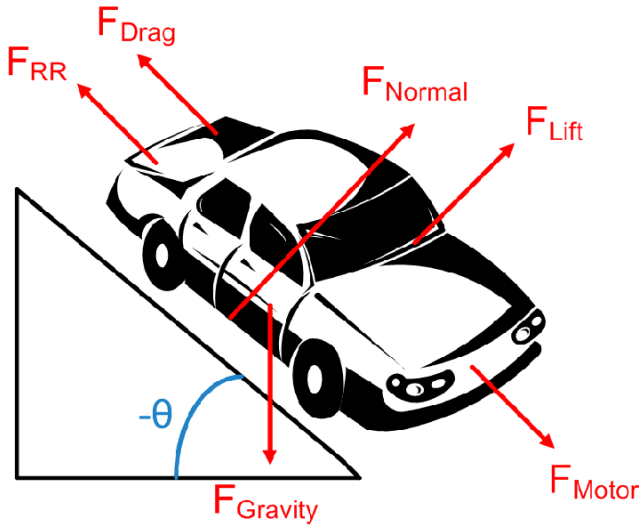


**Figure 3-7: Governing forces during vehicle movement [59]**

*Grade force:* The grade force, $f_g$ is what the vehicle has to overcome when climbing hills, and is calculated using Newton's second law of motion. Parameters such as vehicle mass and grade angle can affect the grade force, and accordingly affect the force required to drive the vehicle.

$$f_g = m.g.\sin\theta \tag{3-5}$$

$m$: The vehicle mass in kg

$g$: Acceleration from gravity in $^{m}/_{s}\,2$

$\theta$: The rode slope

Aerodynamic drag force: A moving vehicle is resisted by the surrounding air around it, and through some simplifications such as ignoring the lateral forces, this force, $f_{Ad}$ can be calculated as follows:

$$f_{Ad} = \frac{1}{2}\rho_a . C_D . A_f . v_{rv}^2 \quad (3\text{-}6)$$

$\rho_a$: *Air density in* $^{kg}/_{m^3}$

$C_D$: *Drag coefficient*

$A_f$: *Vehicle frontal area*

$v_v$: *Vehicle velocity in* $^{m}/_{s}$

*Rolling resistance:* This resistive force $f_{RR}$ results from deformation of the tires at their contact point to the ground during rolling movement. While modeling this parameter depends on several other factors and generally complex enough, there are simplifications adopted from the literature to represent it in the following form:

$$f_{RR} = m . g . (k_1 + k_2 . v_v) . \cos\theta \quad (3\text{-}7)$$

$k_1$ and $k_2$ are rolling resistance coefficients that are determined by experiment. The required force at a specific speed to drive the vehicle is the sum of three forces discussed above.

$$f_{total} = f_{RR} + f_{Ad} + f_g \quad (3\text{-}8)$$

Watt is converted to kW as the required engine power. The engine power output is equal to the resistance power plus the dynamic power for acceleration of the vehicle. This

is the required power to overcome the forces at grade, which is accordingly calculated as follows:

$$P_{grade} = \frac{v_{v,grade}}{1000.\eta} . f_{total} \quad (3\text{-}9)$$

$\eta$: The overall propulsion system efficiency

$v_{v,grade}$: Velocity at the grade

$P_{grade}$: Vehicle power (in Kilowatts) required to maintain a constant speed at the specified grade

The minimum motor/engine size to meet the road grade requirement equals to the vehicle power requirement to maintain a constant speed at the specified grade.

The Gear Ratio (GR) can be used to convert the tractive effort of the power source (PS) to the tractive effort at the drive wheels [60].

$$F_{wh} = F_{PS} . GR \quad (3\text{-}10)$$

$F_{wh}$: tractive force at the drive wheels

$GR$: Gear Ratio (Introduced in Equation (3-4))

$F_{PS}$: Tractive force at the power source

It shall be noted that the vehicle mass is dependent on the power source size, so such problem needs to solved iteratively, and after calculation of the PS mass at each iteration (depending on the power), the road load is then updated.

## 3.4. Powertrain components and performance equations

### 3.4.1. Engine

A generic spark ignition (SI) engine model is used for this study, using gasoline to produce mechanical energy. The generic engine model in SimDriveline provides the maximum torque available for a given engine speed, and has the following torque function [61]:

$$\tau = \left(\frac{P_{max}}{\omega_o}\right) * \left(\frac{p(w)}{w}\right), \text{where } \omega_o \text{ is the speed at } P_{max}, w = \frac{\omega}{\omega_o} \quad (3\text{-}11)$$

$$p(w) = p_1 w + p_2 w^2 - p_3 w^3, satisfying\ p_1 + p_2 - p_3 = 1, p_1 + 2p_2 - 3p_3 = 0 \quad (3\text{-}12)$$

For spark-ignition type, all of the power demand coefficients, $p_1, p_2, p_3$, equal to one. For diesel type, $p_1 = 0.6526$, $p_2 = 1.6948$, and $p_3 = 1.3474$ [61].

Experimental data form test data and PSAT available in lookup tables are used in this study to calculate the output of the engine. A time constant of 0.2 seconds is used in this system.

### 3.4.2. Fuel Consumption and Engine Efficiency

A brake specific fuel consumption (BSFC) lookup table, indexed by engine speed and torque, is taken from the PSAT initialization file of the same engine type. The BSFC relates to the fuel consumption rate. By using the equations below, the fuel rate, total amount of fuel consumption, and engine efficiency could be calculated.

- Fuel consumption rate = engine power * bsfc/3600/1000, where bsfc is in g/kWh, power in Watt, and fuel rate in gram/sec.
- Consumed amount of fuel= $\int fuel\ consumption\ rate$
- The efficiency of engine: $\eta = \frac{P}{\dot{m}_{f} * Q_{HV}}$ (3-13)

Where $\dot{m}_f$ is the fuel rate in gram/s, and $Q_{HV}$ is the heating value of the fuel ranging from 11.7~12.2 kWh/kg, which is defined as the heat released from unit fuel with complete combustion at standard conditions and the combustion products cooling down to their original temperature [57]. In this model, $Q_{HV}$ is approximated as 12 kWh/kg.

### 3.4.3. Gear Ratio

The planetary gear set is the key part in power-split PHEV. Torque is supplied through the carrier to ring and sun gears. The key of the power-split mechanism is that power is split according to the number of teeth of the ring and sun gears.

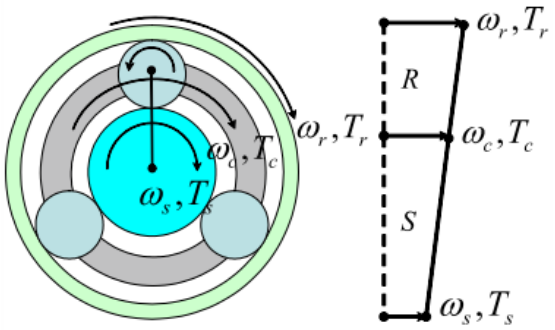


**Figure 3-8: The planetary gear set and the lever diagram [62]**

For a THS, the ring has 78 teeth and the sun has 30 teeth [63]. The governing equations are:

$$T_r = \frac{R}{R+S} * T_c \quad (3\text{-}14)$$

$$T_s = \frac{S}{R+S} * T_c \quad (3\text{-}15)$$

$$\omega_c = \frac{R}{R+S}\omega_r + \frac{S}{(R+S)}\omega_s \quad (3\text{-}16)$$

$\omega_c$, $\omega_r$, $\omega_s$: The speed of the carrier, ring gear, and the sun gear, respectively

$T_c$, $T_r$, $T_s$: The torque of the carrier, ring, and sun gear, respectively

*R* and *S* represent the number of teeth or the radius of the ring and sun gears, respectively. Equation (3-16) is the same as Equation (3-4), but represents the relationship in terms of the gear speeds, while Equation (3-4) shows the angular velocity of powertrain components.

The SimDriveline model only requires the ring-to-sun gear ratio as the input, while the meshing and viscous losses are optional. In this model, the sun-planet efficiency and ring-planet efficiency is 0.96 and 0.98, respectively.

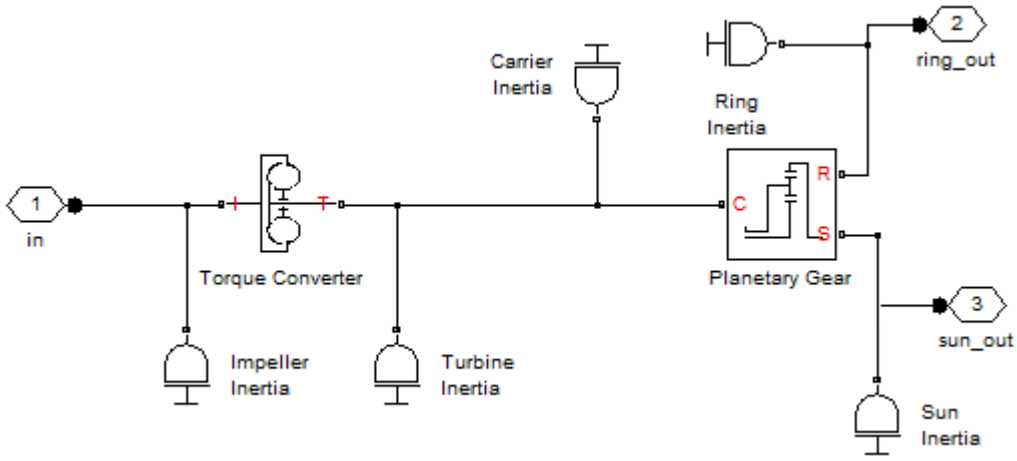


**Figure 3-9 Torque Converter & Planetary Gear Models in SimDriveline**

## 3.4.4. Emissions and After-treatment

The emission data of the engine, HC, CO, and NOX, are obtained from the test data available from PSAT which is provided by Argonne National Laboratories, then fed into an exhaust after-treatment model. The rate of $CO_2$ is calculated based on the distance traveled by the vehicle. The equation is:

$$\dot{CO}_2 = \frac{Ag * Fuel\ Consumption}{distance}\ [\frac{\text{g}}{\text{km}}] \qquad (3\text{-}17)$$

Where $\text{Ag is the gasoline } \text{CO}_2 \text{ emission coefficient} = 2380\frac{g}{L}$

Fuel consumption is plugged-in here in Liter, and distance is in Kilometers.

### 3.4.5. Battery Model

The open circuit voltage, $V_{oc}$ lookup table, indexed by temperature and state of charge (SOC), is taken from the PSAT initialization file of the same type of battery, i.e., Li-ion Saft battery with 3 cells in each module and a nominal 3.6 Volt per cell. The conductive and convective heat transfer data is taken from the PSAT initialization file as well. The battery is modeled mainly based on mathematical approach for computational simplicity, for which the fundamental equations are explained shortly. The battery pack treats all the sub-cells as a whole, and the nominal voltage is the aggregate of these sub-cells. The change in internal resistance of the battery is omitted since the variation is not significant. The mathematical battery model takes battery capacity and temperature into account to calculate the current, voltage, and state of charge (SOC). The inputs are the current of motor and generator which are added up to obtain the battery current. Negative current means the generator or motor is charging battery, whereas positive current means discharging. The outputs of the battery are the instantaneous voltage and the SOC. The fundamental equations to model a battery are as follows:

$$battery\ voltage = Voc - I * R_{int} \tag{3-18}$$

$Voc$: The open circuit voltage

$I$: Current passing the battery

$R_{int}$: Internal resistance of the battery

The time that a battery can sustain is a function of its capacity divided by its current:

$$capcity\ used = \int I + (1 - Voc) * max.capacity \tag{3-19}$$

$$SOC = capcity\ remained / maximum\ capcity \tag{3-20}$$

$$Q_{gen} = R_{int} I_{in}^2 - V.I_{in}(1 - \eta_{coulombic}) \text{ For } (I_{in} < 0) \tag{3-21}$$

$Q_{gen}$ : The power loss from the battery

$\eta_{coulombic}$: The columbic efficiency of the battery

$I_{in}$: Discharging current

$SOC$: State of charge of the battery, as a percentage of the capacity

### 3.4.6. Electric Motor

The traction motor occasionally functions as a generator, but mainly as a prime mover. Depending on the control strategy, it could be a dominant source of power or an assistive device. In a typical Prius configuration, the motor is an AC permanent magnet synchronous machine. However, since the battery is a DC device, an inverter must be used (ad hence included in the model) to connect the DC source to the AC motor. Since the inverter involves complex electronic elements such as transistors, and the AC circuits between the AC motor and inverter are also complicated, the AC motor is simplified as a DC motor with equivalent properties from the SimElectronics toolbox. The motor model is built through using a dynamic equation to show the torque, which is the rate of change in the angular momentum of the motor. The total torque is calculated through Equation (3-25), as the summation of the motor torque, plus the value of motor inertia multiplied by the angular acceleration of the motor.

$$L = I_m \omega \tag{3-22}$$

$$\tau = \frac{dL}{dt} \tag{3-23}$$

$$\tau = \omega . \frac{dI_m}{dt} + I_m . \frac{d\omega}{dt} \tag{3-24}$$

$$\tau_{total} = \tau_{motor} + I_m . \frac{d\omega_m}{dt} \quad (3\text{-}25)$$

Where:

$\tau_{motor}$: The motor torque

$I_m$ : The motor moment of inertia

$\omega_m$: The angular velocity of the motor.

$L$: The angular momentum

Another assumption is that the motor could achieve peak power all the time. As been tested, the temperature of the 50 kW motor rarely exceeds the upper limit. This is tested based on a PSAT block which calculates the heating index of the motor, as shown in Figure 3-10. In fact, the simulation results show that the maximum torque of the motor stays below the maximum continuous limit, so the assumption is more or less not important.

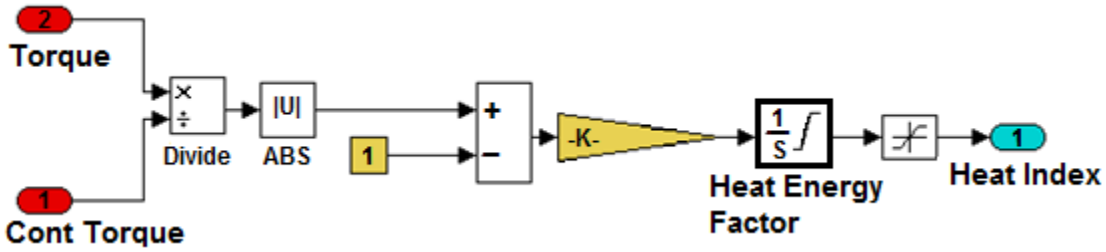


**Figure 3-10 Heating Index Calculation**

## 3.4.7. Generator

The generator is modeled by the same SimElectronics model as the motor, but with different parameters, including the maximum torque (which is dependent on the motor size,

while for the generator it is equal to 200 N.m and fixed), and the speed at which the efficiency is measured (2300 rpm for motor, vs. 4500 rpm for the generator). Most of other parameters such as the electrical loss are the same. It is connected to the sun gear shaft to either allow the engine to charge the battery, propel the vehicle or start the engine from the off state. Through controlling the torque and the speed of the generator, the speed of the engine can be controlled to achieve higher operating efficiency and less emissions [63].

In this PHEV model, the engine start process is done by connecting a duplicated generator model to the output shaft of the engine. A constant current is fed into the generator to provide enough speed for the engine to start generating torque. The amount of current is considered as what the generator consumes. For different generator sizes, this amount of current might need to be adjusted.

### 3.4.8. Vehicle Body and Tires

The vehicle subsystem consists of a vehicle body, two sets of tires, braking system, and a differential gearbox. The inputs are the braking force, the longitudinal force from the tires, the wind speed, and the road incline angle. The outputs are the vehicle velocity and the normal force of the vehicle. The top level equation for the vehicle propulsion is:

$$P_o = \frac{1}{\eta_T}\left(\frac{mgf_r v}{3600} + \frac{C_D A v^3}{76140} + \frac{\delta m v}{3600}\left(\frac{dv}{dt}\right) + \frac{mgvsin\beta}{3600}\right) \quad (3\text{-}26)$$

where $P_o$ is the demand power in kW, $\eta_T$ is the transmission efficiency, m is the vehicle mass in kg, g is the acceleration of gravity in m/$s^2$, $f_r$ is the rolling coefficient, v is the vehicle speed in km/h, $C_D$ is the aerodynamic drag coefficient, A is the frontal area of the vehicle in $m^2$, $\delta$ is the rotating mass coefficient, and $\beta$ is the slope angle of the road in rad [63]. This equation is widely used in literature to provide a baseline for calculating the required power for the vehicle propulsion. The rest of fixed parameters used in the modeling of this study are shown in Table 3-1. The dynamic equations for the vehicle body used in SimDriveline are:

$$m\dot{V_x} = F_x - F_d - mgsin\beta \quad (3\text{-}27)$$

where $V_x$ is the longitudinal vehicle velocity, $F_x$ is the longitudinal force on wheels, $F_d$ is the aerodynamic drag force.

$$F_x = n(F_{xf} + F_{xr}) \tag{3-28}$$

where *f* represents front wheels and *r* represents rear wheels, *n* is the number of wheels on each axle.

$$F_d = \frac{1}{2} C_D \rho A (V_x - V_w)^2 sgn(V_x - V_w) \tag{3-29}$$

where $\rho$ is the mass density of air = 1.2kg/$m^3$; $V_w$ is the headwind speed.

**Table 3-1: Fixed parameters used in the PHEV model for this study**

| **Parameter** | **Value** |
|---|---|
| Vehicle glider mass (kg) | 1228 kg |
| Number of wheels per axle | 2 |
| Horizontal distance from CG to front axle (m) | 1.4 |
| Horizontal distance from CG to rear axle (m) | 1.6 |
| CG height above ground (m) | 0.5 |
| Frontal area ($m^2$) | 3 |
| Drag coefficient | 0.29 |
| Initial velocity (m/s) | 0 |
| Transmission efficiency | 95% |
| Rolling friction coefficient | 0.007 |
| Wind speed (m/s) | 1 |
| Tire effective radius (m) | 0.305*0.95 |

## Brake

The braking system consists of the built-in brake model. The input is a normal force that locks the frictional plates depending on the threshold value. The initial condition of the brake needs to be correctly specified according to the state of other components. The

braking force is calculated based on the negative torque demand from the driver. The governing equation is

$$Braking\ force = \frac{torque\ demand * Gear\_ratio}{wheel\ radius} \quad (3\text{-}30)$$

In the calculation of torque demand, the overall torque demand is divided by the gear ratio, as the gear ratio is an intensifier of the torque. For calculating the braking force, however, the ratio is multiplied in the above equation to compensate and show the actual force required for stopping the vehicle.

### Clutches

The clutches are similar to braking systems, but requiring a pressure signal as the input. Two sets of clutches are used to decouple the motor from the driving shaft, to enable the engine starter, and to lock the sun gear to the ground. These clutches are signaled by the controller to implement the control strategy.

### Driver

As Wang [64] suggests, the driver is modeled as a PI controller in the following form:

$$P + I.T_s \frac{1}{z-1} \quad (3\text{-}31)$$

where p = 800, I = 0.5, and the initial time response constant is 0.2 seconds.

The speed error between the target speed and instantaneous speed of the vehicle is fed into the PI controller to calculate the torque demand for propelling the vehicle. The PI controller is tuned to give a reasonable value of torque while maintaining a fast response of the engine and motor to the speed error. The torque lost due to aerodynamic drag, rolling resistance, and road incline should also be added to the torque demand which is finally divided by the transmission ratio. Once the actual velocity exceeds the desired, the brake

signal is triggered. The torque demand could also be converted into power demand based on the equation below.

$$Power\ demand = \left(\frac{torque_{demand}}{wheel_{radius}}\right) * target\ speed \quad (3\text{-}32)$$

The torque loss is calculated through Equation (3-33):

$$F_{loss} = (fr + 0.00012V)m_{veh}g + \frac{\rho C_d A V^2}{2} + m_{veh}gsin(grade) \quad (3\text{-}33)$$

$$T_{loss} = F_{loss} * r_{wheel} \quad (3\text{-}34)$$

## 3.5. Control Strategies

Due to the plug-in ability, the PHEV is designed to mainly take advantage of the electric machines. Ideally, the PHEV is expected work in all-electric-range (AER) mode in which the vehicle is propelled only by the electric power. However in many commercial PHEVs, the strategies are to maintain the engine at high efficiencies with the assistance from the battery.

### 3.5.1. Electric Dominant Strategy

This type of control mostly is to utilize the traction motor to drive the vehicle as long as the constraints are not met. The engine only provides the extra amount of power regardless of efficiency [65]. The challenge of this strategy is that the size of the battery should be large enough to allow the vehicle for a long distance of drive, but the price of the battery also constrains the size. Because of the sustainability problem, true AER vehicles are not as practical as commercial PHEVs that take advantage of the engine dominant strategy.

### 3.5.2. Rule-Based Engine Dominant Strategy

#### Engine Optimal Region

The operation of engine depends on the torque and speed. An ideal operation region is the desired state for engine to operate at the best efficiency [66], as shown in Figure 3-11. Usually this state is accomplished by controlling the torque and speed of the engine. The efficiency of the model is shown to be mostly affected by the power of the engine. Within a rough range between 15 to 50 kW, the efficiency could be maintained above 30%. However, further tests reveal that by controlling the torque output of the engine by a PID controller, the efficiency could be maintained above 30% as well. The torque range for the best efficiency is 63 to 114 Nm. The advantage of controlling the torque output is that the amount of torque required could be easily converted to a throttle signal that feeds into the engine model.

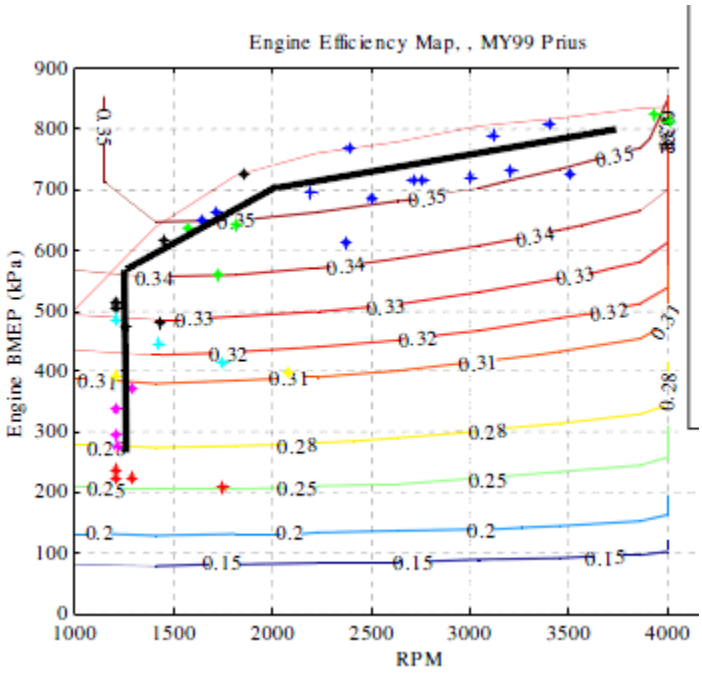


**Figure 3-11 Engine Ideal Operational Line [57]**

The engine torque depends on the engine size which is the engine displacement and is defined as the volume swept by the piston from top dead center (TDC- the furthest point in piston's travel, where the upward stroke changes to downward stroke) to bottom dead center (BDC). The mean effective pressure (mep), is a more useful relative performance measure defined as the work per cycle per displacement [66]. The Brake

Mean Effective Pressure (BMEP) is a measure of the efficiency of a given engine at producing torque from a given displacement.

Being able to control the minimum and maximum torque for the best efficiency, different operational mode could be achieved. Taking the SOC of the battery and the vehicle speed as constraints, the controlling of acceleration could be divided into three regions: low torque, medium torque, and high torque. The general control implementation is to control the input of the engine and motor and to enable or disable particular clutches.

## Accelerating Mode

The accelerating mode consists of two sub-modes which are charge depleting (CD) and charge sustaining (CS) modes. As long as the SOC is above the lower limit, the CD mode implements the engine-dominant strategy to continuously decrease the SOC. When the SOC hits the lower limit, 30%, the Equivalent Consumption Minimization Strategy, or ECMS, is applied to maintain the SOC at 30% while propelling the vehicle as demanded.

## Charge Depleting Mode

### Low Torque Region

The low torque region in this Prius 2004 model is defined for torque demands less than 63 Nm, under which the motor is the only source to assist propulsion if the SOC is above the threshold of 30%. This mode could also be triggered when the vehicle speed (engine turn-on speed) is less than 5 m/s. In this case, the torque demand for the motor is controlled by the output voltage of the battery which is scaled by the torque gain defined as the torque demand to maximum continuous torque ratio. This way of controlling motor torque may not be sufficiently accurate but as many trials have been done, the results show that such way of controlling could generate almost the same torque as demanded.

**Table 3-2: Rules in Low Speed Region**

| Low speed region | Engine torque [Nm] | Motor torque [Nm] | Battery state |
|---|---|---|---|
| SOC > 0.3 | 0 | $T_{dmd}$ | Discharging |

### Medium Torque Region

As long as the torque demand is within 63 ~ 114 Nm, the vehicle enters the medium torque region. The torque of the generator should be compensated by the motor because a fraction of torque from engine is converted into electricity by the generator. Different modes of operation are listed in Table 3-3.

**Table 3-3: Rules in Medium Speed Region**

| Medium speed region | Engine torque [Nm] | Motor torque [Nm] | Battery state |
|---|---|---|---|
| SOC > 0.3 | 63 | $T_{dmd}$- 63 +$T_{gen}$ | Discharging |

### High Torque Region

When the torque demand exceeds 114 Nm, the vehicle works in blended mode. The operation modes are similar to the medium region except the minimum torque of the engine should be 114 Nm, as shown in Table 3-4.

**Table 3-4: Rules in High Speed Region**

| High speed region | Engine torque [Nm] | Motor torque [Nm] | Battery state |
|---|---|---|---|
| SOC > 0.3 | 114 | $T_{dmd}$-114 + $T_{gen}$ | Discharging |

### Sharp Acceleration

To satisfy the demand from the driver, sharp acceleration is accomplished by set the engine throttle to 1 to indicate when the throttle is open, and let the motor provide of the required power. In this case, the engine is not necessarily working in its best efficiency range. The torque threshold, 200 Nm, of turning on this mode might not be realistic. The acceleration mode contains the above CD and CS modes which are designed to control the propulsion of the vehicle. The deceleration mode, overwriting the acceleration mode once triggered, decouples the motor from the driving shaft, and enables the braking subsystems.

## 3.6. SimDriveline for creating generic PHEV models

Professional software such as PSAT and ADVISOR have been effectively used in vehicle modeling of various studies in the literature. However, more detailed models could be accomplished using SimDriveline in Simulink. SimDriveline includes an adequate number of mechanical models such as brake, clutch, coupling, drive, engine, gearbox, tire, and vehicle body. It takes advantage of Simulink abilities for developing comprehensive models, which allow modeling of numerous external and internal factors and studying their effect on vehicle performance.

By choosing other mechanical elements from the fundamental library under Simscape, a complete and illustrative mechanical model of the powertrain could be built. The Simscape fundamental library contains all the basic elements in mechanical, electrical, and thermal fields. These elements could be used with the physical modeling product family, including SimDriveline, SimElectronics, and Simpowersystems, to make a complete model. On the electrical side, different motors are available in SimElectronics, and other elements could be found in the electric fundamental library under Simscape. More advanced modeling of the electric components could be done by the Simpowersystems toolbox which includes better models of motors and some other electrical and electronic elements. Simscape also provides models for thermal elements which could also be applied in vehicle modeling.

The advantage of this Simulink-based modeling tool is that an illustrative physical model that resembles a real powertrain could be developed rather than pure mathematical models in PSAT. With all the parameters specified, Simulink processes the equations behind each component and provides the results.

## Validation

A validation process is done typically by comparing the simulation results with the previous validated results. Since the test data for the MY04 Prius model is available, the simulation results are compared with the test data. The output of each component is verified to be similar to realistic components in term of rated performance.

## Selected Control strategy

A strategy similar to the electric dominant strategy is applied in this study, where engine assists the vehicle as needed, and is not strictly turned off. As such, it is observed in Figure 3-13 that a decrease in SOC until a specific threshold. However, depending on the power demands at various times of the drive cycle, SOC is showing a relatively flat line with occasional small increases in the form of little spikes in the graph during the charge sustaining mode). The urban dynamic drive schedule, or UDDS, is used for testing the performance of the PHEV under urban driving conditions since PHEV is primarily used within cities. The properties of the drive schedule are shown in Table 3-5.

**Table 3-5: UDDS specifications**

| | **Max speed (mph)** | **Average speed (mph)** | **Max acceleration (m/s2)** | **Max deceleration (m/s2)** | **Cycle distance (miles)** |
|---|---|---|---|---|---|
| UDDS | 56.7 | 19.6 | 1.48 | -1.48 | 7.45 |

The vehicle speed closely follows the speed demand of UDDS, as shown in Figure 3-13.

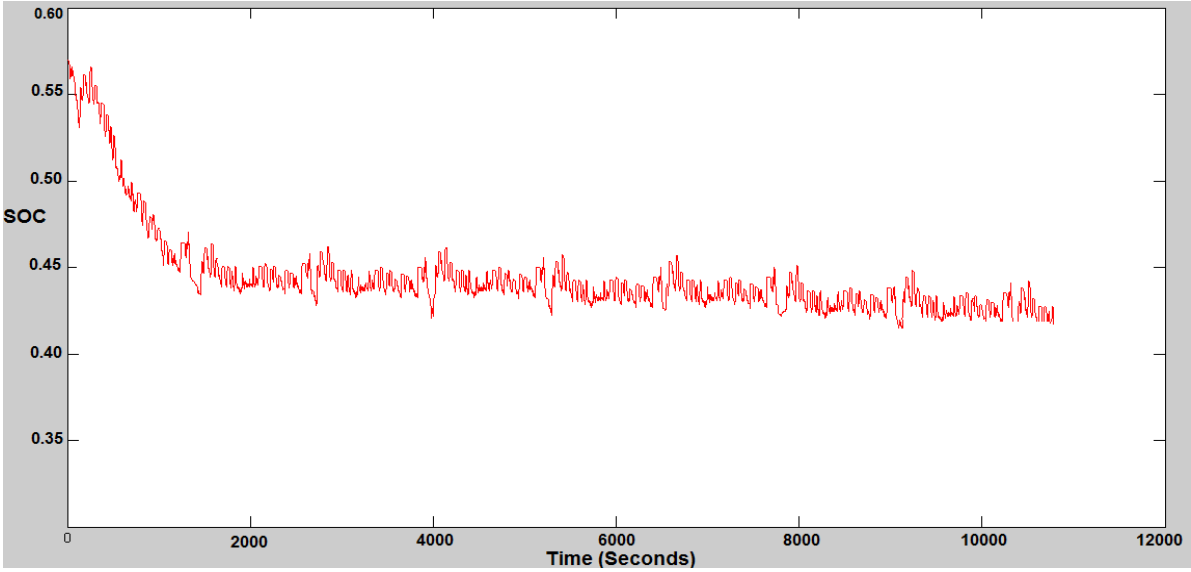


**Figure 3-12 SOC diagram over time for an electric dominant strategy**

The plot in this picture is captured during a run of the simulation, and as it can be observed, the vehicle velocity is closely following the expected velocity imposed by the UDDS drive cycle.

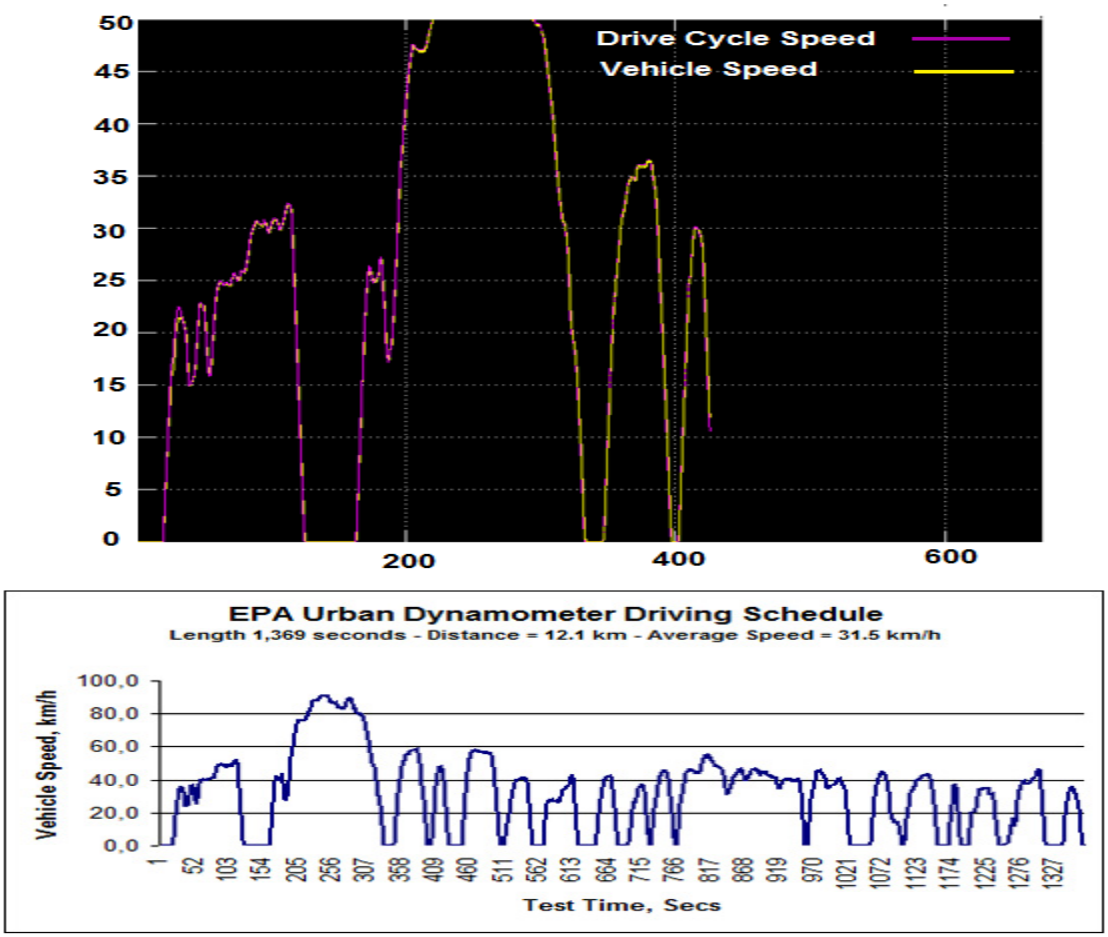


**Figure 3-13: Results of the simulation model following the UDDS cycle**

## Performance Tests

The maximum vehicle speed, acceleration, and gradeability were tested by setting the engine throttle to one, and the motor only supplies the extra power. The general performance constraints for PHEV are:

| | | |
|---|---|---|
| Max. vehicle speed | ≥ 85 mph | (3-35) |
| Max. vehicle acceleration | ≥ 0.5g | (3-36) |
| 5-second distance | ≥ 140 feet | (3-37) |

| | | |
|---|---|---|
| 0-60 mph time | ≤ 12 sec | (3-38) |
| 0-85 mph time | ≤ 23.4 sec | (3-39) |
| 40 – 60 mph time | ≤ 5.3 sec | (3-40) |
| HC emissions | ≤ 0.125 g/mile | (3-41) |
| CO emissions | ≤ 1.75 g/mile | (3-42) |
| $NO_x$ emissions | ≤ 0.075 g/mile | (3-43) |

The tests Implemented in separate and simplified models, show that the model operates within all the above constraints. As such, the model is capable of serving design optimization purposes, and will be used toward adapting our desired problem formulation in the following chapter. The details results of model validation are presented in Appendix B.

In summary, this chapter provided a presentation of the developed simulation model which has adopted the governing equations and fixed parameters from the literature for utilization toward our optimization and family design purposes in the next chapters.

# Chapter 4. Proposed Family Design Method

In this chapter the proposed product family design methodology of this dissertation will be explained in detail. An efficient non-conventional sensitivity analysis, the detachability property of each variable, and the coefficient of variation are among the techniques mainly used towards making platform configuration decisions. As mentioned in Chapter 1, the need for this methodology comes from lack of efficient techniques to address simulation-based family design problems, and the set of techniques integrated into the proposed methodology here, are shown to ensure computational saving throughout the family design stages.

Meta-modeling techniques are employed to provide reliable correlation intensities information, with remarkable savings in the number of function calls. It is shown that the proposed method is efficient for designing scalable product families through its application to a family of universal electric motors. The outstanding features are: 1) It obtains the design solution with more commonality levels over a number of previously developed methods; 2) The resultant family design is within allowable performance loss range, and there is improvement in the aggregated preference objective function value, as compared to the previously published family design methods; 3) The method provides comparable computational efficiency, with promises to work efficiently for high-dimensional expensive black-box (HEB) design problems. A test case is also designed to study more about the impact of the leveraged parameters on the performance of our proposed method. It is shown that the proposed method suits well to high dimensional expensive black-box (HEB) design problems, which makes it an efficient approach for designing product families based on simulations with no explicit mathematical equations. For such HEB problems, metamodeling is usually used. Based on recent works in [67, 68], knowledge can be gained about the black-box function, along with the variable correlations and sensitivities. The

proposed method leverages this new technique for product family design on HEB problems, which results in significant savings in the function calls.

This chapter leverages a non-conventional sensitivity analysis of the design variables for identification of the appropriate platform candidate set. Rather than sensitivity analysis used in Dai and Scott [27], the information on the sensitivity of the variables are obtained through a strategy that combines the Radial Basis Function-High Dimensional Model Representation (RBF-HDMR) and the Random Sample HDMR (RS-HDMR) meta-modeling techniques, in order to quantify the impact of each variable on the performance function and provide a measure of the correlations among variables. Differing from previous works, the sensitivity analysis is performed on the meta-model, not on the original expensive function, and the cost of the sensitivity analysis procedure is thus remarkably reduced through using computationally cheap sample points rather than original expensive ones. The results of our family design will be compared to the results obtained by Dai and Scott [27] and Ninan and Siddique [41]. Further comparisons are also made to the PPCEM and VBPDM in the later stages of our study, and conclusions are made on the performance of our method in terms of the level of commonality obtained, the objective function value, and the computational effort needed for making platform configuration decisions.

## 4.1. Introduction

As indicated in the literature review, product family design is an efficient strategy for increasing the manufacturing cost savings through commonalizing the components/variables or functions in different products, while attempting to maximize the diversity in order to gain more market shares. Product family includes a group of related products, called variants, which are differentiated from a group of common functions, components, modules, or sub-systems (i.e., a platform) to serve different market segments' needs. The challenge in designing a product family relates to the increased complexity resulting from the added task of finding the components to be shared, and assigning them common values that would increase commonality among family members without sacrificing their individual performance [69].

Many studies have imposed restrictions such as pre-determined platform architecture, assuming single-platform cases in which, each platform variable is either shared across the entire product family or is kept unique for each variant without any sharing. Our proposed approach does not impose the limitation of pre-determined platform architecture, and finds the optimal configuration based on information about the impact of each variable on the aggregated performance function. It also allows multiple-platform product design, in which the design variables can be shared among any subset of product variants within the family. The approach possesses a number of similarities to the proposed design method developed by Dai and Scott; however, we will show that our proposed method can perform more efficiently for the same test problem, in terms of the aggregated performance of the family, as well as the obtained level of commonality.

The major difference is that our proposed method only requires the function values to decide on the platform configurations (as compared to leveraging gradient-based techniques as some of the references do). Also under the assumption of expensive black-box evaluation, our approach presents greater efficiency due to the use of efficient metamodeling strategy as compared to evolutionary algorithms, which normally require many function calls. Therefore our method can be claimed to be the first of its kind to tackle expensive black-box problems in family design.

To explain this in more detail, it is elaborated on the following two important aspects:

**1. Higher efficiency as compared to population-based algorithms**: Our proposed method is shown to be more efficient than population-based algorithms due to the frugal sampling and knowledge gained through metamodeling. It is thus believed to be applicable to black-box functions with acceptable cost.

**2. Independence from gradient information**: The joint problem adds complexity to the initial problem by defining new variables and new constraints accountable for the sharing cases among the variants. Therefore, relaxation into continuous space is a remedial action to cope with the added complexity of such discrete commonality variables. As noted by Khajavirad and Michalek [38], "*while GAs (Genetic*

*algorithms) offer global search, their stochastic nature limits the ability to ensure local or global optimality, and requires significant time for parameters tuning. Therefore, for cases where variant design can be analytically formulated, gradient-based methods are preferred in that they guarantee at least local optimality and global optimality for convex problems, and are computationally efficient.*" This obviously indicates on the need for either population-based methods, or shifting to a gradient-based optimization method. Since the method proposed in this dissertation not only does not add further variables for potential sharing cases, but also does not need the problem to be analytically formulated, therefore, use of gradient-based methods is not necessary and the method can be applied to black-box problems with less difficulty.

Among other developed approaches that are explained in Section 2.3, CP3 [34] is of superiority in terms of its greedy look to performance optimization. However, while the CP3 framework can be generally applied to all types of design problems such as MDINLP, but its required number of evaluations and complexity will be remarkable due to the added commonality variables/constraints, which is a challenge for black-box type of problems. In the best case, an approximation of the black-box shall be provided for further proceeding with that approach. Therefore, our proposed approach and CP3 framework differ from each other in terms of their challenges when being applied to black-box design problems.

There are limited studies addressing the family design for black-box problems. The work by Fellini et al. [70] leveraged a surrogate model for designing a family of three automotive engines, by using radial basis function artificial neural network and sampling from a Latin Hypercube design of experiments. Also, Fellini et al. [45] have recommended approximating three to four-variable simulations (for automotive powertrain models) and using Kriging approximations towards generating Pareto sets and optimizing the power train family. The other notable study is Simpson et al. work [71], which employed second order response surface models to approximate the mean and standard deviation of performance parameters towards robust design of a family of aviation aircraft. This approach focuses on designing scalable families through minimization of the noise that is the variations in the scale factor.

## 4.2. The proposed method

The following steps form the proposed method in this dissertation:

1. *Individual optimization of the variants*

   Through optimizing each variant, the set of optimal values for each variable as well as the optimal values of the performance function are obtained for further use in later stages of platform configuration.

2. *Sensitivity and correlation (detachability) analysis*

   Through applying the RBF-HDMR and RS-HDMR meta-modeling techniques, the information about sensitivity of each variable and its quantified correlation with other variables will be obtained and will be used for platform candidate set selection.

3. *Platform candidate set selection*

   Decision points will be determined to allow selection of appropriate variables for sharing, by selecting the variables with desired sensitivity value and level of correlations.

4. *Platform members and value(s) selection*

   The decision on single vs. multiple platforms and the preferred value for each platform or sub-platform will be made, based on a proposed partitioning strategy.

5. *Entire family design optimization*

   The selected platform and sub-platforms values are fixed, the family variants design will be optimized with the remaining variables

6. *Performance evaluations*

   The family performance will be compared to the individual performance of each variant.

   If the performance loss is unacceptable, the variable with the highest sensitivity is excluded from the platform set and the variants are optimized with the new set of

scale variables. This procedure is repeated until the desired performance is obtained for the whole family.

The proposed method has common steps with a number of the existing methodologies, including the initial and Steps 5 and 6. However, as a result of applying the differentiating steps of this methodology, the obtained platform configurations and the family design solutions would be different from the literature. The flowchart of this approach is shown in Figure 4-1.

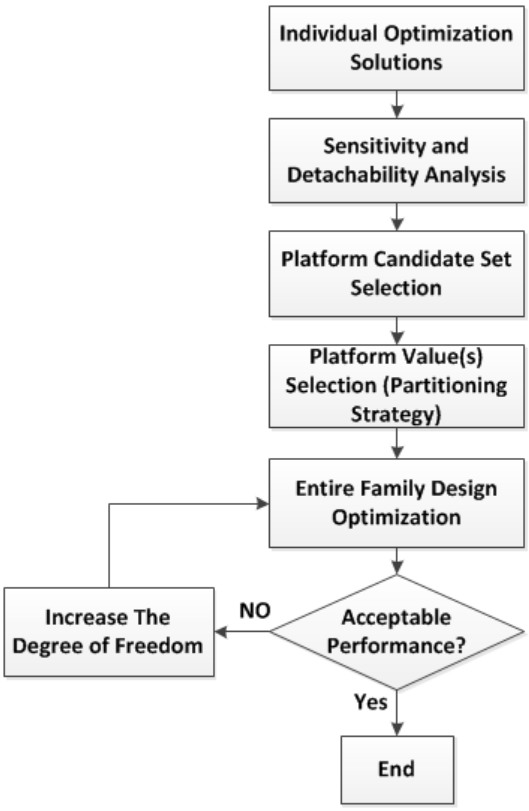


**Figure 4-1: Flowchart of the proposed family design method**

## Step 1: Individual optimization of variants

The general form of the design optimization problem is:

$$\forall\, i = 1,2,..,m \tag{4-1}$$

Find $x^i = \{x_1^i, x_2^i, \dots, x_k^i\}$

To minimize $AOF(x^i, p^i)$

*s.t.:*

$$g_j(x^i, p^i) < 0, j = 1,2, \dots, n$$

$$x_L^i \le x^i \le x_U^i$$

This definition is adopted from [27], and the aggregated objective function (AOF) is a scalar function that aggregates the preference functions of the problem, combining the multiple performance objectives and integrating all different performance targets into a single objective function, so that a measure of overall performance for each design solution can be obtained. $g_j(x^i, p^i)$ represents the design constrains on the ith product in the family, and $x_L^i$ and $x_U^i$ are the lower and upper bounds for a given design variable,

### *Aggregated Objective Function (AOF)*

The adopted AOF in this study is the same as the AOF used in Dai and Scott's study, following the form of:

$$\mathcal{P}_s = \left(\frac{\omega_1 {\alpha_1}^s + \omega_2 {\alpha_2}^s}{\omega_1 + \omega_2}\right)^{1/s} \tag{4-2}$$

Where $\omega_1$ and $\omega_2$ are is the relative importance of each preference function $\alpha_i$; $s$ is a measure of level of compensation; and $\mathcal{P}_s$ is the aggregated preferences function which has included all the objectives of interest into a single objective function. As noted by Dai and Scott [27], adjustment of the set of these decision parameters (i.e., **p** = $\omega_1$, $\omega_2$, $s$, $\alpha_1$, $\alpha_2$ )

will result in the best platform decision. However, the efficacy of the method does not depend on an optimized set of such parameters. The selected values for the test problem in our study are adopted from the same research study, as follows:

$$\begin{aligned} \omega_1, \omega_2 &= (0.5, 0.5) \\ s &= -1 \end{aligned} \tag{4-3}$$

The preference functions $\alpha_\eta$ and $\alpha_M$ will be explained for the used test problem in later sections.

## Step 2: Platform candidates set selection

### *2-a) RBF-HDMR*

The technique used in this stage is driven from the method proposed by the authors for decomposing HEB (high dimensional expensive black-box) functions. The main strategy and techniques for this part are briefly presented in this section.

In many of the physical systems and phenomena, the system output is dependent on several input variables. For many systems, such dependencies might be unknown and finding the structure of such relations can be quite challenging. The widely used technique for addressing this issue is interpolation of a mathematical model based on sampling a number of output points. However, the required number of samples grows exponentially in order to obtain the desired modeling accuracy, and extensive sampling can impose remarkable computational costs to the system. High Dimensional Model Representations (HDMR) follows the general form of:

$$\begin{aligned} f(x) = f_0 + \sum_{i=1}^{d} f_i(x_i) + \sum_{1 \le i < j \le d} f_{ij}(x_i, x_j) + \sum_{1 \le i < j < k \le d} f_{ijk}(x_i, x_j, x_k) + \cdots \\ + \sum_{1 \le i_1 < \cdots < i_l \le d} f_{i_1 i_2 \cdots i_l}(x_{i_1}, x_{i_2}, \cdots, x_{i_l}) + \cdots + f_{12\cdots d}(x_1, x_2, \cdots, x_d) \end{aligned} \tag{4-4}$$

where $f_0$ is a constant value, representing the zero-th order effect on $f(x)$. $f_i(x_i)$ is the first-order effect, i.e., the effect of the variable $x_i$ acting independently on the output $f(x)$, which

can be linear or non-linear. Second-order effect $f_{ij}(x_i, x_j)$ is the residual correlated contribution of variables $x_i$ and $x_j$ on $f(x)$ after accounting their first-order contributions through the first-order components. Other correlated effects are represented similarly by the corresponding components. A fundamental feature of HDMR expansion is that the component functions are orthogonal and are the optimum reflectors for the input contribution to the output. In practice, it is shown that in most of the cases, high-order component functions have small effects and the HDMR expansion can be reduced to a second-order expansion [72].

$$f(x) = f_0 + \sum_{i=1}^{d} f_i(x_i) + \sum_{1 \le i < j \le d} f_{ij}(x_i, x_j) \tag{4-5}$$

The RBF-HDMR leverages the RBF function to model each of the component functions in the HDMR model [73]. Test points are used to identify the needed component function and then sample points are added adaptively until the desired accuracy is achieved. In this way, when there is no correlation between two specific variables, the corresponding component is not built in the model and there is no need to sample in the corresponding sub-space.

## Sensitivity and Detachability Analysis

The strategy of our proposed PFD method starts from modeling the black-box function by the RBF-HDMR technique, and then the RS-HDMR is used for easing the calculation of sensitivity indices that were introduced by Sobol [74], and Alis and Rabitz [75]. The existing studies on RBF-HDMR show that the variable correlations and the relative strengths of the correlations are estimated well by this technique [67]. The HDMR component functions are built one-by-one from one-dimensional to *L*-dimensional components based on the complexity of the problem, and the sampling for the corresponding lines, planes and hyper-planes are continued until a pre-defined accuracy is met. Based on the obtained information, the variables with sufficiently low sensitivity can be selected as platform candidates. Other pieces of information that are useful for platform

candidate set selection include the correlations of each variable to the rest of variables. This parameter can show the variables that are more isolated and have less mutual effect with the rest of variables, and in case that a variable has low sensitivity and low correlations, it can be one of the most appropriate candidates to be considered for platform configuration. Also the coefficient of variation is leveraged for the vector of individual optimal values of each variable, in order to identify the relative freedom of sharing that variable vs. sharing other variables. Among the platform candidate set members, the variables with lower coefficient of variation are better candidates to take common values, indicating that less performance loss would result from sharing that variable.

In comparison to other meta-modeling approaches, RBF-HDMR can significantly reduce the number of expensive function calls (i.e., simulations) for constructing the meta-model of HEB problems, thus reducing the computational intensity. RBF-HDMR helps to reveal the functional form of the black-box function, and provides qualitative information about the variable correlations [76]. The authors developed an strategy called "decomposition of HEB problems through quantified correlation" to tackle the HEB challenge by quantifying the variables correlations for "black-box" objective function, and then used such information toward decomposing and optimizing HEB problems. The proposed method is shown to overcome the limitation of RBF-HDMR for decomposition in [67] through capturing the information about the most important input variables and correlations. The strength of the variable correlations is obtained by applying the Sobol sensitivity analysis method to the RBF-HDMR meta-model. The main novelty of this part is performing sensitivity analysis on basis of the variable structure uncovered by RBF-HDMR. Empirical results show that the results of sensitivity analysis on RBF-HDMR meta-model are sufficiently close to those implemented on the black-box function [67].

### *2-b) Obtaining the sensitivity information*

For the sensitivity analysis, RS-HDMR meta-model is built and its component coefficients are used to calculate Sobol sensitivity indices [75]. The sensitivity indices are used as the input in a two dimensional matrix, $S$, in which the diagonal components represent the variables intensities (their independent impact on the performance), and the

off-diagonal components show the intensities of the variable correlations. Note that although the RBF-HDMR meta-model is built for all of the existing orders of correlations, the sensitivity analysis is performed on the second order, and the higher orders are neglected, following the observations in [72, 77], i.e., the less important correlations are removable and smaller sub-problems can be obtained to reduce the computational cost. The efficiency of this approach has been evaluated for eight problems in [67] and according to the comparisons presented in that study, the proposed decomposition-based optimization technique is of high efficiency in terms of accuracy of modeling and the number of needed function calls. The same idea has been used in the product family design study here, for identifying the variables with the lowest to highest impact on the objective function. The variables with sufficiently low sensitivity are candidates for entering a platform and taking a shared value to enable commonalization.

The required steps and decisions for platform candidate selection are as follows:

a) Sensitivity Indices ranking: Based on the heuristically determined sensitivity index (SI) threshold, the variables for which the average SI value (ASI) is lower than the $\boldsymbol{ASI_{min}}$, are selected and recorded as a platform candidate set. This set is called set #1.
b) Detachability ranking: Since the variables with small correlations to other variables can have small mutual effects on the objective function and are more isolated with more independence from other variables, paying attention to the correlations can help to reduce the performance loss through commonalization. Through sorting the global correlation measures in a non-descending order, the variables with sufficiently low correlation to the rest of variables are identified and recorded as the second platform candidate set (set #2).
c) Ultimate candidate set selection: The intersection of these two sets will result in the finalized set of variable candidates for platform configuration. Such variables are guaranteed to result in the least possible performance loss in case of commonalization, as well as their little impact on the design, if being considered as a constant and excluded from the variables set.

d) The ultimate set will be sorted in non-descending order of the GSI values, and will be assessed for commonalization based on the partitioning strategy that will be presented in the next step.

### Step 3: Platform value(s) determination

The basic idea to determine the common value for each candidate variable is to leverage the coefficient of variation (CV) parameter information. The CV for a single variable aims to describe the dispersion of the variable in a way that does not depend on the variable's measurement unit. This idea is taken from the robust design principles which have been addressed and applied to the product family design by Simpson et al. [71]. Although this idea is used here with some modification and simplifications, the main logic behind both are the same, i.e., to attempt to keep the mean of the new design as close as possible to the target mean, and to minimize the deviation in separate goals. The robust design in their study attempts to adjust some control factors through a compromise decision support problem (DSP). However, since it is necessary to commonalize the platform candidates among the appropriate variants, and since the attempt is to achieve the minimum performance loss, the idea of using the standard deviation and mean of the individual optimal values are adopted from [71] and modified for suiting our purposes in this study.

The coefficient of variation is preferred to the standard deviations in this study and the reason is that the standard deviations of two variables cannot be compared to each other meaningfully to determine which variable has greater dispersion. As a result, since the design variables are of different units and fall within a diverse range of design bounds, in order to be able to treat them equally in the platform candidate selection procedure (as well as the platform value determination decisions), CV is calculated for each candidate, taking the individual optimal values for that variable into account. Let the matrix $P$ represent the optimal values for the design variables ($j=1\ldots, m$) over the entire family of $p$ products, obtained from the first step when no platform has been used.

$x_i^{*j}$: *The optimal value of i$^{th}$ product for the j$^{th}$ variable*

$$P = \begin{bmatrix} x_1^{*1} & \cdots & x_1^{*m} \\ \vdots & \ddots & \vdots \\ x_p^{*1} & \cdots & x_p^{*m} \end{bmatrix} \quad (4\text{-}6)$$

The equation of this parameter is shown in Equation (4-7):

$$\mathrm{CV} = \frac{\sigma}{\mu} * 100\% \quad (4\text{-}7)$$

$$CV = \left[\frac{\sigma(:,1)}{\mu(:,1)} * 100\% \quad \cdots \quad \frac{\sigma(:,m)}{\mu(:,m)} * 100\%\right] \quad (4\text{-}8)$$

Where $\sigma$ and $\mu$ are the standard deviation and mean operators, respectively. A higher value of this parameter indicates more dispersion of the vector values. Since the units of the standard deviation and mean of a variable are the same, taking the ratio of these two cancels the units.

By using this parameter as a reference for the platform member selection, the commonalization scheme is expected to result in the least possible deviation of the variants from their individual optimal value. This strategy allows single platform configuration for the variables with sufficiently low CV value, and attempts to identify the minimum number of multiple platforms with a desired average CV after clustering. This strategy is referred to here as the optimal partitioning strategy, which includes a clustering step, and then assigning the desired value to each platform or sub-platform.

### *3-a) Clustering for determining the platform members*

The tool used for clustering for multiple platforms is the *k*-means clustering analysis. This technique is popular for cluster analysis in data mining, which partitions the observations into k clusters. This technique allows clustering a set of data into k

clusters, and the clusters are formed through an iterative algorithm that minimizes the sum of distances from each object to its cluster centroid, over all clusters. The algorithm finds a partition in which objects within each cluster are as close to each other as possible, and as far from objects in other clusters as possible. Each observation or data point is treated as an object with a location in space, and each resulting cluster has a centroid, to which the sum of distances from all objects in that cluster is minimized [78]. Different measures can be used to compute cluster centroids, and k-means minimizes the sum with respect to the specified measure. The objects are moved between clusters by this technique until the sum cannot be decreased further. The result is a set of clusters that are as compact and well-separated as possible.

In order to decide the best value assigned to each single platform and sub-platform, the individual optimal values from the first step are used for considering different clusters and identifying the best number of clusters that would result in the desired average coefficient of variation. As mentioned earlier, the main basis for deciding on the platform configurations is the ASI. As per our set strategy, for a member of the platform candidate set that has a GSI value less than 0.025, the single platform configuration is suggested in our approach. For the variables with $\mathrm{ASI} \in [0.025, 0.05]$, the clustering analysis will be performed and the smallest possible number of sub-platforms will be selected. It should be noted that the GSI range is depending on the problem under study, and the decision points are heuristically determined for the applied test problem.

In order to achieve the optimum platform configuration, the sub-platform members are selected such that the average of ***sub-CV*** *values (i.e.,* the new CV values for the resulting clusters) will be less than a particular value. Through applying this criterion, for each of the variables under consideration, the proximity of the sub-platform members' value to their individual optimal value is guaranteed. Also, the unnecessary granulation of the platform can be avoided through starting from one cluster and considering more clusters until meeting the stop criteria. Since more sharing is desired for commonality improvement objectives, as soon as a desired level of reduction in the total CV is obtained (i.e., the stop criterion for the clustering section), the partitioning or clustering can be terminated.

If the average ***sub-CV*** *values* is not sufficiently reduced until several clusters are considered, the underlying variable is excluded from platform set and will be considered as a scale variable for preserving performance of the variants. Two reasons can be noted for this decision:

1) It is assumed that there is little advantage having too many sub-platforms, each consisting of very few variants, since it defeats the purpose of product family design. For instance, if five clusters are allowed for a 10-variant family, the number of possible values for each variable is then reduced from ten to five. If considering only one variable, the number of set-ups for manufacturing the 10-variant family will be reduced by 50%. Therefore, when the clustering analysis does not result in the expected CV reduction, it indicates that commonalization would be of little or no benefit and the performance loss would be too much to commonalize that variable. This $Sub\text{-}CV_{min}$ value can be fine-tuned for the best trade-offs in terms of production cost and commonality target.

2) In case of having chosen an inappropriate candidate variable from Step 2, the assessment of the average CV value can reveal the nature of the variable and thus avoid commonalization of this variable.

### *3-b) Platform and sub-platform values determination*

Recall that the partitioning strategy uses k-means algorithm to cluster the individual optimal values (of the multiple platform candidates) into different number of clusters, and for each variable under study, the variants in each sub-platform are determined based on assessment of the average coefficient of variation.

To illustrate the procedure of selecting a common value for each sub-platform (i.e., a set of variants sharing a variable), the following mathematical presentations are necessary. Let the matrix *P* represent the optimal values for the variants from the first step. The sensitivity vectors for each product are obtained through the RBF-HDMR and RS-HDMR, and those vectors are then collected into a matrix we call Sensitivity Index or SI:

$$SI = \begin{bmatrix} SI_1^{*1} & \cdots & SI_1^{*m} \\ \vdots & \ddots & \vdots \\ SI_p^{*1} & \cdots & SI_p^{*m} \end{bmatrix} \quad (4\text{-}9)$$

For the test problem of this study, there are eight variables and ten product variants, therefore the matrix P will have ten rows and eight columns.

For a given variable $x_i$, assume that the following clusters are suggested through the partitioning scheme, which is shown as an example below with 2 clusters or sub-platforms:

$$subplatform1 = \{\mathbf{P1}, \mathbf{P2}, \ldots, \mathbf{P(i)}\}$$

$$subplatform2 = \{\mathbf{P(i+1)}, \mathbf{P(i+2)}, \ldots, \mathbf{P(p)}\}$$

According to this information, now two values should be determined for $x_i$, one to be shared by the first five products, and the second one as the platform value for products number six to ten. The common value for the corresponding variants (in the first sub-platform) are selected from the following set of values:

$$W = \{ W_1^1 = \frac{(\sum_{k=1}^{5} SI_k^i * x_k^{*i})}{\sum_{k=1}^{5} SI_k^i};\ W_1^2 = \frac{(\sum_{k=1}^{5} x_k^{*i})}{5};$$
$$W_1^3 = centroid;\ W_1^4 = \underset{x_k^{*i}}{\arg\max}\, SI_k^i\ , (k = 1\ to\ 5)\} \quad (4\text{-}10)$$

The common value for the corresponding variants in each sub-platform for a platform variable are selected from the following set W including the cluster centroid, a weighted sum of members (i.e., the local sensitivity indices are used as weights), the average of optimal values, and the individual optimal value of the variable, for the variant that has the highest local sensitivity in that sub-platform. The platform/sub-platform will take the value shown in Equation (4-12).

$$For\ z = 1\ to\ 4:$$

$$SUM_z = \sum \left| W_1^z - X_{subplatform1}^{*1} \right| \tag{4-11}$$

$$x_{subplatform1}^{*1} = \underset{W_1^z}{\arg\min} Sum_z \tag{4-12}$$

$X_{subplatform1}^{*1}$ represents the vector of optimal value of $x_1$ in the first sub-platform which includes five variants. $SUM_z$ is the summation of the absolute value difference between $W_1^z$ and each member of the sub-platform vector. Equation (4-12) shows which option among the four candidates, $W_1^z$ $(z = 1 \dots 4)$, will be selected as the common value for $x_1$ in the first sub-platform. A flowchart of the whole partitioning and commonalization strategy is shown in Figure 4-2. The steps are numbered to show the order of proceeding through the flowchart.

### Step 4: Entire family design optimization

After obtaining the optimal configuration and the values assigned to the platform variables, the design problems with a fewer number of variables will be obtained for each variant, which will be optimized similar to Step 1, with the following problem definition:

$\forall\ i = 1,2,..,p$ *and given the fixed platform from Step 3*

Find $x_{non-platform(NP)}^{i} = x_{NP_1}^{i}, x_{NP_2}^{i}, \dots, x_{NP_{m-N}}^{i}$

To minimize $AOF(x^i, v^i)$

*S.T.:* (4-13)

$$g_j(x^i, v^i) < 0, j = 1,2, \dots, n$$

$$x_L^i \leq x^i \leq x_U^i$$

Where $x_{NP}^i$ is the non-platform variable for the *ith* variant, and *N* is the number of platform variables that are now fixed.

### Step 5: Performance evaluation

The obtained objective function value of each variant will be compared to the individual optimal target values and if the performance change is within the allowed range (i.e., maximum of 10% loss according to the previous studies for the same design problem), the design can be accepted for the family.

In case of violating the performance requirements (obtaining infeasible design), the following strategy will be implemented until a feasible design is obtained:

(1) Considering multiple sub-platforms instead of a single platform, adjust the value of individual variable in order to reduce the variation from the individual optima among the new sub-platform members.

(2) Increase the degree of freedom by adding to the number of non-platform variables, i.e., excluding the last member in the platform candidate set, and optimizing the variant with the new set of non-platform variables.

In summary, this chapter provided the details of the proposed product family design methodology of this dissertation, which is different from the existing methods from two aspects, i.e., leveraging a meta-model based sensitivity analysis technique, which results in less number of function evaluations needed, and applicability to simulation-based design problems which are expensive and complex to handle by other existing PFD methodologies.

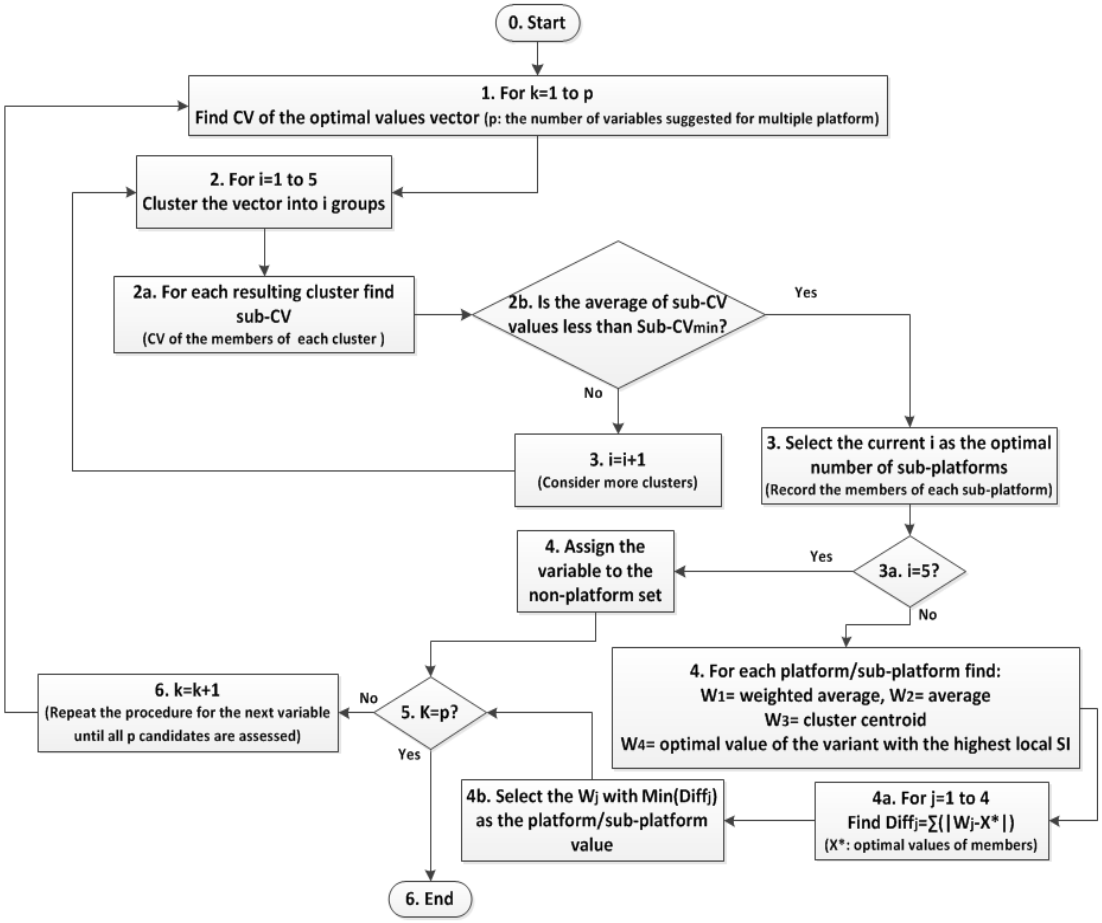


**Figure 4-2: The partitioning strategy for finding platform members and values**

In the next chapter, this methodology will be applied to a test problem, and its performance will be discussed from aspects such as the percentage of performance loss as well as the obtained commonality.

# Chapter 5. Application of the proposed PFD method to universal electric motors family design

In this chapter, the performance of the proposed approach in Chapter 4 is tested by designing a family of scalable products. A family of universal electric motors with a scalable product platform includes ten universal electric motors, which are supposed to meet ten market segments' needs by affording specific power and unique torque values for each variant. The desired market segmentation grid is created by Simpson et al. [30] for this problem, and the same definitions and design ranges are adopted here. The entire problem specifications can be found in Appendix A.

Since ten separate preference functions exist for mass depending on the torque requirement, the objective function of each product in the family will be unique. The mass preference for each motor indicates that the closer the mass value gets to the value shown in row two of Table 5-1 (adopted from the literature), the higher value is obtained for the mass preference function, and considered completely satisfactory, while any mass above the value shown in the third row of the table for that variant is of no preference and considered unacceptable. These limits are determined based on different torque requirements, with 0.05 added to both upper and lower limit [27].

**Table 5-1: Mass range for different torques (Kg)**

| Variant | 1 | 2 | | 4 | 5 | 6 | 7 | 8 | 9 | 10 |
|---|---|---|---|---|---|---|---|---|---|---|
| **Best** | 0.25 | 0.3 | 0.35 | 0.4 | 0.45 | 0.5 | 0.55 | 0.6 | 0.65 | 0.7 |
| **Worst** | 1.75 | 1.8 | 1.85 | 1.9 | 1.95 | 2.0 | 2.05 | 2.1 | 2.15 | 2.2 |

The preference functions derived from the performance targets are defined as follows:

## 5.1. Application of the methodology

As explained in later parts of section 4.2, in order to integrate various objectives of interest into a single objective function, the aggregated objective function (AOF) concept is used here as well, which allows defining preference functions for each objective of interest, and then integrating them into a single statement through use of weights for each preference function, as well as applying a parameter called level of compensation (*s*).

### Preference functions (α):

Efficiency (η):

$$\alpha_{\eta} = \frac{\eta - 0.15}{0.7 - 0.15} \tag{5-1}$$

Mass (M):

Depending on the desired torque for the motor, the acceptable range of mass will be different, as Table 5-1 shows. The preference function follows Equation (5-2).

$$\alpha_{M} = \frac{M_{worst} - M}{M_{worst} - M_{best}} \tag{5-2}$$

### Step 1: Individual optimization of variants

At this step, each variant is optimized for its specific objective function. The abbreviations used over the rest of the paper are shown in Table 5-2.

**Table 5-2: The abbreviations used for the proposed approach details**

| | | | |
|---|---|---|---|
| *m* | *Number of variants in the family* | *SI* | *Sensitivity Index* |
| *n* | *Number of constraints* | *QC* | *Quantified Correlation* |
| *k* | *Number of design variables* | *CV* | *Coefficient of Variation* |

The algorithm used for optimizing the variants is Sequential Quadratic Programing (SQP) and the results of individual optimizations are shown in Table 5-3.

**Table 5-3: Individual variant design optimization solutions**

| Variant ---------- | P1 | P2 | P3 | P4 | P5 | P6 | P7 | P8 | P9 | P10 |
|---|---|---|---|---|---|---|---|---|---|---|
| $N_c$ | 144 | 155 | 159 | 162 | 164 | 165 | 165 | 165 | 164 | 159 |
| $N_s$ | 324 | 413 | 443 | 467 | 500 | 500 | 500 | 500 | 500 | 500 |
| $A_{wa}$ | 0.2586 | 0.2639 | 0.2703 | 0.2762 | 0.2812 | 0.2813 | 0.2836 | 0.2855 | 0.2879 | 0.2899 |
| $A_{wf}$ | 0.2586 | 0.2640 | 0.2703 | 0.2762 | 0.2812 | 0.2813 | 0.2836 | 0.2855 | 0.2879 | 0.2899 |
| $r_0$ | 17.338 | 20.02 | 21.08 | 21.96 | 23.29 | 24.38 | 25.31 | 26.19 | 26.90 | 28.05 |
| $t$ | 4.2896 | 5.2437 | 5.6543 | 5.9787 | 6.3827 | 6.4764 | 6.5883 | 6.7481 | 6.866 | 7.06**7** |
| $I$ | 3.0314 | 3.2485 | 3.3314 | 3.4062 | 3.5670 | 3.7142 | 3.8569 | 3.9931 | 4.127 | 4.439 |
| $L$ | 18.897 | 21.278 | 22.054 | 22.793 | 24.302 | 26.571 | 28.521 | 30.08**4** | 31.59 | 33.94 |
| $\eta$ | 0.8605 | 0.8030 | 0.7830 | 0.7658 | 0.7313 | 0.7023 | 0.6763 | 0.6532 | 0.6320 | 0.5876 |
| $M$ | 0.2960 | 0.4347 | 0.4968 | 0.5547 | 0.6509 | 0.7396 | 0.8215 | 0.8991 | 0.9717 | 1.0899 |
| AOF | 1.2805 | 1.1821 | 1.1433 | 1.1082 | 1.0447 | 0.9883 | 0.9376 | 0.8905 | 0.8467 | 0.7669 |

Sensitivity index values for each variable in each variant are obtained through building the RBF-HDMR meta-model of the objective function, and then performing the sensitivity analysis on the RS-HDMR model, and modifying the Sobol sensitivity indices to quantify the correlations. The values for each variant are obtained from the diagonal elements of the matrix S which is representing the variation explained by each variable. An average SI is calculated for each variable afterwards, which is the average of the ten local SI values. The obtained local and average SI's are presented in Table 5-4. The design variables of interest and the ranges include:

1. Number of turns of wires on the armature ($100 \leq N_c \leq 1500$) turns
2. Number of turns of wire on each field pole ($1 \leq N_s \leq 500$) turns
3. Cross-sectional area of the wire used on the armature ($0.01 \leq A_{wa} \leq 1.0$) $mm^2$
4. Cross-sectional area of the wire used on the field poles ($0.01 \leq A_{wf} \leq 1.0$) $mm^2$
5. Radius of the motor ($10 \leq r_0 \leq 100\ mm$)
6. Thickness of the stator ($0.5 \leq t \leq 10\ mm$)

7. Current drawn by the motor ($0.1 \leq I \leq 6.0\ Amp$)
8. Stack Length ($1 \leq L \leq 100\ mm$)

## Step 2: Platform candidates set selection

The information about correlations and mutual effect of variables is also used in the selection of candidates for platform configuration. The variables with small correlations to the rest of variables can be more freely detached from other variables, and assuming a fixed value for them will have less significant impact on the performance or objective function, as compared to a variable that is highly correlated to the rest of design variables. The off-diagonal elements of matrix *S* represent the correlations among variables. The quantified correlations are presented in Table 5-5. This information can be used toward selecting candidates to form a platform. Variable 7 is the current, so it is excluded from platform candidate considerations, since it is a state variable rather than a manufacturing variable. In other words, there is no manufacturing advantage in holding current as a platform [41].

**Table 5-4: Local and Average sensitivities of variables**

| Design Variable | $N_c$ | $N_s$ | $A_{wa}$ | $A_{wf}$ | $r_0$ | $t$ | $I$ | $L$ |
|---|---|---|---|---|---|---|---|---|
| **SI(1)** | 0.0022 | 0.0199 | 0.0112 | 0.0266 | 0.0737 | 0.0058 | 0.1344 | 0.0603 |
| **SI(2)** | 0.0213 | 0.0444 | 0.0133 | 0.0233 | 0.0717 | 0.0216 | 0.1742 | 0.0479 |
| **SI(3)** | 0.0214 | 0.0431 | 0.0133 | 0.0256 | 0.0722 | 0.0217 | 0.1675 | 0.0495 |
| **SI(4)** | 0.0216 | 0.0421 | 0.0134 | 0.0280 | 0.0727 | 0.0218 | 0.1617 | 0.0511 |
| **SI(5)** | 0.0217 | 0.0411 | 0.0134 | 0.0302 | 0.0732 | 0.0219 | 0.1565 | 0.0526 |
| **SI(6)** | 0.0217 | 0.0402 | 0.0134 | 0.0324 | 0.0737 | 0.0220 | 0.1519 | 0.0540 |
| **SI(7)** | 0.0218 | 0.0395 | 0.0134 | 0.0345 | 0.0741 | 0.0221 | 0.1478 | 0.0554 |
| **SI(8)** | 0.0219 | 0.0388 | 0.0134 | 0.0366 | 0.0745 | 0.0222 | 0.1441 | 0.0568 |
| **SI(9)** | 0.0219 | 0.0382 | 0.0135 | 0.0386 | 0.0749 | 0.0223 | 0.1408 | 0.0581 |
| **SI(10)** | 0.0219 | 0.0376 | 0.0135 | 0.0406 | 0.0753 | 0.0223 | 0.1378 | 0.0593 |
| **Average SI (ASI)** | 0.0197 | 0.0385 | 0.0132 | 0.0316 | 0.0736 | 0.0204 | 0.1517 | 0.0545 |

**Table 5-5: Correlations and mutual effects**

| Design Variable | $N_c$ | $N_s$ | $A_{wa}$ | $A_{wf}$ | $r_0$ | $t$ | $I$ | $L$ |
|---|---|---|---|---|---|---|---|---|
| **QC(1)** | 0.0123 | 0.0175 | 0.0129 | 0.0177 | 0.0139 | 0.0201 | 0.0173 | 0.0201 |
| **QC (2)** | 0.0123 | 0.0175 | 0.0129 | 0.0177 | 0.0138 | 0.0200 | 0.0173 | 0.0200 |
| **QC (3)** | 0.0123 | 0.0174 | 0.0129 | 0.0177 | 0.0138 | 0.0200 | 0.0173 | 0.0200 |
| **QC (4)** | 0.0122 | 0.0174 | 0.0129 | 0.0176 | 0.0137 | 0.0199 | 0.0172 | 0.0199 |
| **QC (5)** | 0.0121 | 0.0173 | 0.0128 | 0.0176 | 0.0136 | 0.0198 | 0.0172 | 0.0198 |
| **QC (6)** | 0.0121 | 0.0173 | 0.0128 | 0.0175 | 0.0135 | 0.0197 | 0.0171 | 0.0197 |
| **QC (7)** | 0.0120 | 0.0172 | 0.0128 | 0.0174 | 0.0134 | 0.0196 | 0.0170 | 0.0196 |
| **QC (8)** | 0.0119 | 0.0171 | 0.0127 | 0.0173 | 0.0133 | 0.0195 | 0.0169 | 0.0195 |
| **QC (9)** | 0.0118 | 0.0170 | 0.0126 | 0.0172 | 0.0132 | 0.0194 | 0.0168 | 0.0194 |
| **QC (10)** | 0.0117 | 0.0169 | 0.0126 | 0.0171 | 0.0131 | 0.0193 | 0.0167 | 0.0193 |
| **Global QC** | 0.0121 | 0.0173 | 0.0128 | 0.0175 | 0.0135 | 0.0197 | 0.0171 | 0.0197 |

## Step 3: Platform value(s) determination

The first part of this step is to find the orders of SI and detachability of the design variables, as well as their coefficient of variation. The information being used toward this decision making stage is shown in Table 5-6.

**Table 5-6: SI, correlation, and Coefficient of Variation- the universal motor problem**

| Parameter | Vector value | Non-descending sorted index of variables |
|---|---|---|
| **ASI** | *[0.0197 0.0385 0.0132 0.0316 0.0736 0.0204 0.1517 0.0545]* | *[3 1 6 4 2 8 5 7]* |
| **Correlation** | *[ 0.0121 0.0173 0.0128 0.0175 0.0135 0.0197 0.017 0.0197]* | *[1 3 5 7 2 4 6 8]* |
| **CV** | *[ 4.12 12.51 3.77 3.76 14.34 13.98 11.91 18.98]* | *[3 4 1 7 2 5 6 8]* |

The selected values to serve as thresholds for SI and QC are presented in Table 5-7 and Table 5-8 respectively. It shall be noted that these thresholds are selected

heuristically and they can be fine-tuned for increasing the robustness of the resulting platform configuration.

**Table 5-7: The applied decision points for platform candidate selection**

| GSI range (for each variable) | Minimum number of clusters to be assessed |
|---|---|
| *ASI<0.025* | All-or-none platform case |
| *0.025<ASI<0.05* | Determined through optimizing the partitioning scheme |
| *0.05<ASI* | Non-platform |

**Table 5-8: Decision points for platform candidate selection**

| Correlation measure range (for each variable) | Minimum number of clusters to be assessed |
|---|---|
| *QC≤0.0175* | Eligible for platform configuration consideration |
| *0.0175< QC* | Non-platform variable |

Based on the values shown above, the following sets of variables are created:

Platform candidate set#1: [X3 X1 X6 X4 X2 X8]

Platform candidate set#2: [X1 X3 X5 X7 X2 X4]

Intersection of set# 1 & 2: [X1 X2 X3 X4]

As presented in Table 5-9, variables 5, 6, 7, and 8 will be non-platform variables. Variables 1 and 3 are assigned to a single platform, since their GSI values are less than 0.025. ASI. Also, variables 2, and 4 are assessed as candidates of multiple platform configurations due to higher sensitivity. Their optimal number of clusters is determined based on the partitioning strategy of Figure 2, which is obtained through clustering until the resulting average CV of the clusters is less than 0.65 of the initial CV for that variable.

**Table 5-9: The determined number of platform/sub-platforms for the proposed method**

| Variable | Number of clusters to be assessed |
|---|---|
| *1,3* | All-or-none platform |
| *2,4* | 2 |
| *5,6,7,8* | Scale variable |

Table 5-10 shows the selected values for each platform/sub-platform, and the members of each sub-platform. As mentioned earlier, the preferred value for a platform or sub-platform is selected from the list of average, weighted average (based on local sensitivity indices), cluster centroid, and the optimal value of the variant with highest sensitivity in each cluster. The chosen value is the one that results in the least total absolute differences with optimal individual values of that cluster.

**Table 5-10: Platform configuration based on the proposed partitioning scheme**

| Platform Candidate | $X_1$ | $X_3$ | $X_2$ | $X_4$ |
|---|---|---|---|---|
| **Number of platforms** | Single platform | | 2 | 2 |
| **Platform variants** | | | $P_1$: {$p_1$, $p_2$, $p_3$, $p_4$<br>$P_2$: $p_5$, $p_6$, $p_7$, $p_8$, $p_9$, $p_{10}$} | $P_1$: {$p_1$, $p_2$, $p_3$, $p_4$, $p_5$, $p_6$, $p_7$<br>$P_2$: $p_8$, $p_9$, $p_{10}$} |
| **Platform preferred value** | 162 | 0.2783 | $X_2(P_1)$=412 | $X_4(P_1)$=0.2642 |
| | | | $X_2(P_2)$= 500 | $X_4(P_2)$= 0.2837 |

## Step 4: Entire family design optimization

With the determined platform values, each variant (i.e., family member) can be optimized with less number of variables by setting the values of platform variables to the fixed values determined in Step 3. The same optimization algorithm has been applied to the final stage optimizations as well, that is the SQP algorithm for nonlinear constrained optimization subject to the performance requirements. The entire family design is shown in Table 5-11, along with the obtained efficiency and mass for each variant, and the communalized values are shown in colors.

**Table 5-11: Platform and scale optimized values based on the proposed partitioning scheme**

| Variant ---------- Design Variable | P1 | P2 | P3 | P4 | P5 | P6 | P7 | P8 | P9 | P10 |
|---|---|---|---|---|---|---|---|---|---|---|
| $N_c$ (x1) | 162 | 162 | 162 | 162 | 162 | 162 | 162 | 162 | 162 | 162 |
| $N_s$ (X2) | 412 | 412 | 412 | 412 | 500 | 500 | 500 | 500 | 500 | 500 |
| $A_{wa}$(X3) | 0.2783 | 0.2783 | 0.2783 | 0.2783 | 0.2783 | 0.2783 | 0.2783 | 0.2783 | 0.2783 | 0.2783 |
| $A_{wf}$(X4) | 0.2642 | 0.2642 | 0.2642 | 0.2642 | 0.2642 | 0.2642 | 0.2642 | 0.2837 | 0.2837 | 0.2837 |
| $r_0$(X5) | 19.795 | 20.837 | 21.377 | 21.880 | 23.514 | 24.601 | 25.691 | 25.895 | 26.886 | 28.962 |
| $t$(X6) | 7.455 | 5.7161 | 5.489 | 5.3861 | 6.7820 | 6.9324 | 7.232 | 6.6546 | 6.993 | 7.7845 |
| $I$(X7) | 3.0425 | 3.235 | 3.3196 | 3.4009 | 3.6417 | 3.8120 | 3.981 | 4.0211 | 4.174 | 4.4929 |
| $L$(X8) | 13.371 | 20.095 | 22.938 | 25.496 | 23.686 | 25.811 | 27.329 | 30.500 | 31.391 | 31.963 |
| $\eta$ | 0.8574 | 0.8063 | 0.7858 | 0.7670 | 0.7163 | 0.6843 | 0.6552 | 0.6487 | 0.6250 | 0.5806 |
| $M$ | 0.3017 | 0.4407 | 0.5027 | 0.5611 | 0.6252 | 0.7075 | 0.7827 | 0.8897 | 0.9566 | 1.0749 |
| $f$ | 1.103 | 1.030 | 1.011 | 0.9942 | 0.9508 | 0.9132 | 0.8801 | 0.8539 | 0.8282 | 0.7661 |

## Step 5: Performance evaluation

### *5-a) Comparison to the individual variants design*

Table 5-12 shows the performance change for both efficiency and mass. The positive change in efficiency indicates performance improvement, while a positive change in mass target indicates performance loss over the reference design solution. For almost all of the variants the performance loss is less than 3%, which indicates an allowable level of performance loss.

### *5-b) Comparison to other approaches*

In order to compare the performance of our proposed approach to the existing methods, the percentages of change in mass and efficiency of our proposed family design are compared to the platform design approach through sensitivity and clustering analysis

by Dai and Scott [27], and the platform cascading approach (PCM) proposed by Ninan and Siddique [41].

**Table 5-12: Proposed family solution comparison to the individual optima**

| Motor No. | Individual optima | | Product Family Solutions | | Difference (%) | |
|---|---|---|---|---|---|---|
| | η | M (kg) | $\eta$ | M(Kg) | $\eta$ | M |
| 1 | 0.8605 | 0.2960 | 0.8574 | 0.3017 | -0.3603 | 1.9257 |
| 2 | 0.8030 | 0.4347 | 0.8063 | 0.4407 | 0.4110 | 1.3803 |
| 3 | 0.7830 | 0.4968 | 0.7858 | 0.5027 | 0.3576 | 1.1876 |
| 4 | 0.7658 | 0.5547 | 0.7670 | 0.5611 | 0.1567 | 1.1538 |
| 5 | 0.7313 | 0.6509 | 0.7163 | 0.6252 | -2.0511 | -3.9484 |
| 6 | 0.7023 | 0.7396 | 0.6843 | 0.7075 | -2.5630 | -4.3402 |
| 7 | 0.6763 | 0.8215 | 0.6552 | 0.7827 | -3.1199 | -4.7231 |
| 8 | 0.6532 | 0.8991 | 0.6487 | 0.8897 | -0.6889 | -1.0455 |
| 9 | 0.6320 | 0.9717 | 0.6250 | 0.9566 | -1.1076 | -1.5540 |
| 10 | 0.5876 | 1.0899 | 0.5806 | 1.0749 | -1.1913 | -1.3763 |
| Average Change | | | | | -1.15% | -1.13% |

Since the problem is multi-objective, conclusion on performance of different approaches might not be straightforward, particularly when one or some of the objectives show performance improvement, while there is performance loss in other objective(s). For handling such cases, the family design solution of the previous approaches is plugged into our objective function equation, and used the aggregated preference function (AOF) as defined in Equation (4-2) to enable comparison. The obtained AOF values for solutions of these reference methods are shown in Table 5-13. Table 5-14 shows the comparison of

results between our solution and Dai and Scott's. The details of comparison to Ninan and Siddique's suggested family design are also presented in Table 5-15.

**Table 5-13: The optimal AOF values for the suggested designs in previous publications**

| Author \| variant | P1 | P2 | P3 | P4 | P5 | P6 | P7 | P8 | P9 | P10 |
|---|---|---|---|---|---|---|---|---|---|---|
| Dai and Scott | 1.086 | 0.998 | 0.974 | 0.947 | 0.935 | 0.9067 | 0.8776 | 0.8605 | 0.8352 | 0.7756 |
| Ninan | 1.093 | 1.02 | 1.01 | 0.975 | 0.866 | 0.7998 | 0.760 | 0.729 | 0.701 | 0.660 |

**Table 5-14: Comparison of the proposed family to the solution from [27]**

| Motor No. | Dai and Scott's PFD solution | | Product Family Solutions | | Difference (%) | | |
|---|---|---|---|---|---|---|---|
| | $\eta$ | M (kg) | $\eta$ | M(Kg) | $\eta$ | M | AOF |
| 1 | 0.862 | 0.347 | 0.8574 | 0.3017 | -0.5336 | -13.0548 | 1.5654 |
| 2 | 0.713 | 0.388 | 0.8063 | 0.4407 | 13.0856 | 13.5825 | 3.2064 |
| 3 | 0.70 | 0.425 | 0.7858 | 0.5027 | 12.2571 | 18.2824 | 3.7988 |
| 4 | 0.671 | 0.478 | 0.7670 | 0.5611 | 14.3070 | 17.3849 | 4.9842 |
| 5 | 0.6600 | 0.534 | 0.7163 | 0.6252 | 8.5303 | 17.0787 | 1.6898 |
| 6 | 0.648 | 0.637 | 0.6843 | 0.7075 | 5.6019 | 11.0675 | 0.7169 |
| 7 | 0.626 | 0.717 | 0.6552 | 0.7827 | 4.6645 | 9.1632 | 0.2849 |
| 8 | 0.630 | 0.826 | 0.6487 | 0.8897 | 2.9683 | 7.7119 | -0.7670 |
| 9 | 0.503 | 0.879 | 0.6250 | 0.9566 | 24.2545 | 8.8282 | -0.8381 |
| 10 | 0.560 | 0.988 | 0.5806 | 1.0749 | 3.6786 | 8.7955 | -1.2249 |
| **Average Change** | | | | | + 8.88% | +9.88% | +1.34% |

The summarized results of average percentage of difference for sections A and B are shown in Table 5-16. The performance loss on the efficiency objective is 1.15% on average, while there is a same percentage of reduction on the mass, which is considered as improvement. As a result, this family design solution is acceptable and within allowed

performance loss range. The commonality of this design includes two single platforms and two multiple platforms, each consisting of two sub-platforms.

**Table 5-15: Results of comparing the proposed family to the suggested family solution in [41]**

| Motor No. | Ninan's PFD solution | | Product Family Solutions | | Difference (%) | | |
|---|---|---|---|---|---|---|---|
| | $\eta$ | M (kg) | $\eta$ | M(Kg) | $\eta$ | M | AOF |
| 1 | 0.81 | 0.35 | 0.8574 | 0.3017 | 5.8519 | -13.8000 | 0.9149 |
| 2 | 0.80 | 0.46 | 0.8063 | 0.4407 | 0.7875 | -4.1957 | 0.9804 |
| 3 | 0.78 | 0.50 | 0.7858 | 0.5027 | 0.7436 | 0.5400 | 0.0990 |
| 4 | 0.72 | 0.51 | 0.7670 | 0.5611 | 6.5278 | 10.0196 | 1.9692 |
| 5 | 0.66 | 0.59 | 0.7163 | 0.6252 | 8.5303 | 5.9661 | 9.7921 |
| 6 | 0.63 | 0.66 | 0.6843 | 0.7075 | 8.6190 | 7.1970 | 14.1785 |
| 7 | 0.58 | 0.70 | 0.6552 | 0.7827 | 12.9655 | 11.8143 | 15.8026 |
| 8 | 0.55 | 0.74 | 0.6487 | 0.8897 | 17.9455 | 20.2297 | 17.1331 |
| 9 | 0.49 | 0.76 | 0.6250 | 0.9566 | 27.5510 | 25.8684 | 18.1455 |
| 10 | 0.43 | 0.77 | 0.5806 | 1.0749 | 35.0233 | 39.5974 | 16.0758 |
| **Average Change** | | | | | +12.45% | +10.32% | +9.5% |

In terms of effectiveness (performance improvement), our approach has 8.88% average improvement on efficiency, and has 9.88% loss on average on the mass target. The lost performance is still acceptable based on the rule of thumb adopted from the literature (i.e., less than 10% of loss is allowed), and since the AOF in our proposed approach is on average 1.3% better than Dai and Scott's proposed family solution, it can be concluded that a the Pareto set of our design is of similar level of performance to that design.

Comparison of the proposed design to the PCM approach by Ninan and Siddique [41] results in a similar trend, and a 9.5% better value on average on the AOF values indicates a more desired Pareto set for the solution obtained through the proposed solution. Such

difference between AOFs of the two reference methods can be explained based on the difference in orientation of those approaches.

**Table 5-16: The results of comparing the proposed method to references [27, 41]**

| **Design solution** | **Individual optimal design** | | **Dai and Scott's design** | | | **Ninan's design** | | |
|---|---|---|---|---|---|---|---|---|
| Objective | $\boldsymbol{\eta}$ | M | $\boldsymbol{\eta}$ | M | AOF | $\boldsymbol{\eta}$ | M | AOF |
| % Average difference | -1.15% | -1.13% | + 8.88% | +9.88% | +1.34% | +12.4% | +10.2% | +9.5% |

Dai and Scott's approach is quite conservative and obtains commonality through step-by-step comparisons and performance evaluations, while the PCM method focuses on commonalization through the single-platform strategy and its attempt to cascade new platforms by the minimum variation from the previous single platforms. Therefore, the better performance of our proposed family solution is expected based on our intent of performance-preserving, as compared to the PCM design solution.

## 5.2. Method verification and improvement

In order to find the effect of sensitivity analysis on the performance of the proposed approach, the plan is to design a test scheme, without taking the SI and correlation information into account and using the CV or dispersion information as the only basis for selecting platform candidates and finding platform configuration. This consideration has resulted in the following scheme, called as "commonality-oriented scheme".

Based on the coefficient of variation for the vector of individual values from the first step, the variants with the closest optimal values are selected as the candidates for platform configuration. The flowchart illustrating this scheme details is shown in Figure 3. This test scheme provides higher levels of commonality, and is expected to result in more performance loss over the previous scheme (i.e., performance-preserving). However, the increased commonality is beneficial per se in terms of manufacturing savings it can create. The heuristically chosen thresholds for CV parameter are shown in Table 5-17.

**Table 5-17: The number of platform(s) to assess for commonality-oriented test scheme**

| CV range (for the optimal values vector) | The number of clusters to be assessed |
|---|---|
| $CV_{max}$=10% | All-or-none platform (i.e., to be shared over the entire family) |
| $sub\ CV_{min}^{i} = \frac{2}{3} * (CV_{max})$ | The decision point for clustering assessments termination |
| If 5≤ j | Non-platform |

Since in this scheme all the variables can be assessed for possible sharing, the strategy of Figure 2 is modified and includes decision points to assign a variable into a single or multiple platforms, based on the coefficient of variation information. The modified strategy for this test scheme is presented in Figure 5-1. The optimal number of platforms or sub-platforms to assess is shown in Table 5-18.

**Table 5-18: The number of platform/sub-platforms based on the commonality-oriented test scheme**

| Variable | Number of clusters to be assessed |
|---|---|
| *1,3,4* | All-or-none platform |
| *2,5,6* | 2 |
| *7,8* | Scale variable |

Table 5-19 shows the platform configuration for this scheme, along with the determined platform values. By repeating the same procedure as described for our proposed method here, the obtained results for the entire family optimization are shown in Table 5-20.

As it can be observed, with the chosen fixed values, there is no feasible design obtained for variants 2, 3, 4, 8, 9, and 10. This can be caused by a number of reasons listed as follows:

**Table 5-19: Platform configuration of the variants based on the commonality-oriented scheme**

| **Platform Candidate** | X1 | X3 | X4 | X5 | X6 | X2 |
|---|---|---|---|---|---|---|
| **Number of platforms** | Single platform | | | 2 | 2 | 2 |
| **Platform variants** | | | | $P_1$: {$p_1$, $p_2$, $p_3$} $P_2$: {$p_4$, $p_5$, $p_6$, $p_7$, $p_8$, $p_9$, $p_{10}$} | $P_1$: {$p_1$, $p_2$, $p_3$, $p_4$} $P_2$: {$p_5$, $p_6$, $p_7$, $p_8$, $p_9$, $p_{10}$} | $P_1$: {$p_1$,$p_2$, $p_3$, $p_4$} $P_2$: {$p_5$, $p_6$, $p_7$, $p_8$, $p_9$, $p_{10}$} |
| Platform values | 162 | 0.2783 | 0.2783 | $X_5(P_1)$=20.0898 | $X_6(P_1)$= 5.3116 | $X_2(P_1)$= 412 |
| | | | | $X_5(P_2)$= 25.6820 | $X_6(P_2)$= 6.584 | $X_2(P_2)$=500 |

**A- Permissive or Restrictive Decision points**

Depending on the chosen thresholds for CV, three adverse effects might result:

1. A variable (or more) might be wrongly chosen as platform candidate. In such case, there is a reduction in the degree of freedom for the last stage family design, and there is much more limited design space to search for an optimal design solution.
2. A variable that would be better to form multiple sub-platforms might be wrongly assigned to the single platform set, resulting in more performance loss.
3. A scale variable that would result in significantly more desired performance, would be confined due to its wrong selection as a candidate for multiple platforms.

**B- Inadequate decision parameter(s)**

The other potential reason is that the decisions on platform configuration are made based on incomplete information and considerations, which is a confirmation on the importance of taking other parameters into consideration towards platform configuration decisions. The effect of each parameter can be studied further to gain more insight about the issue. However, in order to find out if the infeasibility problem is mainly resulted from

the second cause rather than the first set of causes, it was decided to apply corrective actions based on the set of causes in the first category, i.e., to allow multiple platforms for variables with high CV and repeat the optimization procedure. In case that this corrective action will not resolve the infeasibility issue, the next action is to increase the degree of freedom and completely exclude such variables from the platform candidate set, so that the design space is reasonably expanded. The procedure is then repeated with the same structure, until the optimal design for the entire family is achieved.

**Table 5-20: Platform and scale optimized values based on a commonality-oriented scheme**

| Variant Design Variable | P1 | P2 | P3 | P4 | P5 | P6 | P7 | P8 | P9 | P10 |
|---|---|---|---|---|---|---|---|---|---|---|
| $N_c$ (x1) | 162 | 162 | 162 | 162 | 162 | 162 | 162 | 162 | 162 | 162 |
| $N_s$ (X2) | 412 | 412 | 412 | 412 | 500 | 500 | 500 | 500 | 500 | 500 |
| $A_{wa}$(X3) | 0.278 | 0.278 | 0.278 | 0.278 | 0.278 | 0.278 | 0.278 | 0.278 | 0.278 | 0.278 |
| $A_{wf}$(X4) | 0.278 | 0.278 | 0.278 | 0.278 | 0.278 | 0.278 | 0.278 | 0.278 | 0.278 | 0.278 |
| $r_0$(X5) | 20.09 | 20.09 | 20.09 | 20.09 | 25.68 | 25.68 | 25.68 | 25.68 | 25.68 | 25.68 |
| $t$(X6) | 5.312 | 5.312 | 5.312 | 6.584 | 6.584 | 6.584 | 6.584 | 6.584 | 6.584 | 6.584 |
| $I$(X7) | 3.060 | Infeasible | Infeasible | Infeasible | 3.637 | 3.774 | 3.913 | Infeasible | Infeasible | Infeasible |
| $L$(X8) | 11.49 | | | | 21.47 | 24.93 | 27.82 | | | |
| $\eta$ | 0.853 | | | | 0.717 | 0.691 | 0.666 | | | |
| $M$ | 0.309 | | | | 0.679 | 0.753 | 0.815 | | | |

Variables 1, 3 and 4 are single platform candidates, and $x_1$ has the highest CV value among them. By moving $x_1$ into the multiple candidate set, a value of $x_1 = 161$ is assigned to the infeasible variants, and ran the optimization again. This action resulted in infeasibility again, and as a result the next action was applied (variable 1 is added to the non-platform set). Through optimizing its value for variants 2, 3, 4, 8, 9 and 10, the family design shown in Table 5-21 was obtained.

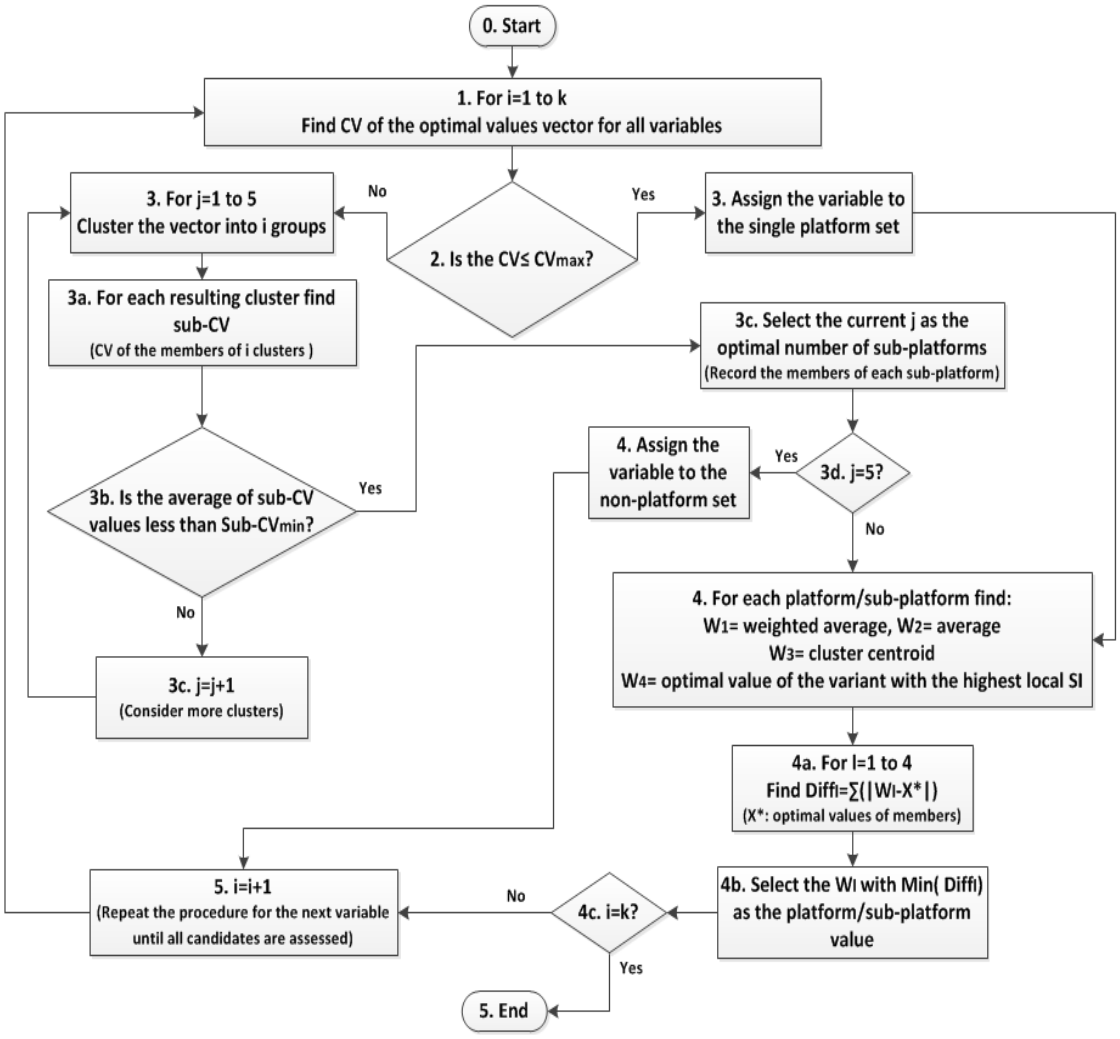


**Figure 5-1: Platform values determination basis in the commonality-oriented scheme**

The resulting family design does not assure feasibility for integer values of $N_c$ for variants 3 and 9, and therefore suffers from performance challenges. However, for this design solution, the results have been compared to our proposed family design, and the results are shown in Table 5-22.

**Table 5-21: The family design after corrective actions on commonality-oriented scheme**

| Variant ---------- Design Variable | P1 | P2 | P3 | P4 | P5 | P6 | P7 | P8 | P9 | P10 |
|---|---|---|---|---|---|---|---|---|---|---|
| $N_c$ (x1) | 162 | 158 | 153.73 | 149 | 162 | 162 | 162 | 158 | 151.75 | 137 |
| $N_s$ (X2) | 412 | 412 | 412 | 412 | 500 | 500 | 500 | 500 | 500 | 500 |
| $A_{wa}$(X3) | 0.2783 | 0.2783 | 0.2783 | 0.2783 | 0.2783 | 0.2783 | 0.2783 | 0.2783 | 0.2783 | 0.2783 |
| $A_{wf}$(X4) | 0.2783 | 0.2783 | 0.2783 | 0.2783 | 0.2783 | 0.2783 | 0.2783 | 0.2783 | 0.2783 | 0.2783 |
| $r_0$(X5) | 20.089 | 20.089 | 20.089 | 20.089 | 25.682 | 25.682 | 25.682 | 25.682 | 25.682 | 25.682 |
| $t$(X6) | 5.3116 | 5.3116 | 5.3116 | 6.584 | 6.584 | 6.584 | 6.584 | 6.584 | 6.584 | 6.584 |
| $I$(X7) | 3.0598 | 3.206 | 3.285 | 3.363 | 3.639 | 3.7735 | 3.913 | 4.0732 | 4.257 | 4.711 |
| $L$(X8) | 11.49 | 21.525 | 26.259 | 33.076 | 21.448 | 24.903 | 27.792 | 30.682 | 33.414 | 37.786 |
| $\eta$ | 0.8525 | 0.8135 | 0.794 | 0.7756 | 0.7172 | 0.6913 | 0.6666 | 0.6404 | 0.6126 | 0.5537 |
| $M$ | 0.3093 | 0.4526 | 0.5193 | 0.6047 | 0.6795 | 0.7534 | 0.8153 | 0.8758 | 0.9321 | 1.020 |
| $f$ | 1.0964 | 1.0297 | 1.0095 | 0.9817 | 0.9299 | 0.9011 | 0.8772 | 0.8522 | 0.8264 | 0.7594 |

**Table 5-22: Average percentage of change in performance for the test scheme vs. the performance-preserving design**

| **% of difference (test case from the proposed family design)** | | |
|---|---|---|
| **$\eta$** | **M** | **AOF** |
| -0.25% | +2.63% | -0.7% |

Compared to our proposed family design, this family design results in decreased efficiency and increased mass at the same time, and has a lower average AOF value. Since this design is obtained after mitigating the effect of permissive or restrictive decision points, it can be concluded that the main reason for less desired performance of this scheme is the less insightful decision parameter applied. Even with an equal degree of freedom to the performance-preserving scheme, the performance of the resulting family is worse. This indicates that the right set of variables was not selected for platform

configuration, due to relying on just the dispersion of the individual optima and not including more parameters into decision making.

## 5.3. Information integration: A moderate scheme

The proposed scheme and the test scheme results show that by including the information on sensitivity of the variables and their detachability, a reliable platform within the desired performance range can be obtained, whereas there is risk of infeasible design when the configuration decision is not based on such information. However, the attempt is to achieve a higher level of commonality in our study while preserving the performance, by leveraging the information on SI, detachability, and CV in a more insightful way, based on what is observed from the past two configuration schemes of this chapter. A moderate scheme is suggested in this section, to achieve this goal by considering both CV and SI information and combining them toward attaining the most possible commonality and the least possible performance loss.

This scheme allows consideration of all variables, based on the information on their sensitivity and coefficient of variation, and provides the opportunity to include all the variables into some level of commonalization, depending on their condition. The criteria used for platform configuration are as follows:

A) If both the sensitivity of a variable and its coefficient of variation for the vector of individual optimal values are sufficiently low, that variable is considered as a platform variable with the shared value over all the variants (i.e., single platform). The shared value determination procedure will be similar to the previous schemes, based on the optimal partitioning strategy.
B) For variables that have a mid-range value for both CV and SI, different clustering schemes will be assessed toward selecting the best number of clusters (sub-platforms).
C) For a variable that has either a high value of SI or CV or both, the sharing will not be considered and the variable will be kept as a scale variable.

In this scheme, the CV thresholds for a variable with sufficiently low sensitivity should be different from that for a variable with higher SI value. Similarly, for a variable with higher sensitivity, even if CV is sufficiently low, the number of sub-platforms shall be carefully decided in order to avoid any substantial performance loss, and capturing more commonalization possibilities. Although it might contain subjectivity to some extent, however a general guideline for setting such thresholds is to select specific percentiles of the distribution of the SI and CI values on each side. The initial categorization of single, multiple, and non-platform variables is determined based on Table 5-23 and Table 5-24. Figures 5-2(a) and (b) show the lookup table and the application to the PHEV family.

**Table 5-23: Decision points based on SI values**

| SI range (for each variable) | Minimum number of clusters to be assessed |
|---|---|
| *SI≤0.035* | All-or-none platform case |
| *0.035<SI≤0.07* | 2 |
| *0.07<SI* | Scale variable |

**Table 5-24: Decision points based on CV values**

| CV range (of the optimal values vector) | Minimum number of clusters to be assessed |
|---|---|
| *CV≤7.5%* | All-or-none platform |
| *7.5%<CV≤15%* | 2 |
| *15%< CV* | Scale variable |

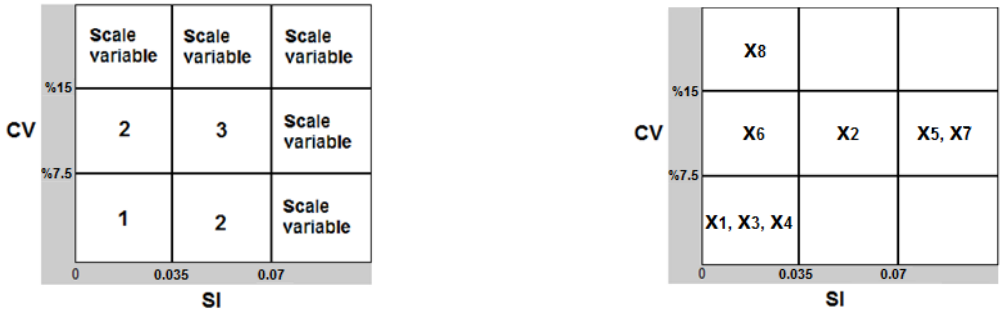


**Figure 5-2: (a) Platform configuration scheme (b) PHEV platform**

The platform configuration and the number of sub-platforms based on the moderate scheme are shown in Table 5-25. The platform composition and the obtained values for each platform or sub-platform variable are shown in Table 5-26.

**Table 5-25: The number of platform/sub-platforms based on the improved scheme**

| Variable | Number of clusters to be assessed |
|---|---|
| 1,3,4 | All-or-none platform |
| 6 | 2 |
| 2 | 3 |
| 5,7,8 | Scale variable |

As our purpose is to obtain more commonality, and since the suggested scheme for $x_2$ includes a single variant detached from the rest of the variants, two configurations are assessed, one with three sub-platforms for $x_2$, and the other with two sub-platforms, by including variant number one into the first sub-platform. The results did not differ significantly, while by sharing a new value among the first three motors, more commonalization is obtained (The average performance loss for commonalizing $x_2$ of the first motor is 0.03% for efficiency, and 0.21% for mass, which is ignorable).

**Table 5-26: Platform and scale optimized values based on the improved scheme**

<table>
<tr><th>Platform Candidate</th><th>$X_1$</th><th>$X_3$</th><th>$X_4$</th><th>$X_6$</th><th>$X_2$<br>(partitioning suggestion)</th><th>$X_2$<br>(After integrating P1 and P2)</th></tr>
<tr><td>Number of platforms</td><td colspan="3" rowspan="2">Single platform</td><td>2</td><td>3</td><td>2</td></tr>
<tr><td>Platform variants</td><td>P1: {$p_1$, $p_2$, $p_3$}<br>P2: {$p_4$, $p_5$, $p_6$, $p_7$, $p_8$, $p_9$, $p_{10}$}</td><td>P1: {$p_1$}<br>P2: {$p_2$, $p_3$}<br>P3: {$p_4$, $p_5$, p6, $p_7$, $p_8$, $p_9$, $p_{10}$}</td><td>P1:{$p_1$, $p_2$, $p_3$}<br>P2: {$p_4$, $p_5$, $p_6$, $p_7$, $p_8$, $p_9$, $p_{10}$}</td></tr>
<tr><td rowspan="3">Platform values</td><td rowspan="3">162</td><td rowspan="3">0.2783</td><td rowspan="3">0.2783</td><td>$X_6(P_1)$= 5.3116</td><td>$X_2(P_1)$= 324</td><td>$X_2(P_1)$= 393</td></tr>
<tr><td rowspan="2">$X_6(P_2)$= 6.584</td><td>$X_2(P_2)$= 428</td><td rowspan="2">$X_2(P_2)$= 500</td></tr>
<tr><td>$X_2(P_3)$= 500</td></tr>
</table>

For the sake of space saving, only the second configuration (with more commonality) is presented in Table 5-27, as a feasible design with no need for any corrective strategy. Since the goal of this scheme was to increase commonality based on intuitive CV and SI thresholds, the results of performance comparison to the individual optima (Table 5-3) shows acceptable level of performance loss, and makes this scheme superior to the performance-preserving scheme, with more commonality obtained through the new platform configuration.

The results are compared to the individual optima, as shown in Table 5-28, and the comparison results to Dai and Scott's design and Ninan and Siddique's design are shown in Table 5-29 and Table 5-30 respectively. Our proposed method has improved the average efficiency by 8.8% at the cost of adding the mass by 11% in comparison to Dai and Scott's design. Our solution's AOF is better by 1.2% in average, indicating acceptable performance of this methodology.

**Table 5-27: Optimal family design for the improved moderate scheme**

| **Variant ---------- Design Variable** | **P1** | **P2** | **P3** | **P4** | **P5** | **P6** | **P7** | **P8** | **P9** | **P10** |
|---|---|---|---|---|---|---|---|---|---|---|
| $N_c$ (x1) | 162 | 162 | 162 | 162 | 162 | 162 | 162 | 162 | 162 | 162 |
| $N_s$ (X2) | 393 | 393 | 393 | 500 | 500 | 500 | 500 | 500 | 500 | 500 |
| $A_{wa}$(X3) | 0.2783 | 0.2783 | 0.2783 | 0.2783 | 0.2783 | 0.2783 | 0.2783 | 0.2783 | 0.2783 | 0.2783 |
| $A_{wf}$(X4) | 0.2783 | 0.2783 | 0.2783 | 0.2783 | 0.2783 | 0.2783 | 0.2783 | 0.2783 | 0.2783 | 0.2783 |
| $r_0$(X5) | 19.599 | 20.565 | 21.032 | 22.094 | 23.0895 | 24.090 | 25.117 | 26.197 | 27.375 | 30.553 |
| $t$(X6) | 5.3116 | 5.3116 | 5.3116 | 6.584 | 6.584 | 6.584 | 6.584 | 6.584 | 6.584 | 6.584 |
| $I$(X7) | 3.0398 | 3.1932 | 3.267 | 3.418 | 3.5768 | 3.735 | 3.898 | 4.070 | 4.257 | 4.761 |
| $L$(X8) | 12.556 | 21.550 | 25.106 | 21.513 | 24.887 | 27.195 | 28.650 | 29.373 | 29.400 | 26.655 |
| $\eta$ | 0.8582 | 0.8169 | 0.7984 | 0.7630 | 0.7293 | 0.6983 | 0.6691 | 0.6409 | 0.6128 | 0.5478 |
| $M$ | 0.3062 | 0.4587 | 0.5268 | 0.5510 | 0.6477 | 0.7324 | 0.8074 | 0.8740 | 0.9328 | 1.023 |
| $AOF$ | 1.101 | 1.0293 | 1.0092 | 0.9954 | 0.9518 | 0.9147 | 0.8824 | 0.8532 | 0.8261 | 0.7527 |

As compared to the individual optimization solution, the moderate scheme has improved the average mass by 0.17% and has a loss of 1.05% on efficiency. This amount of loss is acceptable, and the design can be approved with two single platforms and three multiple platforms, each consisting of two sub-platforms. Also, as compared to the PFD approach suggested by Dai and Scott, our family design solution is of 8.8% improvement in average on efficiency target, and of 11% loss on mass in average. The value of AOF function in our study is better than that of Dai and Scott's family design by average of 1.2%, indicating acceptable performance for our moderate design scheme. As compared to Ninan and Siddique's solution, in average there is a +12.2% improvement on the efficiency objective, and the resultant average mass of our family solution is 0.08 kg more in average (i.e., 11.03%) than the average mass obtained through the PCM suggested solution. The aggregated performance functions are also compared, and the AOF of our family is better by 9.3% in average (in a maximization problem), indicating superior performance of our proposed moderate scheme. Table 5-31 also summarizes the entire comparisons implemented for this scheme.

**Table 5-28: Comparison of individual solutions to the improved family design**

| Motor No. | Individual optima | | Family Solutions | | Difference (%) | |
|---|---|---|---|---|---|---|
| | $\eta$ | M (kg) | $\eta$ | M(Kg) | $\eta$ | M |
| 1 | 0.8605 | 0.2960 | 0.8582 | 0.3062 | -0.2673 | 3.4459 |
| 2 | 0.8030 | 0.4347 | 0.8169 | 0.4587 | 1.7310 | 5.5210 |
| 3 | 0.7830 | 0.4968 | 0.7984 | 0.5268 | 1.9668 | 6.0386 |
| 4 | 0.7658 | 0.5547 | 0.7630 | 0.5510 | -0.3656 | -0.6670 |
| 5 | 0.7313 | 0.6509 | 0.7293 | 0.6477 | -0.2735 | -0.4916 |
| 6 | 0.7023 | 0.7396 | 0.6983 | 0.7324 | -0.5696 | -0.9735 |
| 7 | 0.6763 | 0.8215 | 0.6691 | 0.8074 | -1.0646 | -1.7164 |
| 8 | 0.6532 | 0.8991 | 0.6409 | 0.8740 | -1.8830 | -2.7917 |
| 9 | 0.6320 | 0.9717 | 0.6128 | 0.9328 | -3.0380 | -4.0033 |
| 10 | 0.5876 | 1.0899 | 0.5478 | 1.0230 | -6.7733 | -6.1382 |
| **Average Change** | | | | | -1.05% | -0.17% |

**Table 5-29: Comparing the proposed family to the family solution of Dai and Scott [27]**

| Motor No. | Dai and Scott's solution | | Our solution | | Difference (%) | | |
|---|---|---|---|---|---|---|---|
| | $\eta$ | M (kg) | $\eta$ | M(Kg) | $\eta$ | M | AOF |
| 1 | 0.862 | 0.347 | 0.8582 | 0.3062 | -0.4408 | -11.7579 | 1.3812 |
| 2 | 0.713 | 0.388 | 0.8169 | 0.4587 | 14.5722 | 18.2216 | 3.1363 |
| 3 | 0.70 | 0.425 | 0.7984 | 0.5268 | 14.0571 | 23.9529 | 3.6140 |
| 4 | 0.671 | 0.478 | 0.7630 | 0.5510 | 13.7109 | 15.2720 | 5.1109 |
| 5 | 0.66 | 0.534 | 0.7293 | 0.6477 | 10.5000 | 21.2921 | 1.7968 |
| 6 | 0.648 | 0.637 | 0.6983 | 0.7324 | 7.7623 | 14.9765 | 0.8823 |
| 7 | 0.626 | 0.717 | 0.6691 | 0.8074 | 6.8850 | 12.6081 | 0.5469 |
| 8 | 0.63 | 0.826 | 0.6409 | 0.8740 | 1.7302 | 5.8111 | -0.8483 |
| 9 | 0.503 | 0.879 | 0.6128 | 0.9328 | 21.8290 | 6.1206 | -1.0896 |
| 10 | 0.56 | 0.988 | 0.5478 | 1.0230 | -2.1786 | 3.5425 | -2.9526 |
| Average Change | | | | | +8.84% | +11% | +1.15% |

**Table 5-30: Comparing the proposed family to the family solution of Ninan and Siddique [41]**

| Motor No. | Ninan's solution | | Our solution | | Difference (%) | | |
|---|---|---|---|---|---|---|---|
| | $\eta$ | M (kg) | $\eta$ | M(Kg) | $\eta$ | M | AOF |
| 1 | 0.81 | 0.35 | 0.8582 | 0.3062 | 5.9506 | -12.5143 | 0.7319 |
| 2 | 0.80 | 0.46 | 0.8169 | 0.4587 | 2.1125 | -0.2826 | 0.9118 |
| 3 | 0.78 | 0.50 | 0.7984 | 0.5268 | 2.3590 | 5.3600 | -0.0792 |
| 4 | 0.72 | 0.51 | 0.7630 | 0.5510 | 5.9722 | 8.0392 | 2.0923 |
| 5 | 0.66 | 0.59 | 0.7293 | 0.6477 | 10.500 | 9.7797 | 9.9076 |
| 6 | 0.63 | 0.66 | 0.6983 | 0.7324 | 10.8413 | 10.9697 | 14.3661 |
| 7 | 0.58 | 0.70 | 0.6691 | 0.8074 | 15.3621 | 15.3429 | 16.1053 |
| 8 | 0.55 | 0.74 | 0.6409 | 0.8740 | 16.5273 | 18.1081 | 17.0370 |
| 9 | 0.49 | 0.76 | 0.6128 | 0.9328 | 25.0612 | 22.7368 | 17.8459 |
| 10 | 0.43 | 0.77 | 0.5478 | 1.0230 | 27.3953 | 32.8571 | 14.0455 |
| Average Change | | | | | +12.2% | +11.03% | +9.3% |

Also, as compared to the PFD approach suggested by Dai and Scott, our family design solution is of 8.8% improvement in average on efficiency target. The loss on mass is 11% less than Ninan and Siddique's solution on average. The results are also compared to two solutions provided by the PPCEM method suggested by Simpson et al. [30] shown in Table 5-32, and a less commonalized solution shown in Table 5-33.

**Table 5-31: Comparison of the family design solution with the individual optima, and existing PFD approaches results for the universal electric problem: the moderate scheme**

| **Design solution** | **Individual optimal design** | | **Dai and Scott's design** | | | **Ninan and Siddique's design** | | |
|---|---|---|---|---|---|---|---|---|
| **Objective** | $\eta$ | M | $\eta$ | M | AOF | $\eta$ | M | AOF |
| **% Average difference** | -1.05% | -0.17% | +8.84% | +11% | +1.15% | +12.2 % | +11.03 % | +9.3% |

**Table 5-32: Results of comparing the improved scheme to PPCEM approaches**

| **Motor No.** | **η** | | | **M (kg)** | | | **AOF** | |
|---|---|---|---|---|---|---|---|---|
| | **This study** | **PPCEM** | **%Diff** | **This study** | **PPCEM** | **%Diff** | **PPCEM** | **%Diff** |
| 1 | 0.858 | 0.768 | 11.7448 | -19.4211 | -19.421 | -19.4211 | 1.0072 | 9.313 |
| 2 | 0.817 | 0.782 | 4.4629 | -11.7885 | -11.788 | -11.7885 | 0.935 | 10.086 |
| 3 | 0.798 | 0.70 | 14.0571 | -8.5417 | -8.5417 | -8.5417 | 0.9173 | 10.019 |
| 4 | 0.763 | 0.679 | 12.3711 | -11.8400 | -11.840 | -11.8400 | 0.9010 | 10.478 |
| 5 | 0.7293 | 0.639 | 14.1315 | -7.8663 | -7.8663 | -7.8663 | 0.8584 | 10.880 |
| 6 | 0.6983 | 0.602 | 15.9967 | -3.5046 | -3.5046 | -3.5046 | 0.8232 | 11.115 |
| 7 | 0.6691 | 0.568 | 17.7993 | 1.3049 | 1.3049 | 1.3049 | 0.7955 | 10.924 |
| 8 | 0.6409 | 0.536 | 19.5709 | 6.5854 | 6.5854 | 6.5854 | 0.7691 | 10.934 |
| 9 | 0.6128 | 0.505 | 21.3465 | 12.3855 | 12.3855 | 12.3855 | 0.7444 | 10.975 |
| 10 | 0.5478 | 0.448 | 22.2768 | 24.7561 | 24.7561 | 24.7561 | 0.6803 | 10.642 |
| | | | **+15.37%** | | | **-1.79%** | | **+10.53%** |

**Table 5-33: Comparison of the moderate scheme to PPCEM solution with less commonality**

| Motor No. | $\eta$ | | | M (kg) | | | AOF | |
|---|---|---|---|---|---|---|---|---|
| | Proposed PFD | PPCEM | %Diff | Proposed PFD | PPCEM | %Diff | PPCEM | %Diff |
| 1 | 0.8582 | 0.747 | 14.886 | 0.3062 | 0.397 | -22.872 | 0.9861 | 11.652 |
| 2 | 0.8169 | 0.721 | 13.301 | 0.4587 | 0.456 | 0.5921 | 0.9628 | 6.907 |
| 3 | 0.7984 | 0.711 | 12.292 | 0.5268 | 0.477 | 10.440 | 0.9656 | 4.5153 |
| 4 | 0.7630 | 0.701 | 8.8445 | 0.5510 | 0.499 | 10.421 | 0.9681 | 2.819 |
| 5 | 0.7293 | 0.675 | 8.0444 | 0.6477 | 0.568 | 14.0317 | 0.9384 | 1.424 |
| 6 | 0.6983 | 0.648 | 7.7623 | 0.7324 | 0.646 | 13.3746 | 0.9054 | 1.023 |
| 7 | 0.6691 | 0.622 | 7.5723 | 0.8074 | 0.712 | 13.3989 | 0.8781 | 0.4874 |
| 8 | 0.6409 | 0.599 | 6.9950 | 0.8740 | 0.774 | 12.9199 | 0.8459 | 0.8546 |
| 9 | 0.6128 | 0.577 | 6.2045 | 0.9328 | 0.833 | 11.9808 | 0.8247 | 0.1661 |
| 10 | 0.5478 | 0.538 | 1.8216 | 1.0230 | 0.941 | 8.7141 | 0.7663 | -1.774 |
| | | | **+8.77%** | | | **+7.3%** | | **+2.8%** |

Comparison to the VBPDM method proposed by Nayak et al. [33] is also presented in Table 5-34. Our suggested design performs better than the highly commonalized PPCEM method solution, in terms of both objectives. For their less commonalized solution, there is again the trade-off including improvement in efficiency, and losing performance on the mass objective. It shall be noted that our approach allows for generalized commonality, while the PPCEM is an all-or-none platform design approach, which imposes less flexibility to the design over the multiple platform configuration cases.

**Table 5-34: Comparison of the moderate scheme and the VBPDM method solutions**

| Motor No. | $\eta$ | | | M (kg) | | | AOF | |
|---|---|---|---|---|---|---|---|---|
| | Moderate scheme | VBDM | %Diff | Moderate scheme | VBDM | %Diff | VBPDM | %Diff |
| 1 | 0.8582 | 0.89 | -3.5730 | 0.3062 | 0.5 | -38.7600 | 1.024 | 7.5195 |
| 2 | 0.8169 | 0.82 | -0.3780 | 0.4587 | 0.5 | -8.2600 | 1.004 | 2.5199 |
| 3 | 0.7984 | 0.79 | 1.0633 | 0.5268 | 0.5 | 5.3600 | 1.0074 | 0.1786 |
| 4 | 0.7630 | 0.76 | 0.3947 | 0.5510 | 0.5 | 10.2000 | 1.0099 | -1.435 |
| 5 | 0.7293 | 0.71 | 2.7183 | 0.6477 | 0.57 | 13.6316 | 0.9719 | -2.0681 |
| 6 | 0.6983 | 0.67 | 4.2239 | 0.7324 | 0.63 | 16.2540 | 0.9453 | -3.237 |
| 7 | 0.6691 | 0.64 | 4.5469 | 0.8074 | 0.67 | 20.5075 | 0.9220 | -4.295 |
| 8 | 0.6409 | 0.60 | 6.8167 | 0.8740 | 0.72 | 21.3889 | 0.90623 | -5.852 |
| 9 | 0.6128 | 0.58 | 5.6552 | 0.9328 | 0.76 | 22.7368 | 0.89216 | -7.405 |
| 10 | 0.5478 | 0.53 | 3.3585 | 1.0230 | 0.83 | 23.2530 | 0.84859 | -11.300 |
| Average difference | | | **+2.48%** | Average difference | | **+8.6%** | | -2.537% |

## 5.4. Effect of varying the number of sub-platforms (k) on the family design

Since the partitioning strategy to some extent relies on subjective parameters such as *k* (the number of sub-platforms), it is worth to assess the resulting family design performance for different values of such parameter. In this section this assessment is

provided in brief. For this purpose, *k* is varied for a variable with sufficiently low *SI* and *CV* value (i.e., $x_1$, as shown to be a good candidate for all-or-non platform in Figure 5-2), and obtained the resulting family design for *k=1* to *4*. The average performance deviation from the individual optima is illustrated in Figure 5-3. Similarly such analysis was applied to $x_2$ which belongs to a middle range in the *SI-CV* look-up chart and is a candidate for multiple platforms.

As Figure 5-3 shows, the deviation reduction is quite small for increased *k*, indicating that no significant benefit would be obtained for increasing the diversity in design for $x_1$. As such, commonalizing this variable over the entire family would be more beneficial in terms of increasing the commonality, while keeping the performance loss at the allowed level. This assessment confirms the important role of the sensitivity analysis to identify the more appropriate candidates toward commonalization.

Also, as Figure 5-4 shows the trend of convergence in performance, *k=3* would be the most appropriate point for the number of sub-platforms for $x_2$. It is worth to note that the slope of this diagram is steeper and more variation is observed for varying *k* for $x_2$, which implies the more impact of $x_2$ on the performance of the family. All-or-none platform for this variable is not acceptable, since its resulting family design solution faces a performance loss greater than the allowed 10% on the mass objective. Also, as shown here and discussed earlier in this study, the performance loss for choosing two sub-platforms for $x_2$ in average is less than 0.1%, as compared to three sub-platforms case. Therefore, *k=2* is the ultimate option for obtaining more commonality.

These figures illustrate the impact of relying on *SI-CV* information for platform configuration, and the trends of each diagram confirm that it is more important to appropriately select the candidates, rather than imposing extra computational cost for optimizing the value of *k* in the partitioning strategy. As discussed in Section 4.5, for the variables which are not appropriate candidates for any commonalization, neither increasing *k*, nor switching them from platform candidate to non-platform variable would result in desired performance.

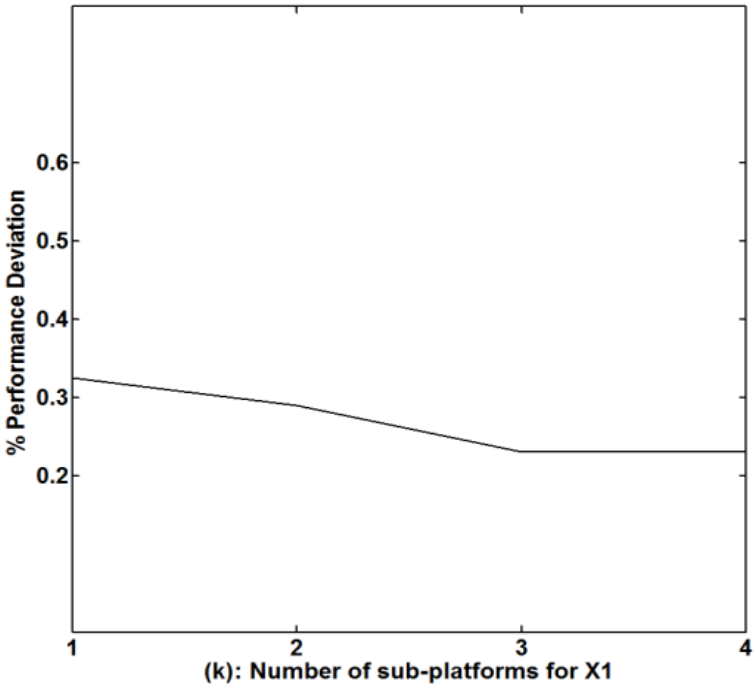


**Figure 5-3: Performance deviation per *k*, for $X_1$**

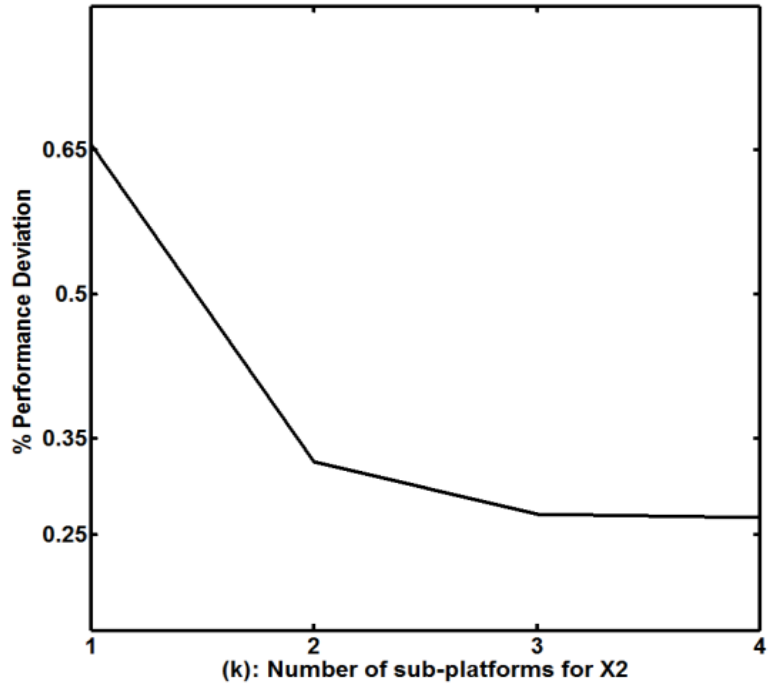


**Figure 5-4: Performance deviation per *k*, for $X_2$**

## 5.5. Commonality measure comparisons

In addition to comparing the objectives and AOF value for each approach, a comparison on the level of commonality achieved through each solution can help to evaluate the efficiency of suggested schemes. Several indices and metrics have been developed for providing insight on the level of commonalization obtained for a family design. Each of the developed metrics need specific inputs, such as the number of common components, cost information, manufacturing and assembly information, BOM of the products, and other relevant information in order to provide a quantified measure about different designs and enable their comparison. A comprehensive comparison of six of such indices can be found in [79]. In order to compare different designs in terms of the tooling cost savings resulted from their commonality degree, the Commonality Index developed by Martin and Ishi [80] is adopted here, because our comparison purposes are similar to that of Khajavirad and Michalek [81]. The CI varies between 0 and 1, and provides a measure of the percentage of commonalization in the whole family. It can be interpreted as the ratio of the number of unique components to the total number of parts [79]. Assuming $p$ variants and $n$ components in each variant (or design variables in our case), for a design with $u$ as the total number of unique components, *CI* will be as follows:

$$CI = 1 - \frac{u-n}{n(p-1)} \tag{5-3}$$

This metric for finding the CI for our desired designs results in the values shown in Table 5-35.

**Table 5-35: The commonality index values for the proposed schemes in this study, and other published methods**

| Commonality measure | Dai and Scott | Ninan and Siddique | Performance-preserving Scheme | Moderate Scheme |
|---|---|---|---|---|
| **(% of variables shared)** | 0.680 | 0.653 | 0.556 | 0.694 |

The obtained value for our moderate scheme is higher than the other existing approaches, and also than the proposed performance-preserving scheme, indicating more

tooling cost saving due to commonalization. Therefore, our proposed approach performs better in terms of the commonality comparisons as well.

The family solution of the moderate scheme is compared to the solutions of the performance-preserving and the commonality-oriented schemes as shown in Table 5-36.

**Table 5-36: Results of comparing the improved scheme to the initial scheme and the test scheme**

| Moderate scheme performance | $\eta$ | M | AOF |
|---|---|---|---|
| % of difference from the commonality-oriented scheme | +0.29% | -1.5% | +1.92% |
| % of difference from the performance-preserving scheme | -0.01% | +1.04% | -0.16% |

As the results show, the performance on both objectives has been improved in comparison to the commonality-oriented scheme where the SI information was not taken into account. Also, by comparing this scheme (moderate) to the performance-preserving scheme, it is observed that commonality has been increased while a very small amount of performance is lost (i.e., on average, the maximum loss is 1% on mass). This scheme confirms that including SI information along with the CV parameter through the suggested configuration scheme would result in a moderate design which is of more commonality, yet within allowable performance loss range. The moderate scheme has more benefits than the performance preserving scheme, as it has obtained higher level of commonality (3 single platforms, and 2 multiple platform variables), and also has more benefits than the commonality-oriented case because its commonality level is the same, while the performance loss (from individual optima) is less.

The results of comparing both schemes to the individual optima, and the solutions of [27, 41] are all shown in Table 5-37. It can be observed that out of the two suggested schemes (scheme1: performance-preserving, scheme2: moderate), both schemes have made improvement on mass target, compared to the individual variant optimal designs. The

AOF value shows improvement on both schemes, compared to both of the existing methods in the literature. This indicates that our proposed approach is performing well and is of comparable performance of to the previously developed methods.

In regard to the Commonality Index (CI), the CP3 method has resulted in a CI=0.28 while our method yields in 0.56 and 0.69, which is much higher than the CP3 method. The average motor efficiency in our method is 71.3%, while CP3 has resulted in an average of 81%. This is expected, since the commonality of CP3 is much less than that of this approach, and as noted earlier in this document, CP3 is a performance-oriented approach as compared to the proposed commonality-oriented proposed method. As such, each method pursues a different objective and it cannot be strictly concluded about the superiority of one over the other.

**Table 5-37: Integrated view of comparison results for the initial proposed and the improved design schemes**

| **compared to→** | **Individual optimal design** | | **PFD(Dai and Scott's design)** | | | **PCM(Ninan's design)** | | |
|---|---|---|---|---|---|---|---|---|
| **↓Scheme** | $\eta$ | M | $\eta$ | M | AOF | $\eta$ | M | AOF |
| **Performance - preserving** | -1.03% | -1.15% | +8.86% | +9.87 % | +1.33% | +12.4% | +10.2% | +9.5% |
| **Moderate** | -1.05% | -0.2% | +8.85% | +10.9 % | +1.17% | +12.2% | +11% | +9.3% |

Regarding the number of function calls, since the universal electric motors design problem is not a black-box function, the comparison to previous publications for this problem is not meaningful. The number of necessary function evaluations for this eight-variable family design problem, based on the structure of the platform configuration and family design method in Dai and Scott's method.

**Sensitivity Analysis**: (10 motors)*(8 variables)*(2 variations/variable)*(n optimization iterations)= 160n

**Cluster analysis**: (10 motors)*(k candidate variables)*(10 points / variable curve fitting) = 100k

**Platform value selection**: (K)*(K+1)/2 performance loss considerations

(K=5 variables)→ 515+160n (5-4)

This number for the proposed method in this dissertation is limited to the number of expensive sample points needed to build the metamodel, which is 45 for the 8-variable design problem, and by running 10 metamodeling algorithms for the entire family, 450 samples or expensive function evaluations will be needed. The number of iterations for optimization is 10n, and the total number will be 450+20n for out proposed method. This value is significantly less than the number needed in the aforementioned family design strategy, which can be an evidence for further concluding on capability of the proposed method for family design of expensive and black-box design problems.

The initial and final stages of the PFD approaches in this chapter are the same as those in Dai and Scott's method, including individual optimization of each variant, as well as the scale variables optimization stage at the end. On the other hand, the function evaluations in our proposed approach concurrently obtain the SI matrix and "whiten" the structure of the black-box function. Since the use of meta-modeling techniques will be inevitable for simulation-based design problems with high dimensions and long running times, it can be concluded that our proposed approach is able to provide reliable family design solutions with less number of function evaluations needed for black-box functions, as compared to the proposed method in [27]. The platform design based on sensitivity and clustering analysis by Dai and Scott needs function evaluations for obtaining sensitivity vectors, clustering analyzes and other performance evaluations in different stages, all of which are unnecessary in our approach. Also, the platform cascading method (PCM) suggested by Ninan and Siddique would be exposed to high computational cost because of optimizing the family design problem with a larger number of variables due to adding commonality variables.

It shall be noted that for the family design problem in this chapter, a number of different lower and upper bounds for the meta-modeling part were examined and it was found out that for a properly narrowed down range, both the sensitivities and correlations follow the

same order for all the variants, and within a sufficiently down-sized design space, the orders of impact of the variables as well as their detachability will be the same, regardless of the variant under study. This is quite helpful in reducing the number of function calls needed for this section, since it helps to identify the indices of variables for set#1 and se#2, based on just one variant rather than the entire family. The meta-modeling step is run for all the variants, while it can be avoided for saving computational cost, if the design range is intuitively shrinked for any intended design problem.

In regard to the proposed method by Khajavirad et al. [81], though it takes advantage of concurrent optimization of the platform configuration and the entire family design, it is of higher computational complexity as compared to two-stage methods for platform and family design. For problems with high dimensional and black-box objective functions, it might require remarkable computational time to optimize a product family.

## 5.6. Conclusion

In this chapter, a new family design method was proposed and its performance was assessed by applying to the universal electric motors family design problem. Two platform configuration schemes were suggested; one for cases with high priority for keeping the performance of the variants as close as possible to their individual optimal performance; and the second one as a moderate scheme attempting to achieve more commonality while sacrificing allowable amount of performance. The main strategy behind the platform candidate selection in both schemes are to leverage the information on the importance of the variables towards aggregated performance, and the dispersion or coefficient of variation (CV) for the vector of individual optimal values of each variable in the family. Information such as the quantified correlations was also exploited towards suggesting platform configurations and variables commonalization. Through an effective sampling, the correlations among variables were identified by RBF-HDMR, and their quantified correlation measures obtained through sensitivity analysis served as the basis for identifying desired candidates for sharing.

The proposed method was shown to perform both efficiently (obtaining a desired level of performance), and effectively (increasing commonality within the family, while satisfying all performance requirements), and showed improvement in the aggregated preference function compared to the previously developed approaches (i.e., [27, 41]). The computational efficiency of the proposed approach is another contribution of the study, enabling design of the product families involving high-dimensional, expensive, black-box (HEB) functions. Even for the same test problem (i.e., the universal motor family), as reported by Simpson et al. [82], the problem would become intractable due to remarkable increase in the number of design variables, constraints, and objectives. Therefore, the use of a two stage design approach instead of the integrated or concurrent optimization is beneficial and efficient in reducing the dimensionality.

As for the method from Wei et al. [40], the role of the SI and ACQ are verified through designing a test scheme, and this clearly shows how our work differs from that work. In summary, the proposed method does not require gradient information and demands a limited number of function evaluations as compared to evolutionary algorithms. These features are developed towards solving black-box type of family design problems. Using a well-known test case can establish our work in the context of the existing literature and can clearly show the steps of the proposed method. It is to be noted that although the test case has explicit equations, they were treated as black-boxes and only the function values are used in the underlying steps. Using test cases and benchmark mathematical problems in metamodel-based design optimization (MBDO) area for black-box type of problems is common and has been widely accepted by the community.

There are a number of parameters used in our study, which have been determined heuristically and their tuning would result in design solutions with better performance (less loss and/or more improvement for the mass and efficiency targets). This sort of parameter selection imposes some limitations on all similar studies, and if fine tuning is implemented to find the best value of each of such parameters (e.g., thresholds for SI, CV, and weights of each preference function), more robust results can be obtained. However, the task of trying different values would also incur some computational cost to the system, and it can be a subject of further research in the area.

This approach is mainly designated for HEB family design problems and the improvements achieved for the test problem in this chapter serves as a motivation for studying its efficiency for the intended HEB family design problems. The next chapter purpose is planned to expand and assess the performance of our proposed approach for such problems, which are simulation-based complex products that have not been considered for family design before.

It is also to be noted that the proposed method only uses function values (no gradients or other information) in metamodeling and decomposition for platform selection. The total number of function evaluations is limited due to the frugal sampling strategy used by RBF-HDMR. These features make the proposed method attractive for solving problems with expensive black-box functions. The efficiency of this approach will be tested in chapter 6, with the PHEV design problem as a real black-box engineering problem that involve such functions.

# Chapter 6. Application of the proposed PFD method to PHEV Family Design

This chapter provides the details of application of the proposed product family design methodology to the PHEVs family. The first part of the chapter deals with presentation of the selected variants and the basis for this selection, i.e., a review of the market penetration scenarios and purchase behaviors of the potential PHEV buyers. Afterwards, the specification of the design problems will be provided along with target performance values for each objective and each variant. The steps of the proposed PFD methodology will then be applied to the PHEV family in hand.

## 6.1. Introduction

The transportation sector has become the largest consumer of the oil resources in the recent decades, absorbing around 49% of such energy resources, and the estimations show that if the current trend continues, all such resources will be depleted by 2038 [83]. Accordingly, the need for reduction of the emissions to control air pollution and global warming, as well as the importance of reduction in the dependency on oil has directed the attention of the developed countries toward technology advancement for vehicles since a few decades ago.

The conventional ICE-powered vehicles are short of impressive overall efficiency when they are operated in lower loads [84]. Although the pure Electric Vehicles (EV) can be of the highest benefits in terms of fuel replacement and Green House Gas (GHG) emissions elimination, they have limited ability for long driving ranges and the battery technology needs remarkable improvement to enhance their functionality.

The Plug-in Hybrid Electric Vehicles can use electric energy over longer distances as compared to HEVs, which comes from the electric outlet connection feature embedded in their design. Use of larger battery packs helps meeting this target and provides the possibility of charging the battery overnight or off the peak hours.

The trade-off among the PHEV configurations can be quite complex to balance the efficiency, cost, manufacturability, and driveability, and there is no globally optimal configuration when all criteria are considered. However, for any chosen configuration, PHEVs can be constructed through optimizing the component sizes [11].

Another issue of importance coupled to the powertrain design is selection of a proper control strategy. The power management strategy is the algorithm that determines the split of power request between the combustion engine and electric drive. It is a vital factor for the efficiency of a PHEV, as different control strategies result in different performance profiles due to the different basis of choosing operation modes. The operation modes of a PHEV include the Charge Depleting mode (CD) in which the battery is the only source of propulsion, and the Charge Sustaining (CS) mode where the engine is leveraged as an auxiliary power source for keeping the battery State of Charge (SOC) within a specific range. In this case, PHEVs operate similarly to HEVs [12]. There are several types of control strategies, such as: 1) electric vehicle mode where the PHEV runs purely on electric energy and like an EV; 2) the charge depleting mode where the SOC decreases until reaching a specified percentage, and the engine may turn on depending on the torque demand within the SOC discharge window, and when its minimum down time has been met; and 3) the charge sustaining mode where the SOC is controlled to stay in a narrow range [13]. $PHEV_x$ can drive a determined distance ($x$) in the electric vehicle mode (the $1^{st}$ type of control) [85].

Understanding the purchase behaviors of the potential PHEV buyers is the key for designing efficient vehicles, and for promoting the benefits of this new technology. Several efforts have been made in this area, including consumer surveys on the owners of HEVs and PHEVs, projection of PHEV purchase probability for the next decades based on different market penetration scenarios, integration of factors such as the daily driven

mileage and the distance between charges of PHEVs along with assessment of their impact on optimality of a specific design. The research studies in this area span from holistic views such as categorization of the customers based on demographic attributes, to more detailed studies such as simulation-based studies for determining the proper design specifications. The desired variants for the family design of the PHEV powertrains are concluded based on a review of such studies [86-96], which are not presented in detail here, but their summary (i.e., the selected variants for family design assessments) will be provided in Section 6.3.

The scale-based family design is of interest for PHEVs in this study, assuming that all the variants will have the same configuration. The chosen powertrain configuration is the power-split PHEV which takes advantage of both parallel and series configurations. Several methods for designing scalable families have been developed, either assuming a fixed platform, or allowing optimization of the architecture as a part of the design. The Product Platform Concept Exploration Method (PPCEM) by Simpson et al. [30], is among the early developments in this area, leveraging robust design principles to minimize the performance sensitivity to the variation of the scale factors. Fixed platform variables have been assumed in Messac et al. [31], where PPCEM and physical programming have been aggregated for product family design. Commonality was treated as a constraint in the design problem by Fellini et al. [51]. Unknown platform architecture involves the task of platform configuration as well, and Nayak et al. integrated this task with the commonality-performance trade-off problem, known as the Variation-Based Platform Design Methodology (VBPDM) [33]. VBPDM attempts to maximize commonality within the family while achieving the performance requirements by varying the smallest number of design variables. The Product Family Penalty Function (PFPF) is another method developed by Messac et al. [34] to find the best set of platform and scale variables for minimum performance losses of commonalization.

The concept of sensitivity analysis was used by Fellini et al. [39] where the performance losses resulting from sharing were measured through sensitivity analysis for identifying the proper candidates as scale variables. Wei et al. developed two-stage multi-objective optimization-based platform design methodology (TMOPDM) to identify the platform

variables based on their impact on the family performance [40]. Dai and Scott also leveraged the sensitivity analysis to find the performance violations per change of design variables and measured a global sensitivity index (i.e., the average of SI values for each variable over the entire family). By assessing pair-wise commonalization cases for less sensitive variables, they provided a family solution with the least possible performance loss among all the possible sharing profiles [27]. For family design of simulation-based problems that might be challenging due to the large number of function calls, in this dissertation an efficienct PFD strategy was developed and was shown to perform well on a test problem [3] . The proposed method uses a metamodel-based analysis approach which enables creating reliable surrogate modes for expensive black-box design problems, and simultaneously provides useful information about the impact of the variables on the performance of the product, and reveals the correlations among the design variables. This method is used in our study to assess a family of Plug-in Hybrid Electric Vehicles, to evaluate the potential of the chosen variants for family design and platform configuration. The only powertrain family design study that exists so far in the literature is Fellini et al. [45], where a family of three powertrains, including a conventional vehicle, an EV, and a mid-sized parallel-configuration HEV powertrain is assessed. Techniques such as derivative-free global optimization and decomposition techniques are explored for addressing the challenges resulting from the high level of the design complexity in their study. This study is the first of its kind in assessing platform configuration and family design for the PHEV

The PHEV variants are determined based on a vertical leveraging strategy, where there are products for small, medium, and high AER range, spanning from low to high cost according to their performance on AER.

## 6.2. Market study of the PHEVS for variants selection

In order to decide which variations of PHEVs would be the most appealing vehicles to different customer segments, a review of the research in the following areas were conducted in this research: a) the studies which have performed market penetration

scenario analyses; b) the ones that have conducted surveys to analyze customer behavior/preferences and to find more about their perceived benefits in regard to these vehicles; and c) those have assessed customer data from resources such as National Household Transportation Survey (NHTS) for finding the fitting available vehicle designs for various segments. These studies were reviewed and the parts which assist identification of proper PHEV candidates for various segments are summarized in this section.

### 6.2.1. Long-term market of PHEVs

In a comprehensive environmental assessment of electric transportation, the Electric Power Research Institute (EPRI) and the Natural Resources Defense Council (NRDC) examined the greenhouse gas emissions and air quality impacts of plug-in hybrid electric vehicles (PHEV). The purpose of the program was to evaluate the environmental impacts of potentially large numbers of PHEVs in the US over a time period of 2010 to 2050. The year 2010 was assumed to be the first year PHEVs would become available in the U.S. market, while 2050 would allow the technology sufficient time to fully penetrate the U.S. vehicle fleet [97]. Detailed models of the U.S. electric and transportation sectors resulted in creation of a series of scenarios for PHEV fleet penetration over the 2010 to 2050 timeframe [97]. The same study developed three distinct market adoption scenarios, each based on PHEVs entering the market in 2010 and achieving maximum new vehicle market share in 2050, results of which are shown in Table 6-1.

**Table 6-1: Peak PHEV market share for 2050, based on 3 market adoption scenarios [97]**

| **Market share of PHEV fleet by 2050 based on scenario under study** | | **Vehicle Type** | | |
|---|---|---|---|---|
| | | **Conventional** | **Hybrid (HEV)** | **Plug-in Hybrid (PHEV)** |
| **Penetration Scenario** | Low penetration | 56% | 24% | 20% |
| | Medium Penetration | 14% | 24% | 62% |
| | High Penetration | 5% | 15% | 80% |

The global market for Plug in Hybrid Electric Vehicles (PHEVs) is estimated to be 130,000 vehicles by 2015, and North America (NA) is expected to hold a strong market for PHEVs with estimated volumes of 101,000 by 2015, while PHEVs will be introduced to Europe by 2012 with reduction of costs but with less numbers. Japan is likely to lag behind since Japanese market is more inclined towards Fuel Cell Vehicles rather than PHEVs [20]. For US buyers, tax credits[1] of up to $7,500 is provided for each new PHEV purchase starting from 2010, according to the American Recovery and Reinvestment Act of 2009 (ARRA), which was signed into law on February 17, 2009 [89, 98].

General Motors (GM), Toyota, Ford and Daimler Chrysler are to be the primary players in Plug-in Hybrid Market. GM is expected to have a market share of over 50 percent for plug in hybrids by 2015 [20].

### 6.2.2. Drivers' perception study

Institute of Transportation Studies at University of California Davis conducted a study to examine early users' experiences with PHEVs, in 2007 [90]. In their study, 25 to 30 vehicles that had been converted from hybrid electric vehicles (HEVs) to PHEVs were on the road, and through interviews with 23 potential buyers of these vehicles, it was explored how they use and recharged their vehicles, and it was investigated how they think about PHEVs, including the benefits and drawbacks they perceive from the new vehicles. Also, the comments and recommendations of these drivers for future PHEV designs was reported, based on which, the following results have been obtained: The preferred All Electric Range (AER) is between 20 to 40 miles, though some drivers have also preferred higher AERs. 20 miles of AER seems to be the minimal acceptable amount according to this study [90]. However, this is an observation from a sample of the potential users, and not all of them. Even for drivers who needed the vehicle for less than 10 miles of driving per day, it seemed that 20 miles is their perception of a minimum acceptable AER. A few users acknowledged interest in PHEVs with lower AER, but they explained AER below 20 miles

[1] US Congress has approved tax credits amounting to $758 million to subsidize the purchase of up to 250,000 PHEVs over the next few years, which amounts to a range from $2500 to $7500 per vehicle, depending on vehicle attributes.

was acceptable only in initial vehicles, and it is expected that manufacturers improve PHEV technology.

### 6.2.3. PHEV purchase probability projection study

Oak Ridge National Laboratory (ORNL) developed a model for projecting the probabilities of purchasing advanced vehicle technologies, as a function of consumer attributes, costs, performance, and energy prices and policies. The developed model is called Market Acceptance of Advanced Automotive Technologies ($MA^3T$), and it is developed for the US DOE to support analyses of vehicle technology policies. It draws information on households and their characteristics from the U.S. census data and national travel surveys, obtains projections of total vehicle sales, and energy prices from the Department of Energy's Energy Information Administration (DOE/EIA). The analysis is enabled through simulation of consumer purchase behavior for the new energy vehicles (including PHEVs), through using vehicle technology characterizations developed by Argonne National Laboratory [86]. All U.S. new light-duty vehicles (LDV) consumers are grouped by this model based on six dimensions (region, area, attitude toward technology risk, vehicle usage intensity, home charge availability, and work charge availability) into 1,458 segments. According to this model, the variants of Spark Ignition (SI) PHEV comes in three types based on their on-board electricity storage capacity and electric motor power: (1) 10-mile all electric range (AER), (2) 20-mile AER, and (3) 40-mile AER. All the PHEV designs (SI PHEV10, SI PHEV20, and SI PHEV40) are blended hybrids with limited all-electric capabilities.

The $MA^3T$ model projects purchase probabilities for PHEV according to disaggregation of the US household Light Duty Vehicle market, and a reference market segment is defined as the set of early adopters of the new technology vehicles, living in the suburban areas, driving frequently, having access to home recharge, and not having access to recharging at work. By variation of these conditions, new segments are formed and compared to this reference segment. A subset of the National Household Travel Survey (NHTS) 2001 data containing 3755 new car owners that work full-time driving to work and rarely working at home, have been selected and clustered into three levels of

vehicle usage intensity. A data set including their weight in the population, annual usage of the primary vehicle, commuting distances, and associated region and residential area has been extracted and 3755 gamma distributions of daily vehicle usage are then estimated by following the modeled relationship between the distribution parameters and the daily usage mean and mode. The shares of these driver types by region and area are estimated from the NHTS2001, and usage levels are as follows:

- Modest-Driver (driving 8,656 miles annually)
- Average-Driver (16,068 miles)
- Frequent-Driver (28,288 miles)

Four fuel efficiency estimates for PHEVs (CD and CS modes, UDDS and HWFET cycles) and 2 electricity efficiency estimates (CD only, 2 test cycles) have been applied to the selected PHEV*x* vehicles, and the results show that frequent drivers benefit more on fuel saving by owning a PHEV and thus frequent drivers may be more likely PHEV buyers [86].

### 6.2.4. Cost-benefit study for PHEVs

National Renewable Energy Laboratory (NREL) conducted a cost-benefit study on PHEVS in order to compare them to conventional vehicles in terms of vehicle cost, and energy cost, as well as Petroleum consumptions [91]. PHEV2, 5, 10, 20, 30, 40, 50, and 60 vehicles were considered in the study, through developing a performance model which allows component sizing based on performance constraints, and provides desired output such as energy use through application of the UDDS drive cycle. A number of criteria have been provided for comparing PHEVs to conventional vehicles, which can be used as means of measuring performance and deviations from a target performance for our powertrain family design problem.

#### Daily mileage

In order to satisfy more customer groups, it is important to consider the mileage or daily driven distance of the potential drivers. Figure 6-1 shows the US vehicle daily mileage

distribution based on data collected in the 1995 National Personal Transportation Survey (NPTS). The majority of daily mileages are relatively short, with 50% of days being less than 30 miles (48 km).

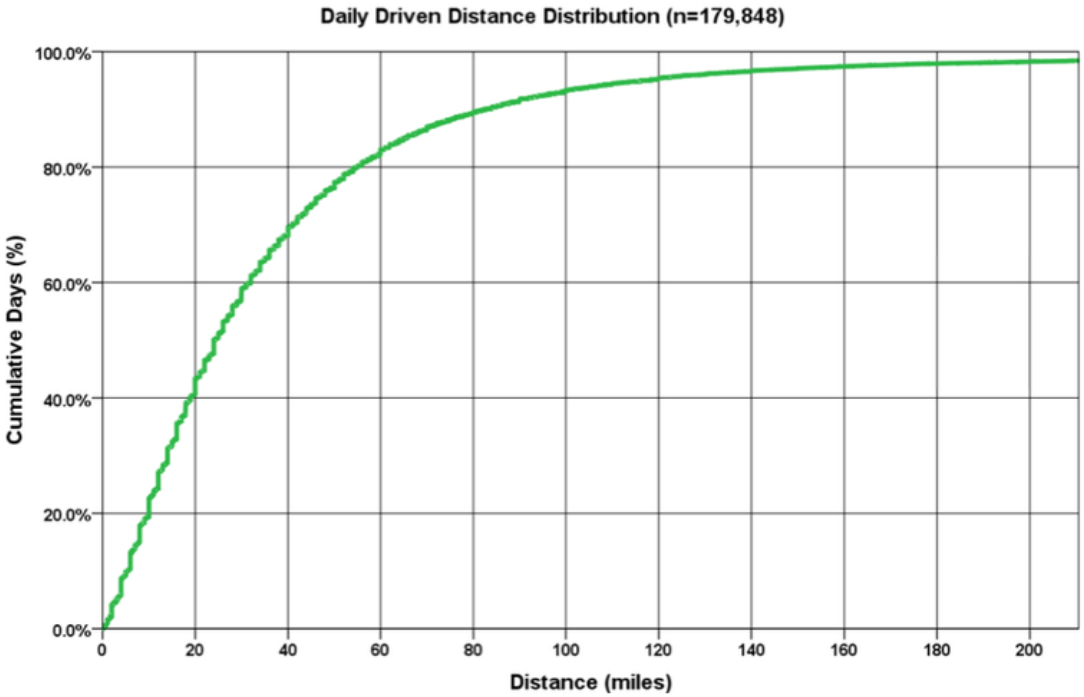


**Figure 6-1: Daily mileage distribution for US motorists based on the 1995 National Personal Transportation Survey [91]**

The Utility Factor (UF) curve for the 1995 NPTS data is shown in the same figure, representing the fraction of total vehicle-miles-traveled (VMT) that occurs within the first D miles of daily travel. For example, for a distance of 30 miles (48 km), the utility factor is approximately 40%. This means that a PHEV30 can displace Petroleum consumption equivalent to 40% of VMT, (assuming the vehicle is fully recharged each day). Similarly, an all-electric PHEV60 can displace about 60%. This low- daily-mileage characteristic shows that PHEVs have potential to displace a large fraction of per-vehicle Petroleum consumption. The daily mileage or kilometers driven in US are classified into three groups in [99], and the trip share of each interval can be shown in Table 6-2.

**Table 6-2: U.S. travel statistics as a function of daily distance driven**

| Daily Distance (Km) | 0-32 | 32-64 | > 64 | Total |
|---|---|---|---|---|
| **Trip Share (%)** | 60.0 | 21.4 | 18.6 | 100 |
| **Share of time spent** | 40.8 | 23.5 | 35.7 | 100 |

According to the data in Table 6-2, it is suggested that either that universal powertrains have to be designed with great versatility or that if a diversity of powertrains is offered in the future, the need for the extra low and high AER values and the fast may be greater than the need for those in the middle.

### Emission Targets in different regions

As mentioned earlier in this section, emission targets are set by different organizations and governments in order to foster sustainable mobility and environmental considerations over the coming years and decades. According to [99], European Union has announced a long-term $CO_2$ emission target for 2020, while US has chosen a more aggressive approach essentially pulling the 2020 National Highway Traffic Safety Administration (NHTSA) target forward to 2016. Japan has only announced a medium-term $CO_2$ emission target and China had set an ambitious $CO_2$ emission target for 2015. By sponsorship of the U.S. Department of Energy's Office of Energy Efficiency and Renewable Energy (EERE), Argonne National Laboratory (ANL) has developed a full life-cycle model called GREET (Greenhouse gases, Regulated Emissions, and Energy use in Transportation), in order to evaluate various vehicle and fuel combinations [100].

### Target fuel economy

The PHEV fuel economy and operating costs are measured and reported using a procedure based on a modification of the Society of Automotive Engineers' (SAE) J1711 Recommended Practice for Measuring the Exhaust Emissions and Fuel Economy of Hybrid-Electric Vehicles [101]. The fuel and electricity use in both CD and CS-modes are measured and weighted according to the Utility Factor (UF), assuming PHEVs are fully-

recharged each day. The measurability of the fuel economy, however, is subject to applying a driving scheme which is categorized as drive cycles, explained below.

Studies show that the markets for HEVs and PHEVs are complementary rather than competitive [99]. PHEVs will be the best choice for suburbanites driving at higher speeds and are suitable for replacing the conventional vehicles (CV) in the suburbs, since garages are desirable locations for plugging in overnight, usually found in suburbia. HEVs will be the best choice for driving at low speeds in congested urban environments. The PHEV option has the potential to expand the market for the fundamental HEV powertrain further into suburbs and small towns. The estimates indicate that the comparative advantage of the PHEV technology will be in suburbia in the United States and generally in upper-income nations and communities with low densities where single-family homes and garages are relatively common. For those who travel long distances per day at relatively high speed, the emerging clean compression ignition, direct injection fuel-distillated vehicles (CIDI) technology may be more desirable than PHEVs [99].

According to MA$^3$T model, the probability of different customer segments to buy PHEVs is the highest for those in urban areas, and those with ability of work recharge. The objective has been to estimate the distribution of daily vehicle usage. Since longitudinal travel data have not been readily available, especially nationwide, the gamma distribution has been proposed for vehicle daily usage and then maximum likelihood estimates of the parameters are obtained based on longitudinal refueling survey data of over 2000 vehicles.

The purchase probabilities for different market segments are subject to different conditions. The consumers in the reference segment become more likely over time to buy a PHEV mainly due to the technology progress that makes PHEVs increasingly cost competitive, but other factors such as improved charging availability, purchase tax credit, and technology novelty also play roles. The temporary and sudden drop of purchase probability is due to the expiration of the PHEV tax incentive. Urban consumers may be more likely to buy a PHEV than suburban consumers because of higher share of stop-and-go driving and therefore larger fuel-saving benefits [86].

In regard to components of the powertrain, the results of simulation performed by Hauffe et al. [102] show that battery weight is a key factor affecting the cost, emissions, and fuel economy of PHEVs. Their recommendation is that best choice of PHEV battery capacity depends on the driven distance between charges, as well as the structural weight required to carry the batteries. They also suggest that since 60% of U.S. passenger vehicle miles are traveled by vehicles driving less than 30 miles per day, cost and GHG emissions can be potentially reduced by appropriate battery capacity sizing to achieve a 30 mile range. On the other hand, there exist three potential complications according to the same study: 1) The significance of the variance in miles traveled per day can adversely affect the optimality of the capacity designed for the average distance; 2) Irregular charging behavior could lead to significantly longer distances between charges than the average daily distances, and thus it might be risky to assume access to charging once a day; 3) Conversely, installation of widespread charging infrastructure in public parking places would enable charging more than once per day, enabling shorter distances between charges [102], which is possibly the case for over-work charging times.

While some analysts view AER as a critical advantage of PHEVs, an interesting observation is recorded in [90], that is the questionability of the AER necessity. PHEV without AER would still deliver fuel economy benefits and could offer faster acceleration and higher top speed [103]. It is suggested that $PHEV_0$ (i.e., similar to HEV, but with a larger batter pack to use less fuel during a trip) would have acceptable potential to penetrate market compared to those with All-Electric driving capability. This is because delivering quick acceleration and operation over a wide range of speeds in all-electric mode requires a larger electric motor as well as a battery with high power output. In contrast, a PHEV that only operates in “blended” mode can constantly provide propulsion power from its internal combustion engine, allowing the use of a smaller electric motor and decreasing the peak power requirements for the battery [90]. As a result, a $PHEV_0$ is likely to be less expensive than a PHEV offering AER and thus, for those consumers who place less value on AER, being a more desirable option. This conclusion is another side of the case, as compared to the drivers perception study results in [90].

Another observation is the multi-objective nature of the PHEV selection problems. Not only do many parameters affect the performance, but also the performance can be defined and assessed from various aspects. Shaiu et al. [104] found that for drivers with distances of less than 10 miles between charging, a PHEV of about 7 miles of AER will result in the least cost, GHG emissions and fuel consumptions, while for distances between 10-20 miles (between charging), depending on the objective, the optimality of PHEV will be different; PHEV7 has the least life time cost, while $PHEV_{20}$ has the least GHG emissions and fuel consumption. Finally, for moderate to long distances between charging (20-100 miles), while PHEVs release less GHG emissions, but HEVs are of less cost. Their study suggests that the small-capacity PHEVs are dominant over larger capacity PHEVs in a wide variety of scenarios, and conclude that government incentives for increasing adoption of PHEVs may be best targeted toward adoption of small-capacity PHEVs by urban drivers who are able to charge frequently [104].

## 6.3. Selected variants for PHEV powertrain family design

As it was mentioned earlier in this study, the PHEVs are varied in the AER range, in a scale of 10 to 60 miles and according to [90], PHEVs 20 to 40 miles are the more desired ones. Some studies have also recommended a case of PHEVs less than 10 for the sake of cost, for particular drivers. Since it is desired to provide a family satisfying more customers, the attempt is to pick the best options among the entire assessed range to include in our product family design study. The basic assumptions made earlier in this regard, includes the powertrain configuration which has been decided to be a power-split configuration that takes advantage of both series, and parallel ones.

As noted earlier in this section, based on Shiau et al. [1], the optimality of the *x* miles and the chosen vehicle (between HEV and PHEVs) highly depends on what objective is under consideration. As such, the vehicle with minimized GHG emissions might be different from the one with minimized life time cost or the fuel consumption. Based on a review of the studies mentioned above, the following variants of PHEVs with a nominal AER of 7, 20, 30, 40, and 60 miles are identified and selected for platform configuration

assessment in this study with a specified range of fuel economy, emissions, and powertrain cost to demonstrate our approach. The following assumptions, considerations and measurements apply to the selected variants [104]:

- The general configuration settings follow the design of Toyota MY04 Prius as modeled in PSAT, with power-split powertrain configuration which is consistent with the intended configuration of our study.
- The studied battery is Saft Li-Ion which is widely used and evaluated in different studies for their great potential as energy storage devices for PHEV due to higher energy density and specific energy.
- A thorough simulation-based study is done for finding the optimal PHEV specifications for meeting different ranges of AER through an extended-range charge-depleting control strategy (which is a modification to the power split hybrid control strategy in PSAT).

The three objectives (i.e., fuel economy, emissions, and powertrain cost) are integrated into an aggregated objective function (AOF), based on the principles adopted from [105]. It should be noted that in case that the optimization convergence would turn out to be challenging, larger objective values can be replaced by the rows labeled as “worst” in Table 6-3 for the cost and emissions. The same applies for the fuel economy (where lower values for the worst value can be allowed, depending on the subsequent optimization challenges). The AOF is created from integrating the preference functions for each design objective, where each preference function attempts to find a value close to the best value, and not more (not less) than the worst value in Table 6-3. For example, for $PHEV_7$, the preference for fuel economy indicates that any fuel economy more than 90 miles/gallon can be considered satisfactory, with a high preference, while any fuel economy below 70 miles/gallon is considered unacceptable, or with a low preference.

The weighted aggregation of these three functions allows a single-objective optimization. The AOF of this problem and the preference functions are as follows:

$$\mathcal{P}_s = \left(\frac{\omega_1 {\alpha_1}^s + \omega_2 {\alpha_2}^s + \omega_3 {\alpha_3}^s}{\omega_1 + \omega_2 + \omega_3}\right)^{1/s} \quad (6\text{-}1)$$

$$\textit{Fuel Efficiency } \alpha_1 = \frac{f_1 - f_{1\_worst}}{f_{1\_Best} - f_{1\_worst}} \quad (6\text{-}2)$$

$$\textit{Cost } \alpha_2 = \frac{f_{2\_worst} - f_2}{f_{2\_worst} - f_{2\_Best}} \quad (6\text{-}3)$$

$$\textit{CO2 Emissions } \alpha_3 = \frac{f_{3\_worst} - f_3}{f_{3\_worst} - f_{3\_Best}} \quad (6\text{-}4)$$

The cost functions are mostly adopted from the literature (i.e., [106, 107]) and the objectives of interest include the operating cost, the ESS cost, motor, and engine cost. The weights are set to be equal (i.e., 1/3), and s=-1.

The design variables and the ranges are as follows:

1. Upper limit for SOC ($0.6 \leq x_1 \leq 0.95$)
2. Lower limit for SOC ($0.25 \leq x_2 \leq 0.5$)
3. Engine size ($40 \leq x_3 \leq 85$) kW
4. Motor size ($30 \leq x_4 \leq 75$) kW
5. Number of Battery modules ($20 \leq x_5 \leq 143$)
6. Power-split device ratio: $\frac{x_6}{x_7} \in \{2.6, 2.75, 2.9, 3.0, 3.2, 3.25, 3.4\}$

Depending on the certain needs in this study, the cost functions have been modified to represent costs in terms of other parameters such as the engine and motor sizes. The new functions have been obtained through interpolation of the cost functions in the literature, and then curves have been fit to the data obtained from the interpolations.

**Table 6-3: Selected range for different objectives**

| Variant | 1 | 2 | 3 | 4 | 5 |
|---|---|---|---|---|---|
| **Fuel economy (miles/gallon)** | | | | | |
| **Best** | 90 | 85 | 80 | 75 | 65 |
| **Worst** | 75 | 65 | 60 | 55 | 42 |
| **Cost (K$)** | | | | | |
| **Best** | 2.5 | 3 | 3.3 | 3.6 | 4 |
| **Worst** | 3 | 3.5 | 4 | 4.5 | 5 |
| **Emission (grams/mile)** | | | | | |
| **Best** | 130 | 150 | 165 | 180 | 205 |
| **Worst** | 145 | 170 | 185 | 200 | 230 |

The cost equations are as follows:

$$Cost = Operating\ Cost + ESS\ Cost + Motor\ Cost + Engine\ Cost \tag{6-5}$$

$$ESS\ Cost = 651.2 \times Battery\ Energy + 680 \tag{6-6}$$

$$Engine\ Cost = 145 \times 10^{-5} \times Engine\ Max\ Power + 531 \tag{6-7}$$

$$Motor\ Cost = 217 \times 10^{-4} \times Motor\ Max\ Power + 425 \tag{6-8}$$

$$Operating\ cost = \frac{1}{Distiance\ in\ miles} \times \left(\frac{Distance_e \times cost_e}{\eta_{CD} \times \eta_{Ch}} + \frac{Distance_f \times cost_f}{\eta_{CS}}\right) \tag{6-9}$$

$Distance_e$: The distance traveled on electric energy

$Distance_f$: The distance traveled purely on fuel

$cost_e$: The cost of electricity= 0.11 $/Kwh

$cost_f$: The cost of gasoline= 3 $/gallon

$\eta_{CD}$: Electrical Efficiency of the vehicle in the charge-depleting mode: 5.2 miles/Kwh

$\eta_{Ch}$: Charging efficiency= 0.88

$\eta_{CS}$: Fuel Efficiency in the charge-sustaining mode that is 59.5 miles/gallon.

The ESS cost is for the Li-ion battery based on the battery energy. The unit prices are adopted from US prices [52]. The control strategy parameters are decided to be fixed except the upper and lower SOC bounds, and the decision points follow a default strategy as created by the Argonne National Library in the PSAT.

The fuel efficiency is calculated based on the logic adapted from [101], where SAE J1711 Recommended Practice has been applied. The required equations for obtaining fuel economy value is presented below.

$Distiance\ in\ miles$: The entire miles of the driven distance

$$mpg_{CS} = \frac{D}{V_{fuel}} \tag{6-10}$$

$$mpg_{CD} = \frac{D}{V_{fuel} + \frac{E_{charge}}{E_{gasoline}}} \tag{6-11}$$

$D$ is the distance traveled and $V_{fuel}$ is the volume of consumed fuel. $E_{charge}$ is required electrical recharge energy in kilowatt-hours, and $E_{gasoline}$ is constant and equal to 33.44 kWh/gal.

The weighted CD-mile per gallon rating is then calculated as follows:

$$mpg_{CD,UF} = \frac{D}{\frac{UF}{mpg_{CD}} + \frac{(1-UF)}{mpg_{CS}}} \quad (6\text{-}12)$$

*UF* is the utility factor, determined based on the findings indicating that 50% of fleet VMT occurs within the first 40 miles of travel [101]. Based on the standard test cycles of UDDS, a full charge test distance of 30 miles is used to determine the $mpg_{CD}$, and the utility factor for this value is 0.42.

The final step according to SAE J1711 is to calculate the cycle fuel economy based on the following equation:

$$mpg_{Cycle} = \frac{2}{\frac{1}{mpg_{CD,UF}} + \frac{1}{mpg_{CS}}} \quad (6\text{-}13)$$

The other dynamic specifications applied in the simulations are shown in Table 6-4. The design variables in our study include a set of component sizes, along with two variables from the control strategy. The control strategy is a blended strategy that enables engine to assist in the propulsion. In this strategy, the vehicle normally operates in the CD mode, but if the torque demand exceeds a specific value, even though the SOC might have not reached the lower limit, the engine is started to assist in propulsion and then turned off as soon as the required torque is reached, resulting a mix of charge depletion and charge sustaining modes.

**Table 6-4: The Vehicle dynamics specifications for simulation**

| Parameter | Feature/Value |
|---|---|
| **Drag Coefficient** | 0.26 |
| **Frontal Area** | 2.25 $m^2$ |
| **Glider mass** | 1228 *kg* |
| **Engine** | 1.5-L, 40-85 kW Atkinson 4 cylinder;<br>5000 rpm Maximum Speed |
| **Motor** | 30-75 kW, 400 Nm,<br>6500 rpm Maximum Speed |
| **Generator** | 30 kW, 10,000 rpm Maximum Speed |
| **Battery** | Li-ion Saft, Series, 3 cells per module, 20-143 NBM |
| **Final Drive Ratio** | 2.6-3.4 |
| **Wheel Radius [m]** | 0.305 |

We assess a range of possible values for the power-split ratio, which span from 2.6 to 3.4, according to a study in this area [107] that leveraged Dynamic Programming to find a range of optimal ratios that can split the torque in the component sizes such that the fuel consumption is minimized and the vehicle performance stays within a desired range. For the sake of maintaining discrete nature of the power-split ratio, we defined a new variable as the ratio of the ring gear to the sun gear, $\frac{x_6}{x_7}$. The sensitivity analysis, however, has been performed on a set of seven variables to allow us analyze the impact of each gear ratio separately. The constraints are shown in Table 6-5.

## 6.4. Platform candidates identification

By obtaining our validated simulation model of the PHEVs (As shown in Appendix B), along with specified ranges for the objectives of designing each variant, the next step is identification of the appropriate platform candidate set. The information on the sensitivity of the variables is obtained through a strategy that combines the Radial Basis Function-High Dimensional Model Representation (RBF-HDMR) and the Random Sample HDMR (RS-HDMR) metamodeling techniques to provide a measure of the correlations among variables and impact of each variable on the objective function.

**Table 6-5: The system constraints for the PHEV design problem**

| | |
|---|---|
| Time from 0 to 60 mile/hour speed | $t_1 \leq 12$ seconds |
| Time from 0 to 85 mile/hour speed | $t_2 \leq 23.4$ seconds |
| Time from 40 to 60 mile/hour speed | $t_3 \leq 5.3$ seconds |
| Maximum acceleration | 0.5×g ≤Max acceleration |
| Traveled distance within the first 5 seconds | 140 ft ≤ 5S distance |
| Maximum grade ability percentage at 55 mile/hr | 6.5% ≤Max %grade |
| Maximum speed | 85 mph ≤ Max speed |
| All Electric Range | AER = 7, 20, 30, 40, 60 miles |

Metamodels are built based on sampling a number of points (or input-output pairs) which allow finding information about the structure of the function under study. Since the required number of samples grows exponentially by increasing the number of variables, extensive sampling can impose remarkable computational costs to the system. High Dimensional Model Representation (HDMR), developed by Sobol [109], is an efficient metamodeling approach, as used in [3] for platform configuration purposes. The component functions in HDMR are orthogonal and optimal in HDMR, as the functions are chosen to minimize the least square approximation error. The RBF-HDMR uses the RBF function to

model each of the component functions in HDMR [73]. The needed component functions will be identified through test points, and then sample points will be adaptively added until obtaining a desired accuracy. In case of no or very small correlation between two variables, the corresponding component function will not be built in the model, and no further samples will be taken from the corresponding sub-space. The variable correlations are shown to be well estimated by use of this technique [67]. Other specifications for design are consistent to Toyota MY04 Prius, as reported in Table 6-6.

**Table 6-6: The general vehicle specifications for all the variants (from [104])**

| Component | Specification | Component | Specification |
|---|---|---|---|
| ***Engine*** | *Baseline Size: 57kW 1.4L 4-Cylinder* | ***Nominal output voltage[1]*** | *3.6 V* |
| ***Motor*** | *Baseline: 50 kW Permanent Magnet* | ***Battery packaging weight factor[2]*** | *1.25* |
| ***Battery*** | *Saft Li-Ion Package* | ***Module weight (3-cell)*** | *0.65 Kg* |
| ***# of cells per module*** | *3 (in Series)* | ***Control strategy*** | *Hybrid Power split* |
| ***Cell Specific Energy*** | *100 Wh/Kg* | ***SOC range*** | *30-70%* |
| ***Cell Weight*** | *0.173 Kg* | ***SOC for switching to CS*** | *35%* |
| ***Cell capacity*** | *6 Ah* | | |

The nomenclature of design variables and the objectives of interest in the PHEV design problem have been listed in Table 6-7.

[1] It shall be noted that these battery characteristics are per cell, and the cumulative parameters such as capacity are scaled for vehicles of higher AER, on a linear basis.

[2] The total battery size and capacity can be scaled by specifying an integer number of battery modules.

***Preference functions (α):***

Depending on the desired range of efficiency, powertrain cost, and expected emissions, the acceptable range of each objective will be different, as shown in the tables above.

1. Fuel Efficiency ($\alpha_1$):

$$\alpha_1 = \frac{f_1 - f_{1\_worst}}{f_{1\_Best} - f_{1\_worst}} \quad (6\text{-}14)$$

2. Cost ($\alpha_2$):

$$\alpha_2 = \frac{f_{2\_worst} - f_2}{f_{2\_worst} - f_{2\_Best}} \quad (6\text{-}15)$$

3. *$CO_2$* Emissions ($\alpha_3$):

$$\alpha_3 = \frac{f_{3\_worst} - f_3}{f_{3\_worst} - f_{3\_Best}} \quad (6\text{-}16)$$

**Table 6-7: The Nomenclature for the PHEV Design Problem**

| | | | |
|---|---|---|---|
| $x_1$ | *Upper limit for SOC [%]* | $\frac{x_6}{x_7}$ | *Power-split device ratio [ring gear/sun gear]* |
| $x_2$ | *Lower limit for SOC [%]* | $f_1$ | *Fuel Economy [miles/gallon]* |
| $x_3$ | *Engine size [KW]* | $f_2$ | *Powertrain cost [$]* |
| $x_4$ | *Motor size [KW]* | $f_3$ | *Co2 emission [g/mile]* |
| $x_5$ | *Number of Battery modules* | *AOF* | *Aggregated objective function* |

While the best weights and value for the level of compensation $s$ can be identified through a trade-off strategy, however in this study since the focus is on finding information on the relation and impacts of the design variables rather than performing optimization, the weights are set to be equal, i.e, $^1/_3$, and $s$ is set to -1.

## 6.5. Application of the PFD methodology to the PHEV family design problem

### Step 1: Individual optimization of variants

At this step, each variant is optimized toward its specific objective function. The algorithm used for optimizing the variants is TRMPS2.

#### *TRMPS2 algorithm*

Mode Pursing Sampling (MPS) is a global optimization algorithm for expensive simulation-based optimization with the ability of performing global optimization [110]. MPS has been tested and is shown to be effective and efficient for low-dimensional design problems. The trust-region based MPS algorithm was later developed to integrate the concept of trust regions into the framework of the PMS algorithm, which was shown to dramatically improve the performance and efficiency of high dimensional problems. The benchmark against Genetic Algorithm (GA), Dividing Rectangles (DIRECT), and Efficient Global Optimization (EGO), through a suite of standard test problems and an engineering design problem by Cheng et al. [111] show that on average it performs better than GA, EGO, DIRECT, and MPS for high dimensional, expensive, and black box (HEB) problems.

MPS relies on stochastic sampling and metamodeling as the primary techniques in order to do optimization. Random sampling is used in MPS to generate a small set of expensive points from the black-box function, and uses them afterwards to create a metamodel of the objective function. A large number of points are fitted onto the metamodel in a discriminative sampling process first and then the metamodel points are used to pick new expensive points and add to the old expensive points set. By identifying the most promising sub-region of the search space, a quadratic model is constructed in the sub-region, and local optimization is performed on this sub-region by using the obtained quadratic model.

For nonlinear high dimensional problems that are highly constrained or are of more than ten design variables, the performance of MPS decreases due to generating a RBF

metamodel in each iteration and using all of the expensive points available which dramatically increases with each iteration. The computational cost of MPS and the required CPU time and memory to store the large matrices makes it not as much efficient for complex problems like the PHEV multi-objective simulation-based design problem.

The TRMPS2 algorithm forms two hyper-quadrilaterals or regions called S and B, which vary in size at different stages of the optimization. At the beginning of the optimization, in both trust regions processes similar to those of MPS are started. If a better optimum point is discovered through the searches, then S expands to let exploration of further areas and avoiding falling into a local minimum region, and B contracts to allow further exploitation of that promising region [111]. If the search does not improve within a specific number of iterations, S contracts to exploit the promising region where seems to have the best points so far, and B expands for better exploration of the search space. The TRMPS2 uses this dynamic balance between exploitation and exploration to increase the efficiency of the sampling in the search space. Complete set of details and parameters for this algorithm can be found in [111]. It is assumed that the distance between charges is beyond the AER considerations, for example more than 60 miles, and by applying the TRMPS2 algorithm to the PHEV design problem, the results shown in Table 6-8 are obtained.

GHG emissions in Shiau study [112] decrease for larger PHEVs. However, for driving a longer distance on a single charge, specifically for blended control strategy used in this research, the total emissions are not far from expectation to increase for bigger AER PHEVs. Since the SOC decreases and ultimately results in more frequent use of engine for longer AER values, it makes sense to have increased GHG emissions and fuel consumption for larger x values in PHEVx. The GHG and fuel consumption are in line to each other. The cost increases for the increments in AER value, but since the AOF is an aggregation of the three objectives, the trends in its value may not be linear.

**Table 6-8: Individual variants design optimization solutions**

| Variant<br>Design Variable | P1 | P2 | P3 | P4 | P5 |
|---|---|---|---|---|---|
| $x_1$ | 0.79 | 0.94 | 0.94 | 0.90 | 0.93 |
| $x_2$ | 0.25 | 0.28 | 0.34 | 0.34 | 0.30 |
| $x_3$ | 83885 | 84697 | 84945 | 84366 | 83717 |
| $x_4$ | 48346 | 50125 | 53623 | 54033 | 55467 |
| $x_5$ | 20 | 42 | 71 | 75 | 88 |
| $x_6$ | 78 | 79 | 82 | 81 | 80 |
| $x_7$ | 29 | 27 | 27 | 27 | 25 |
| **Fuel Efficiency (Miles/gallon)** | 198.4 | 192.73 | 187.15 | 113.9 | 97.03 |
| **Cost ($)** | 2820.8 | 2860.6 | 2936.9 | 2944.9 | 2975.1 |
| **CO2 Emissions (Grams/mile)** | 154.47 | 155.94 | 157.78 | 170.7 | 180.83 |
| **AOF** | 2.25 | 1.27 | 1.93 | 1.87 | 1.74 |

### *Convergence of optimization*

Figure 6-2 to Figure 6-6 show the reasonable convergence trend for all the variants over 700 iterations.

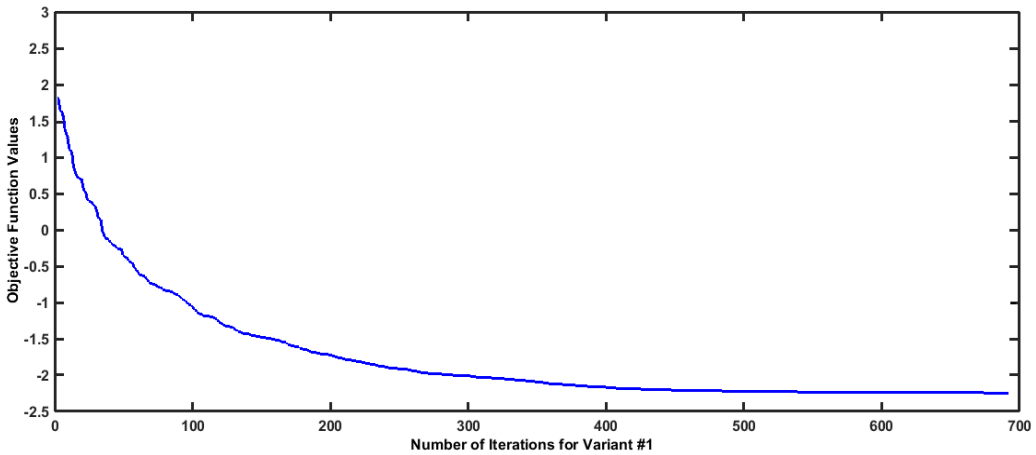


**Figure 6-2: Convergence diagram for optimization of $PHEV_7$**

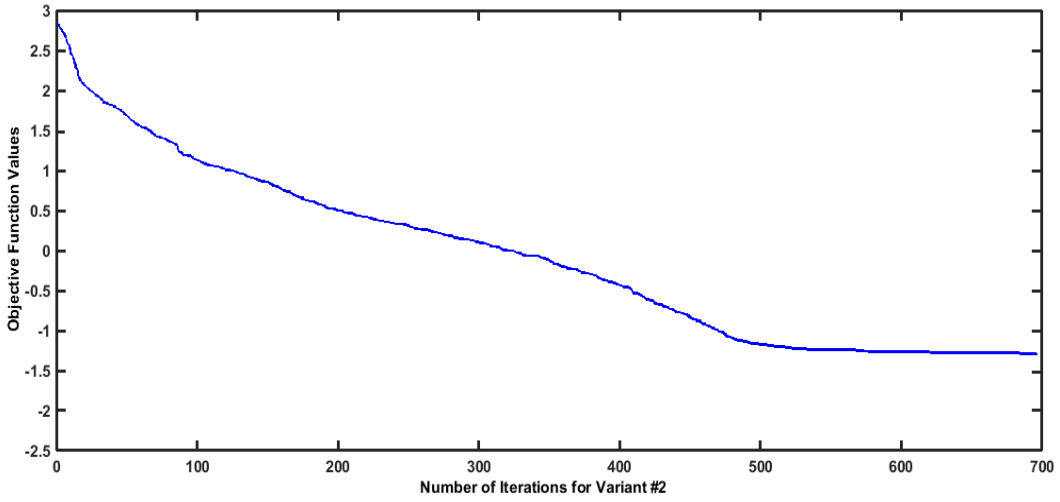


**Figure 6-3: Convergence diagram for optimization of $PHEV_{20}$**

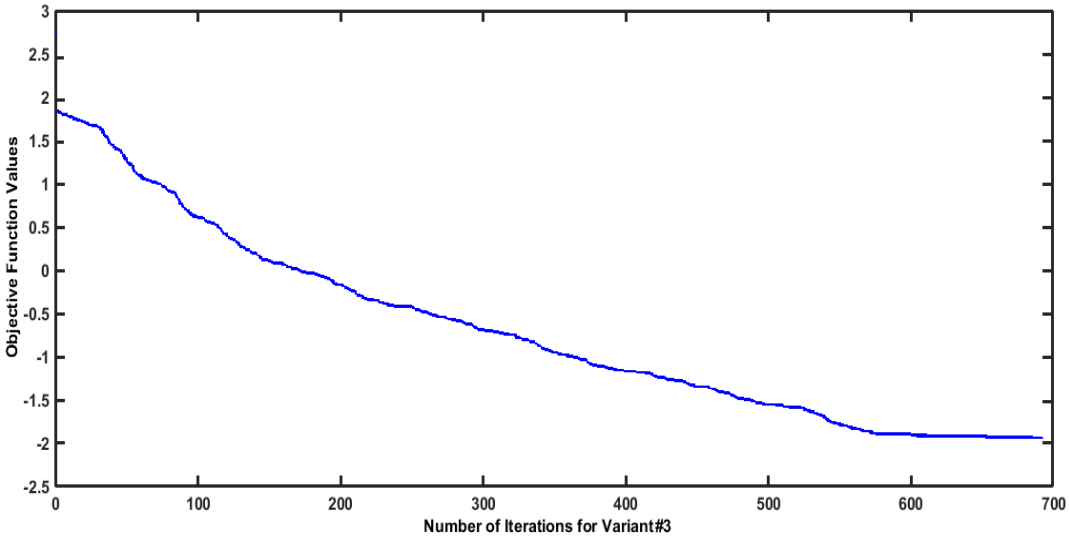


**Figure 6-4: Convergence diagram for optimization of $PHEV_{30}$**

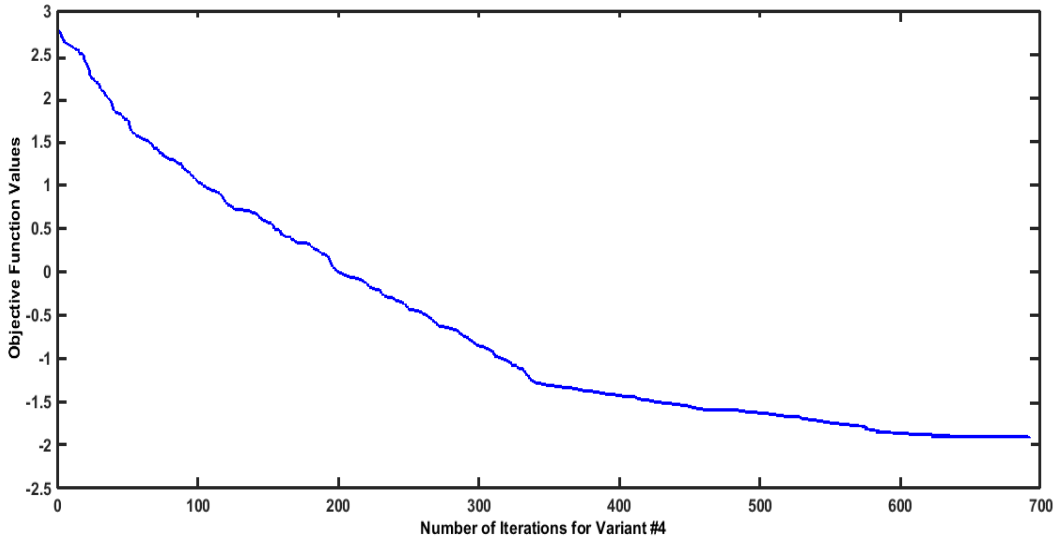


**Figure 6-5: Convergence diagram for optimization of $PHEV_{40}$**

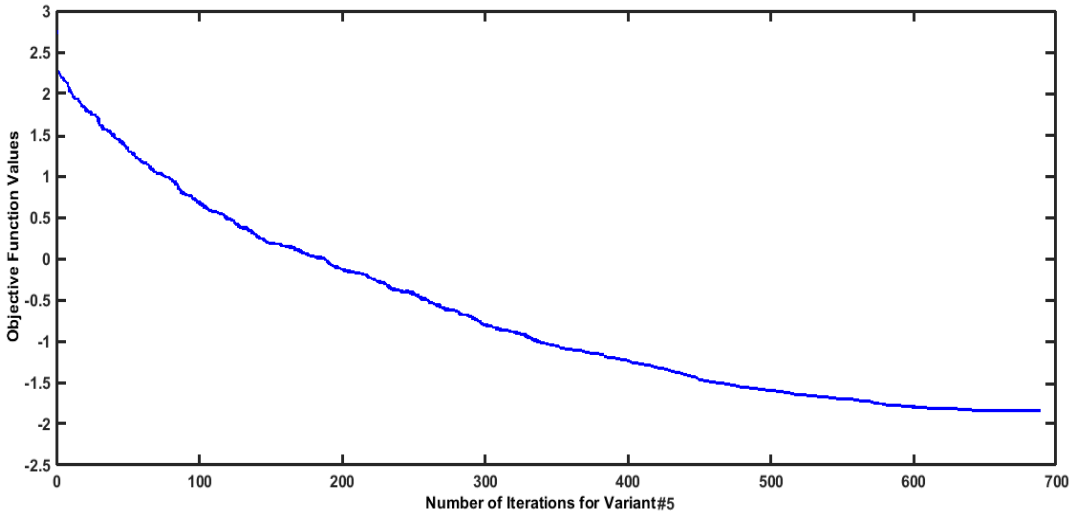


**Figure 6-6: Convergence diagram for optimization of $PHEV_{60}$**

The first variant optimization was run for 1000 iterations, but since from about the $600^{th}$ iteration the objective function value remained fixed around the optima, it was decided to reduce the number of iterations for the sake of avoiding excessive and unnecessary optimization run time. As the convergence diagrams above show, the 700 is a reasonable number of iterations which has resulted in an acceptable level of convergence for all the variants in our first optimization stage.

## Step2: Platform candidates set selection

After obtaining the sensitivity index values for each variable in each variant, a global SI is calculated for each variable, which is the average of the five local SI values. The obtained local and global SI's are presented in Table 6-9. Similarly, by collecting the maximum of the off-diagonal elements in the S matrix of each variant, the quantified correlations (QC) among the variables for each of the five variants, i.e., PHEV7, PHEV 20, PHEV 30, PHEV 40, and PHEV60 are obtained as shown in Table 6-10.

**Table 6-9: Local and Global Sensitivities of variables in PHEV family design problem**

| Design Variable | $x_1$ | $x_2$ | $x_3$ | $x_4$ | $x_5$ | $x_6$ | $x_7$ |
|---|---|---|---|---|---|---|---|
| SI(1) | 0.0008 | 0.0003 | 0.0025 | 0.9242 | 0.0006 | 0.0030 | 0.0003 |
| SI(2) | 0.0086 | 0.0139 | 0.0150 | 0.5933 | 0.0105 | 0.0039 | 0.0110 |
| SI(3) | 0.0098 | 0.0083 | 0.0321 | 0.2588 | 0.0095 | 0.0196 | 0.0030 |
| SI(4) | 0.0110 | 0.0114 | 0.0468 | 0.1048 | 0.0126 | 0.0014 | 0.0015 |
| SI(5) | 0.0151 | 0.0395 | 0.0444 | 0.0282 | 0.0372 | 0.0132 | 0.0265 |
| Global SI | 0.0091 | 0.0147 | 0.0282 | 0.3819 | 0.0141 | 0.0082 | 0.0085 |

**Table 6-10: Quantified Correlation of variables in the PHEV family design problem**

| Design Variable | $x_1$ | $x_2$ | $x_3$ | $x_4$ | $x_5$ | $x_6$ | $x_7$ |
|---|---|---|---|---|---|---|---|
| QC (1) | 0.0060 | 0.0055 | 0.0067 | 0.0066 | 0.0067 | 0.0066 | 0.0034 |
| QC (2) | 0.0344 | 0.0185 | 0.0185 | 0.0344 | 0.0385 | 0.0385 | 0.0271 |
| QC (3) | 0.0353 | 0.0508 | 0.0742 | 0.0384 | 0.0508 | 0.0742 | 0.0381 |
| QC (4) | 0.0665 | 0.0644 | 0.0665 | 0.0460 | 0.0625 | 0.0551 | 0.0644 |
| QC (5) | 0.0546 | 0.0463 | 0.0463 | 0.0546 | 0.0901 | 0.0901 | 0.0588 |
| Global QC | 0.0394 | 0.0371 | 0.0424 | 0.0360 | 0.0497 | 0.0529 | 0.0384 |

The metamodeling accuracy was assessed for the sampled points and the results of this comparison are shown in Figure 6-7, and a more zoomed view for a portion of the graph is shown in Figure 6-8.

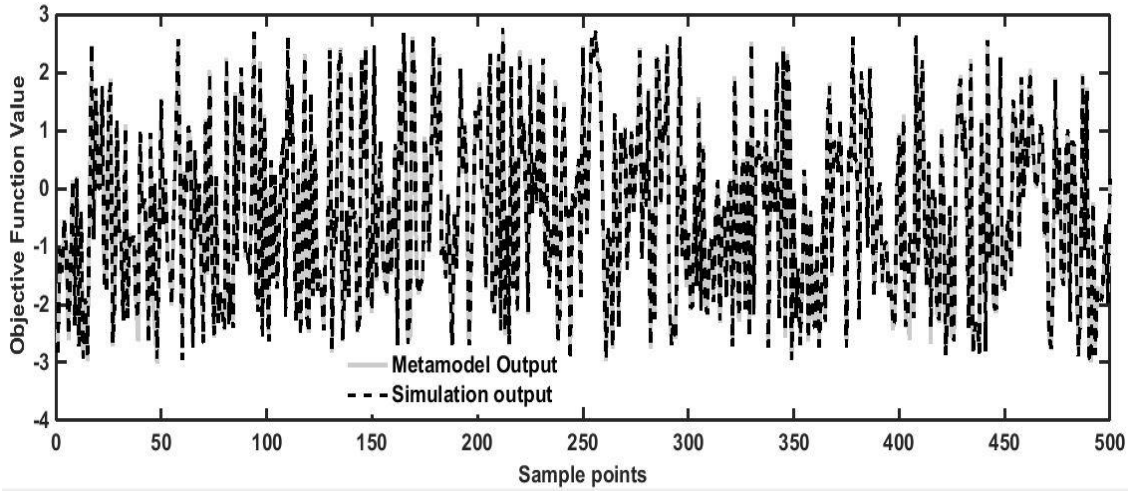


**Figure 6-7: Metamodel accuracy for 500 sample points**

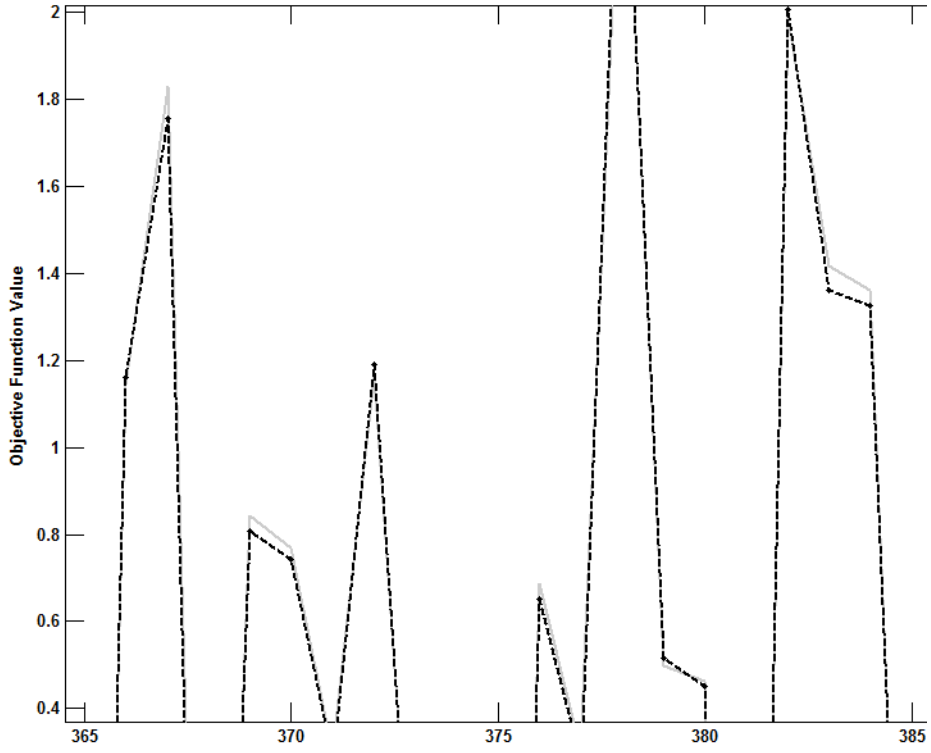


**Figure 6-8: Zoomed view of the metamodel for 20 sample points**

The graphical presentation of the simulation output versus the metamodel output shows high conformance or accuracy. However, to have a quantified measure of the

accuracy, the widely known accuracy measures such as R-Square and RMSE are shown in Table 6-11.

**Table 6-11: The accuracy measures for the metamodel**

| Parameter | Value |
|---|---|
| R-square | 0.9981 |
| RAAE | 0.0242 |
| RMAE | 0.4919 |

Root mean square error: $$RMSE = \sqrt{\frac{\sum_{i=1}^{m}(y_i - \hat{y}_i)^2}{m}} \quad (6\text{-}17)$$

Relative average absolute error: $$RAAE = \frac{\sum_{i=1}^{m}|y_i - \hat{y}_i|}{\max(STD)} \quad (6\text{-}18)$$

Relative maximum absolute error: $$RMAE = \frac{MAX}{STD} \quad (6\text{-}19)$$

R-square shows the accuracy in sampling points; RAAE and RMAE show the global and local accuracy in test points, respectively. Since RBF-HDMR goes through the sampling points, R-square should be ideally 1, while RAAE and RMAE ideally should be as close to zero as possible. In our case, the small value of RAAE and the value of RMAE indicates that a local area might have lower modeling accuracy than the rest of areas, due to potential complexities in the relationships of variables in that specific area [73].

While these measures along with the plot for sample points show reliability of the metamodel information, however, for the sake of more observations and comparisons, a one-variable conventional sensitivity analysis is also performed on the design problem.

### *2-a) Analysis of linearity for the impact of design variables*

It can be helpful to assess the linearity of effects for the design variables, as for the strong linearity it can be concluded that the objective function can be decomposable for specific variables, resulting in reduced efforts for optimization and family design.

### *A) SOC bounds ($x_1$, $x_2$)*

When setting smaller values as the bound for lower SOC, the vehicle has a wider range of operation on electric energy, and consuming less fuel potentially, which as the figure shows, results in more fuel economy. In contrary, when a smaller value is chosen as the upper bound of SOC, there is reduced opportunity of leveraging electric energy, as the window of SOC is narrowed down.

For the case of varying the upper bound of SOC, more sensitivity can be seen. This implies that a larger value of the upper bound allows leveraging more of the electric energy for propulsion, which results in increased fuel efficiency, less emissions, and as expected, no change in the powertrain costs. The AOF value slightly improves by increasing the upper SOC.

However, the sensitivity analysis based on the RBF-HDMR technique shows that for the higher range of upper SOC values, this variable does not come into affecting the performance of some variants. The reason is that our variants have a main differentiation point, which is the range to be driven on pure electric power. Since the initial SOC matters significantly in affecting the control strategy decision points specifically for small AER ranges (e.g., the first and second variants), if initial SOC would be selected as a design variable, different optimization results and sensitivity information might be obtained from the current observations. Second, the upper and lower SOCs, to some extent, couple with each other, meaning that isolated assessment of impact of them on the performance can be misleading, depending on the range under study for these variables. The impact of these variables on our objectives of interest is shown in Figure 6-9 and Figure 6-10 respectively.

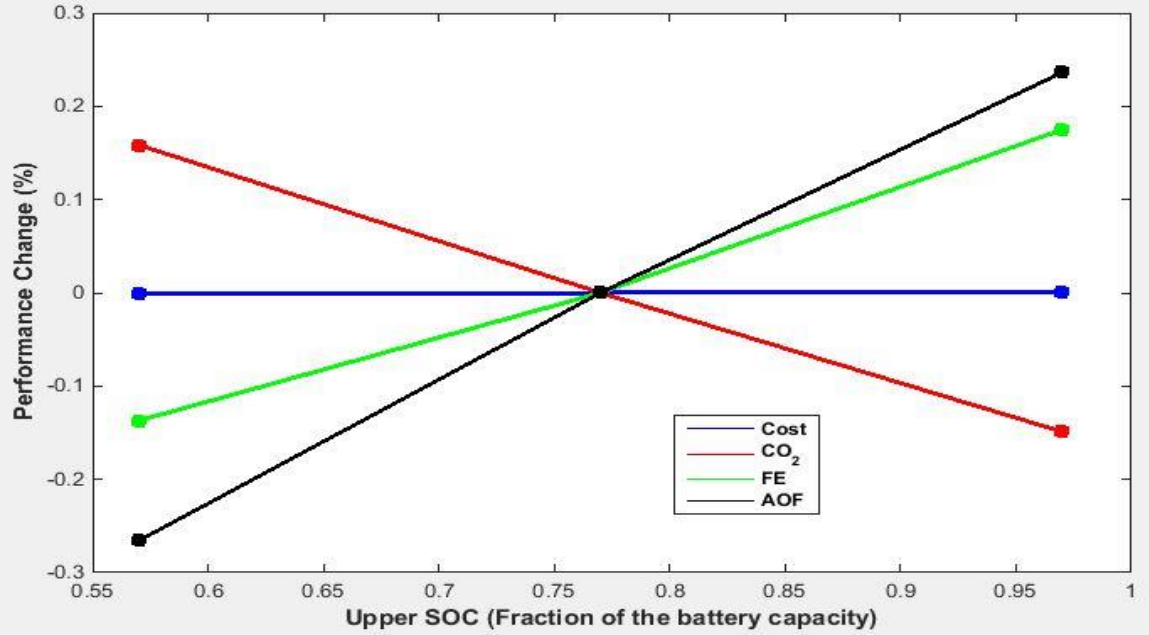


**Figure 6-9: Impact of upper SOC on the design objectives (for Variant #1)**

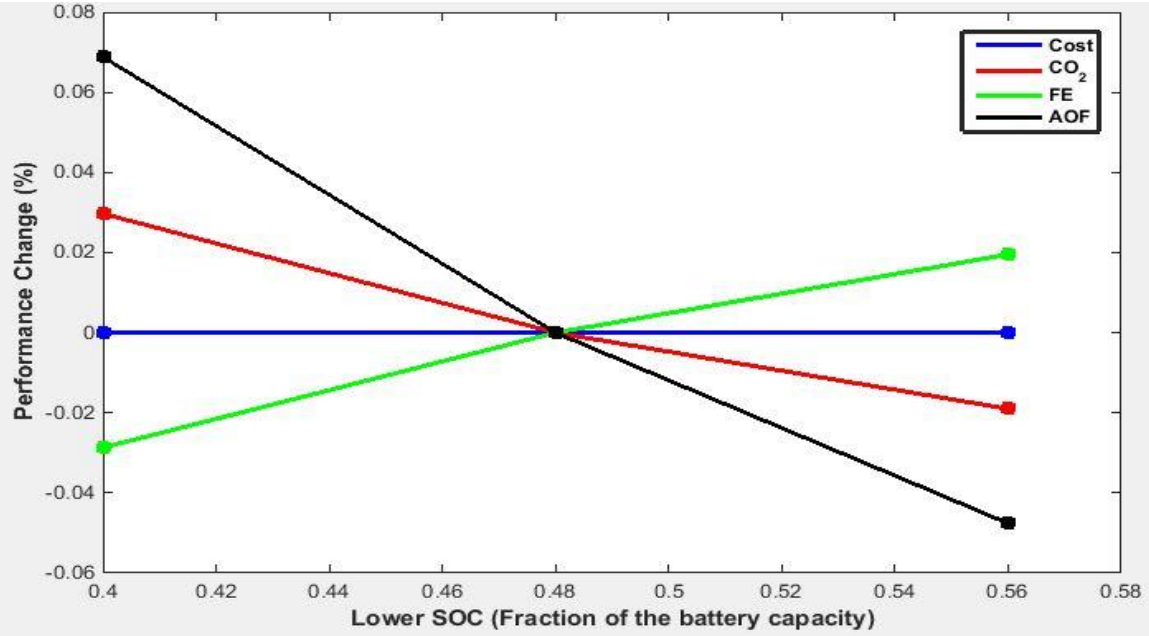


**Figure 6-10: Impact of lower SOC on the design objectives**

### *B) Engine Size ($x_3$)*

The increase in the engine size results in more consumption of the fuel and more emissions, and increase in the cost of the powertrain. The engine size might be minimized

by the optimization algorithm for reducing emissions and improving the efficiency. However, the decrease in the aggregated objective function is not significant due to the cancelling impacts of the emissions and fuel efficiency. The fuel consumption is an issue that can be impacted significantly by the selected control strategy and the thresholds for switching between alternate sources of power. As such, further research on the coupled impact or control parameters and the fuel consumption can be an interesting area for investigation, as it can reveal or impose a different behaviour at the optimization stage. The impact of engine maximum size on all the objectives of interest is shown in Figure 6-11.

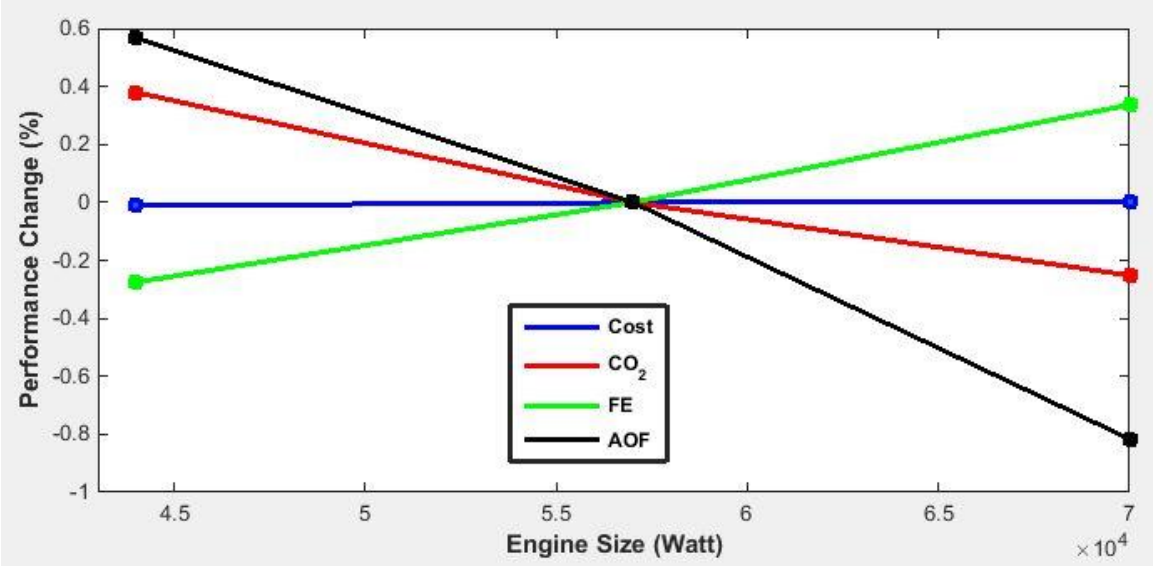


**Figure 6-11: Impact of engine maximum power on the design objective**

### *C) Motor Size ($x_4$)*

The motor size (maximum power in kW) positively affects the aggregated objective function, implying that the increase in its size is more desired for higher fuel efficiency and less emissions. The slope of increase and decrease in the aggregated performance function seem to be larger for the motor size than other factors, which might be a sign of high impact of this variable on the AOF, which is consistent with the SI value obtained through the RBF-HDMR technique. Figure 6-12 shows this impact on the objectives. It should be noted that though in the market there are discrete sizes available for motor and engine so far, this study is based on the ideal case assumptions, indicating that in an ideal case where there will be no manufacturing constraints limiting the options, what sizes can result in optimal performance of the PHEV.

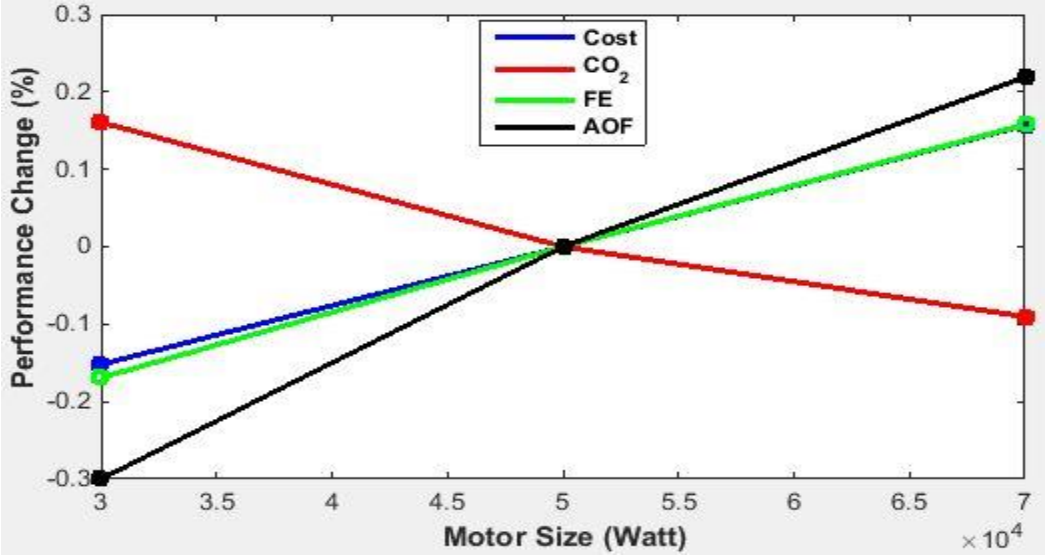


**Figure 6-12: Impact of motor maximum power on the design objectives**

### *D) NBM ($x_5$)*

The performance change with increasing the battery modules is similar in trend and significance to that of the motor size, but the AOF is less sensitive to the changes, and this is consistent with the SI values obtained through the RBF-HDMR technique. It should be noted that the cost modeled in this study is a supervisory level cost. A detailed cost modeling which can incorporate the manufacturing and depreciation costs of batteries will be a worthwhile part for future studies, as it can change the sensitivity analysis results due to its more significant impact on the overall performance of the vehicle. In this study, the cost model is developed based on an extrapolation of the information in the literature, specifically from the study by Markel et al. [106], where the battery pack cost is formulated as a function of the battery energy (kWh), and a fixed cost of 680 dollars. The visual impact is shown in Figure 6-13.

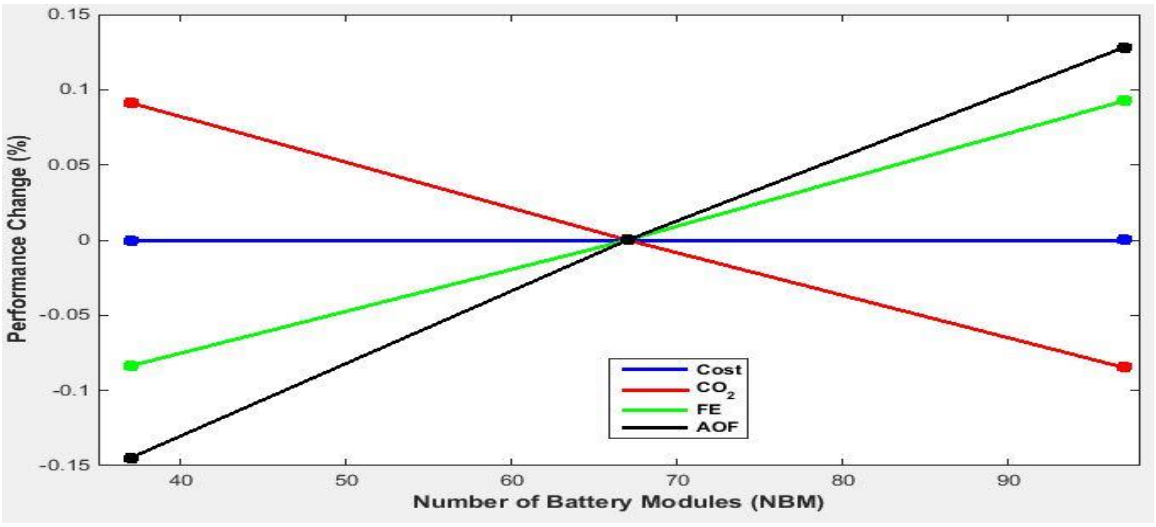


**Figure 6-13: Impact of the number of battery modules on the design objectives**

### *E) Power-split device Ratio ($\frac{x_6}{x_7}$)*

The power-split device ratio is similar to SOC bounds in terms of affecting the powertrain cost, but of an opposite impact on fuel efficiency and emissions. The increase in the fuel efficiency for higher ratio values implies that more torque (and consequently power) is taken from the motor in propulsion, resulting in a similar effect to that of the increase in the motor size which was discussed above. The percentage of change per changing this variable is shown in Figure 6-14.

In summary, the individual sensitivity analyses of this section show reasonable consistency with the metamodeling results. The visualized impact of each variable has some advantages and some limitations. An advantage is its ease of observation and conclusion about the trends per change of each variable. However, this feature might not be very helpful for cases that the output is of insignificant changes, or the range of change is very small, as compared to other output. This is the case for AOF in our study, where the value spans the range of [1 2.5] for the entire design space. In such cases, the comparison between the impacts of different variables becomes challenging and with high chances of errors. Besides, a graphical presentation only provides information about the first order effects, and is based on the assumption of linear impacts. In case of non-linearity and correlations among various variables, some other important pieces of information would be

missed in such type of assessment. Also, since for each and every point an expensive simulation is needed to run, this type of conventional sensitivity analysis can be of significant costs.

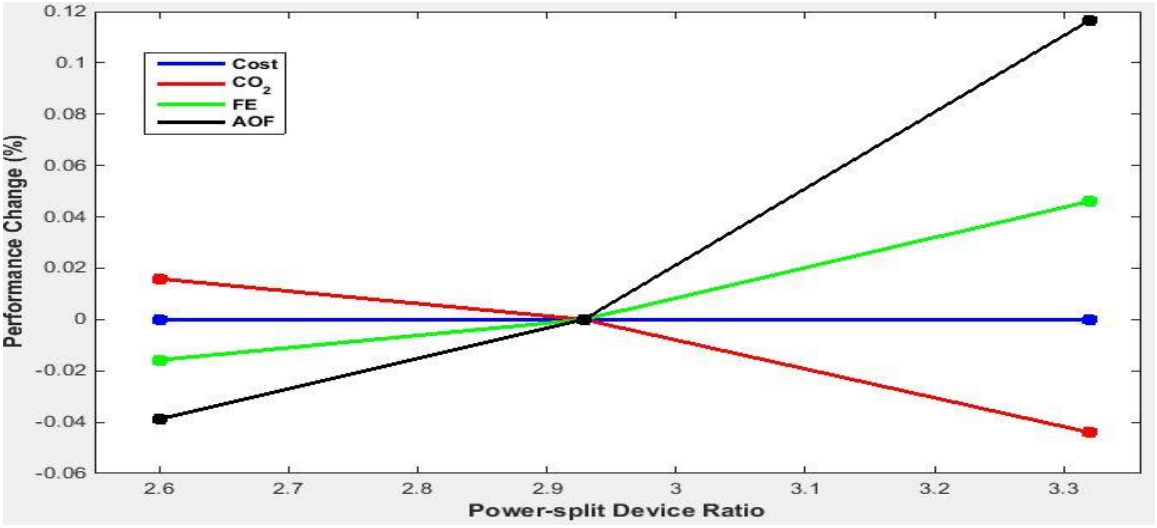


**Figure 6-14: Impact of the ring to sun gears ratio on the design objectives**

### *2-b) Analysis and findings on candidates for platform configuration*

The sorted SI vector shows that the numbers of teeth for the ring gear and the sun gear (in the power-split device), $x_6$ and $x_7$, respectively, are the least impacting factors on the performance of the vehicle. This might be due to the narrow range for these teeth numbers that assure meeting the performance requirements. Also, since these gears are connected to the component sizes, it is expected that their impact mostly depends on the chosen sizes for the underlying component. As such, their own impact is not as much concerning as that of the component sizes in changing the output of the objective function. Accordingly, from the commonalization perspective, a fixed power-split device gear ratio can be a promising candidate toward the family design of PHEVs.

The next rank set of impacts relates to the upper and lower bound of SOC and the battery modules ($x_1$, $x_5$, $x_2$). For the upper and lower SOC, sine they are control strategy parameters, they are not expected to be as much impactful as the component sizes. However, the proximity of effect of NBM to the effect of $x_1$, and $x_2$ makes sense since the battery size and its SOC window are a set of highly coupled parameters governing the

electric power supply for the vehicle. It should be noted that for $x_1$, and $x_2$, there is no benefit or manufacturing cost saving in choosing any shared value.

The engine size, $x_3$, comes next in the SI sorted vector. Though in the SI ranks, it seems that the engine is on the extreme right side of the sorted GSI vector, but all the GSI values except for the motor size are quite similar and in a range less than 0.03, which is significantly less than the GSI value for $x_4$, i.e., 0.38 or more than ten times. As such the engine size can be considered for commonalization to some extent as well. While further determination of its potential for being a multiple sub-platforms vs. the need for keeping it as a scale variable can only be possible after the detailed family design is obtained, however, the insight provided from the sensitivity analysis can be beneficial for manufacturers and designers in early stages.

At the extreme right side of the sorted SI vector in Table 6-9, the motor size, $x_4$, with a high SI value, which indicates significant impact of the motor size on the PHEV performance, and potentially significant performance loss for commonalization of this variable. Since the engine is able to be decoupled from the propulsion sources and because it can be controlled to operate in its most efficient mode, it is expected that its impact on the performance can be less than the impact of the electric motor. The highest impact of the motor size comes from the fact that appropriate battery size alone would not result in the desired performance of the vehicle, unless the motor is also of the right size to be powered by the battery and transfer the power to the transmission. The observations discussed above are consistent with the logic of automatic component sizing, which is one of the widely-used component sizing strategies. In that strategy, the motor size that meets the peak mechanical power required to follow the desired driving cycle is the very first item to be determined. The battery peak discharge power is then defined as the electrical power that the motor requires to produce that peak mechanical power. The engine is then sized to achieve the gradeability requirement of the vehicle and the 0-60 mph performance requirement [113, 114].

The observations on this section are summarized in Table 6-12. Since another effective parameter on making platform configuration decisions is the coefficient of variant,

the decision on whether a variable such as the motor size is beneficial or disadvantageous for any commonalization level highly depends on the span of the optimal values for any given variable on the variants under study, as well as the expected performance range for the variants. In other words, based on the improved scheme developed in Chapter 5 (section 5.7), even the high ranks of SI value will not preclude a variable from being a good option to take a common size for some variants, if not all of them.

**Table 6-12: Suggestions for commonalization based on the sensitivity and correlation analysis findings**

| Variable | Platform configuration suggestions |
|---|---|
| **1, 2** | No benefit in commonalization |
| **3, 6, 7** | Candidate for single or multiple platforms |
| **4, 5** | Scale variables or potential multiple platforms |

## Step 3: Platform value(s) determination

As per the structure of our platform configuration strategy, at this step an additional parameter toward decision making is to find the coefficient of variation (CV) for the vector of optimal values from Step 1. The CV value for each variable is obtained and the resulting vector sorted in non-descending order, shown in Table 6-13.

**Table 6-13: SI, Correlation, and Coefficient of Variation for the variables in the universal motor problem**

| Parameter | | Sorted |
|---|---|---|
| **GSI** | $GSI = [0.0091\ 0.0147\ \ 0.0282\ \ 0.3819\ \ 0.0141\ \ 0.0082\ \ 0.0085]$ | [6 7 1 5 2 3 4] |
| **Correlation** | $AQC = [0.0394\ 0.0371\ \ 0.0424\ \ 0.0360\ \ 0.0497\ 0.0529\ 0.0384]$ | [4 2 7 1 3 5 6] |
| **CV** | $CV = [7.0711\ 12.9097\ 0.6184\ 5.6657\ 46.6504\ 1.9520\ 5.2378]$ | [3 6 7 4 1 2 5] |

The partitioning scheme is updated in this chapter based on the range of obtained values for global sensitivity indices (GSI) and the CV values, to allow multiple platforms. As

concluded from Chapter 3, while the CV and SI values might recommend keeping specific variables as scale or non-platform variables, however the assessments of the universal electric motors family problem revealed that commonalization of those specific variables (i.e., recommended to be non-platform variable) might also be possible, at least to some extent. A cautious commonalization of the variables at the right end of the non-descending sorted vectors of SI and CV not only may not result in significant performance loss, but also may result in savings due to a higher degree of commonalization. Besides, in case of exceeding the allowed performance loss, it is always possible to increase the degree of freedom and reduce the commonality level. As such, it is desired to implement a moderate scheme like the third part of chapter 4, where more possibilities of commonalization were provided to most of the variables. The platform candidates are accordingly obtained as shown in Figure 6-15.

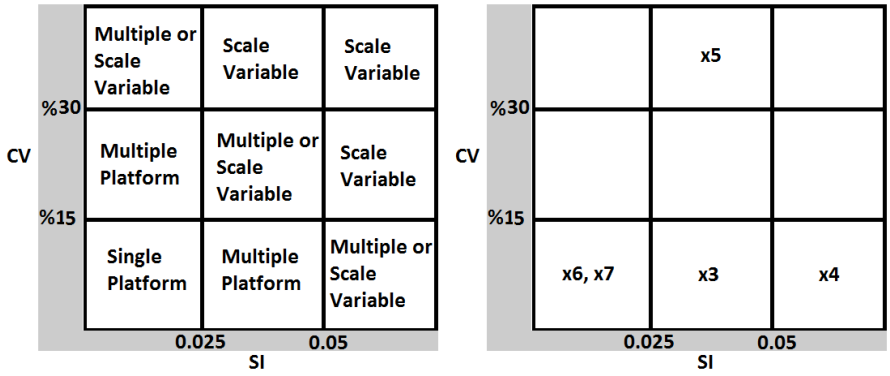


**Figure 6-15: The partitioning scheme for the PHEV family design problem**

The next step is to determine sub-platform values for multiple platform candidates, and common value for single platform candidates. By applying the clustering strategy to the multiple platform candidates, the obtained values and sub-platforms is shown in Table 6-14, and the best values for commonalization is shown in Table 6-15.

**Table 6-14: The determined number of platform/sub-platforms- PHEV PFD**

| Variable | Commonalization level |
|---|---|
| 6,7 | All-or-none platform |
| 3,4 | 2 sub-platforms |
| 1,2,5 | Scale variable |

The values of sub-platforms are obtained through applying the strategy discussed in Part (b) of Section 5 from Chapter 3. The two sub-platforms suggested for engine size and motor size result in groups of variants whose CV value is reduced by 70%, as compared to the case of a single platform for these variables.

**Table 6-15: Platform configuration of the variants based on the proposed optimal partitioning scheme**

| Platform Candidate | $X_6$ | $X_7$ | $X_3$ | $X_4$ |
|---|---|---|---|---|
| **Number of platforms** | Single platform | | 2 | 2 |
| **Platform variants** | | | $P_1$= {$p_1$, $p_5$}<br>$P_2$= {$p_2$, $p_3$, $p_4$} | $P_1$= {$p_1$, $p_2$}<br>$P_2$= {$p_3$, $p_4$, $p_5$} |
| **Platform preferred value** | $X_6$=81 | $X_7$=27 | $X_3$ ($P_1$)= 83801 | X4($P_1$)=49236 |
| | | | $X_3$($P_2$)= 84670 | X4($P_2$)= 53865 |

For the motor size, since there is a significant variance for the SI values, the best suggested value by our algorithm is the weighted average for sub-platform 2, where the SI values span the range of [0.02,0.25], as shown in Table 6-9. This makes sense in terms of the algorithm vision that is avoiding performance loss by staying as close to the optimal values from step 1, as possible. Therefore, when variants 3, 4, and 5 are suggested to form a separate sub-platform for this variable, obviously variant number 3 gets a higher priority due to its larger SI value for $x_4$.

## Step 4: Entire family design optimization

With the determined platform values, each variant is now optimized with less number of variables by setting the values of platform variables to the fixed values determined in Step 3. The results of the entire family design are shown in Table 6-16, along with the obtained efficiency, emissions, and cost for each variant. The commonalized values are shown in hatches and shaded forms for an illustrative presentation of the multiple platform family design.

**Table 6-16: Family Design based on the proposed method- PHEV PFD problem**

| Variant<br>----------<br>Design Variable | P1 | P2 | P3 | P4 | P5 |
|---|---|---|---|---|---|
| $x_1$ | 0.8100 | 0.8578 | 0.9334 | 0.9292 | 0.9497 |
| $x_2$ | 0.3388 | 0.2979 | 0.2554 | 0.2786 | 0.2551 |
| $x_3$ | 83801 | 84670 | 84670 | 84670 | 83801 |
| $x_4$ | 49236 | 49236 | 53865 | 53865 | 53865 |
| $x_5$ | 20 | 52 | 52 | 65 | 70 |
| $x_6$ | 81 | 81 | 81 | 81 | 81 |
| $x_7$ | 27 | 27 | 27 | 27 | 27 |
| **Fuel Efficiency (Miles/gallon)** | 203.82 | 189.98 | 184.55 | 118.99 | 87.45 |
| **Cost ($)** | 2840.0 | 2841.3 | 2941.7 | 2941.7 | 2940.5 |
| **CO2 Emissions (Grams/mile)** | 152.54 | 156.07 | 157.83 | 169.60 | 183.09 |
| **AOF** | 2.39 | 1.27 | 1.91 | 1.94 | 1.46 |

## Step 5: Performance evaluation

At this stage, the best reference for assessing the family design solution obtained in the previous step is the individual optimal designs from Step 1. By pair-wise comparison of the new values for all the three objectives as well as the aggregated objective function (AOF), the percentage of change in each variant performance is measured and collected in Table 6-17.

### *5-a) Comparison with individual optimal designs*

The results show that for fuel efficiency objective, in the worst case, there is 9.8% loss for $PHEV_{60,}$ in case of sharing the variables as per the suggested configuration. This indicates about 10 miles per gallon reduction in the fuel efficiency, as compared to the expected performance of the $PHEV_{60}$ at its optimal design before family design. There are some improvements for $PHEV_7$ and $PHEV_{40}$, indicating the better performance of the

vehicle with the new component sizes. The average loss on the fuel efficiency is 1.1% which is within the acceptable loss range.

**Table 6-17: The results of comparing our proposed method to the individual optima**

| Variant | Difference (%) | | | |
|---|---|---|---|---|
| | **Fuel Efficiency** | **Cost** | **Emissions** | **AOF** |
| 1 | 2.7319 | 0.6807 | -1.2494 | 5.7778 |
| 2 | -1.4269 | -0.6747 | 0.0834 | 0 |
| 3 | -1.3893 | 0.1634 | 0.0317 | -1.0363 |
| 4 | 4.4688 | -0.1087 | -0.6444 | 3.7433 |
| 5 | -9.8732 | -1.1630 | 1.2498 | -16.0920 |
| **Average Change** | **-1.0977** | **-0.2204** | **-0.1058** | **-1.5214** |

The losses on the cost objective are all less than 1%, indicating insignificant increase in the cost after commonalization. The biggest increase on the cost is for $PHEV_7$ that is $20 in a scale of ~ $2800. There are even slight reductions in the cost, based on the selected configuration, which indicates the fixed sizes for the components at the family design stage have resulted in slightly reduced cost of the powertrain. The overall change in the powertrain cost for the entire family is a few dollars reduction in the cost.

A quite similar variation in the emission objective values can also be recorded, as all the ups and downs in the emission after the family design stage are less than 1.5%, that is about 3 grams per mile of $CO_2$, as compared to the range of 180 grams/mile. As expected, fuel efficiency and emissions are moving in the same direction, i.e., for the variants with improved fuel efficiency after the commonalization, there is reduction in the emissions, and vice versa. However, there is not such a straight forward relation between the trends for fuel efficiency and the cost. In other words, increase in the fuel efficiency may not necessarily result from a more costly component size (such as battery and motor), and therefore as the results show, there are cases where cost shows increase for increased

fuel efficiency (e.g., $PHEV_{40}$), while there are also instances of reduced cost with better efficiency (e.g., $PHEV_{7}$). In addition to the component sizes, some of the other parameters in effect for fuel efficiency include the driven distance, the control strategy parameters.

AOF values before and after family design show more changes, as compared to the individual objectives of interest. One observation is that the AOF value is highly affected by the fuel efficiency, even though all the objectives have the same weight in AOF formulation. $PHEV_{7}$ and $PHEV_{40}$ have better AOF values after the commonalization by 5.7% and 3.7% respectively, and $PHEV_{30}$ and $PHEV_{60}$ have lost 1.3% and 16% of the AOF after the commonalization respectively. This can be an interesting subject for further exploration, in the sense that other weight values can be examined to find out how the optimization results and family design can be affected. As the linearity assessment in section 6.5.1 showed, emission and efficiency could be perceived to be of a cancelling effect, and due to the insignificant changes of the cost, the AOF also showed insignificant changes. However, more significant impacts of the individual objectives on AOF is revealed here, and the observations can provide directions for fine-tuning of the weights in the aggregated objective function formulation.

The 16% loss of performance on the AOF value for the PHEV60 is worth more consideration. Since this value is a measure of the overall performance on fuel efficiency, emissions, and the cost of powertrain as well as the operating cost, it can be concluded that the overall performance of these objectives in the aggregated mode has a 16% loss. For better analysis and conclusion, however, the single objectives are better to be assessed for this variant. The detailed performance values are 10 MPG reduction in fuel efficiency, $20 cost reduction, and 3 g/mile increase in CO2 emissions in the design of this vehicle after the platform configuration. The fuel efficiency has the highest loss among the three objectives of interest, indicating that the family design solution for this variant has the largest impact on increasing the assumption of fuel in this variant. As compared to the individual optimal design for $PHEV_{60}$, the observation is that the motor size reduction of ~1.5 KW as well as the reduced number of battery modules (from 88 to 70) has resulted in more dependency on the engine during the simulation, or in an increase in the fuel consumption over the cycle that this variant is run for our optimization purposes. However,

regardless of the current optimal solution in the family design, this variant is expected to have more fuel consumption due to its longer nominal AER miles. The seemingly large amount of 16% is dependent on the priorities set by the manufacturer, and it might be acceptable (in the trade-of between benefits of commonalization), or unacceptable (in the trade-off between customer preferences and product positioning purposes). In this case, the increase of CO2 emissions and decrease in fuel efficiency penalize the AOF value for $PHEV_{60}$, even though the cost is reduced. Looking at the family as a whole, the average performance loss of 1.52% over the whole family is not a significant loss. Besides, as noted in the market studies, the majority of the driven miles per day is less than 30 miles for 50% of the drivers in US, which can be an important factor in decision making for the level of allowed performance loss for $PHEV_{60}$.

### *5-b) Commonality Index Measurement*

As per the CI index, with $p$ variants (5 in this problem) and $n$ components in each variant (or design variables in our case to be 7), for a design with $u$ as the total number of unique components,(15 as per our obtained family solution in Table 6-16), the value obtained for this family design solution is 71.4% which is a fairly high value for the family. Since the problem under study is not applied elsewhere, at this stage no further comparisons can be made in regard to the commonalization capability of the proposed family design strategy.

## 6.6. Effect of varying the number of sub-platforms (k) on the family design

Similar to the analysis implemented in Section 4.9, it is desired in investigating the effect of the number of sub-platforms on the performance of the resulting family. Since the AOF value is an aggregated representation of the overall performance, a better reflector of the fitness of the platform candidates is to assess the impact of various number of sub-platforms on the three objectives of interest. This is done through assessing more sub-platforms for variables with high SI value, and doing the family design optimization stage again to compare the new family results. The motor size is the best candidate to assess

such consideration for, based on its high impact on the objective function value. Through considering one to 3 sub-platforms for the motor size, it is obtained the platform configuration cases as shown in Table 6-18.

**Table 6-18: Three platform configurations for x4 based on clustering of k**

| **Platform Candidate** | $X_4$ | $X_4$ | $X_4$ |
|---|---|---|---|
| **Number of platforms** | 1 | 2 | 3 |
| **Platform variants** | All variants sharing the motor size | $P_1$= {$p_1$, $p_2$}<br>$P_2$= {$p_3$, $p_4$, $p_5$} | $P_1$= {$p_1$, $p_2$}<br>$P_2$= {$p_3$, $p_4$}<br>$P_3$= {$p_5$} |
| **Platform preferred value** | X4(P)= 52319 | X4($P_1$)=49236 | X4($P_1$)= 49235 |
| | | X4($P_2$)= 53865 | X4($P_2$)= 53828 |
| | | | X4($P_3$)= 55467 |

The family design results for all-or-non platform of the motor size is obtained and shown in Table 6-19.

**Table 6-19: Family design optimal results for all-or-none platform for $x_4$**

| **Variant**<br>**----------**<br>**Design Variable** | **P1** | **P2** | **P3** | **P4** | **P5** |
|---|---|---|---|---|---|
| $x_1$ | 0.8430 | 0.9341 | 0.9480 | 0.9292 | 0.9497 |
| $x_2$ | 0.3518 | 0.2719 | 0.2511 | 0.2786 | 0.2551 |
| $x_3$ | 83801 | 84670 | 84670 | 84670 | 83801 |
| $x_4$ | 52319 | 52319 | 52319 | 52319 | 52319 |
| $x_5$ | 20 | 48 | 50 | 58 | 67 |
| $x_6$ | 81 | 81 | 81 | 81 | 81 |
| $x_7$ | 27 | 27 | 27 | 27 | 27 |
| **Fuel Efficiency (Miles/gallon)** | 203.02 | 193.32 | 179.49 | 113.10 | 81.11 |
| **Cost ($)** | 2880.3 | 2918.6 | 2930.2 | 2939.9 | 2949.5 |
| **CO2 Emissions (Grams/mile)** | 152.31 | 158.51 | 162.23 | 167.91 | 194.37 |
| **AOF** | 2.37 | 1.32 | 1.63 | 1.86 | 1.10 |

As for the case of three sub-platforms, the family solution is shown in Table 6-20.

By comparing the results with the individual PHEVs design in Table 6-8, the following results on the percentage of lost performance for the three objectives of interest, as well as the AOF values per variant are obtained.

**Table 6-20: Family design optimal results for three sub-platforms for $x_4$**

| Variant<br>----------<br>Design Variable | P1 | P2 | P3 | P4 | P5 |
|---|---|---|---|---|---|
| $x_1$ | 0.8100 | 0.8575 | 0.9451 | 0.9459 | 0.9321 |
| $x_2$ | 0.3389 | 0.2979 | 0.2513 | 0.2561 | 0.2600 |
| $x_3$ | 83801 | 84670 | 84670 | 84670 | 83801 |
| $x_4$ | 49235 | 49235 | 53828 | 53828 | 55467 |
| $x_5$ | 21 | 52 | 56 | 68 | 69 |
| $x_6$ | 81 | 81 | 81 | 81 | 81 |
| $x_7$ | 27 | 27 | 27 | 27 | 27 |
| **Fuel Efficiency (Miles/gallon)** | 197.97 | 190.02 | 184.11 | 115.46 | 94.45 |
| **Cost ($)** | 2840.7 | 2841.9 | 2934.3 | 2936.2 | 2969.85 |
| **CO2 Emissions (Grams/mile)** | 152.5 | 155.87 | 154.32 | 166.50 | 173.23 |
| **AOF** | 2.3 | 1.28 | 1.91 | 1.93 | 1.56 |

As it is observed in Table 6-21, the all-or-none platform for the motors size results in more performance loss, which is about 8% in AOF, where the two sub-platform case results in 1.52% average loss on AOF, and the three sub-platform case results in 10.3% average loss, which is quite a decrease as compared to our initial family solution of two sub-platforms for the motor size. Also, as shown in Table 6-22, the level of performance loss is decreased with three sub-platforms for the motor size, as compared to our family solution where there are two sub-platforms for the motor size. The biggest loss is 10% for PHV60 on the AOF value. This design is better than the one with 2 sub-platforms, but the difference is insignificant as shown in the last row of Table 6-22. This observation again reassures us toward the appropriate decision criteria selected in our proposed family design methodology in this dissertation, and shows the capability of this method is providing information on the more fitting platform candidates, as well as their fitting level of commonalization or differentiation.

The plot in Figure 6-16 shows the trends of performance loss per k, for the motor size, which illustrates the benefit of multiple platform over all-or-none platform, and also shows the insignificant gain in using 3 sup-platforms as compared to the 2-sub-platform case.

**Table 6-21: The results of comparing the individual PHEVs design to the family solution for one platform for the motor size**

| Variant | Difference (%) | | | |
|---|---|---|---|---|
| | **Fuel Efficiency** | **Cost** | **Emissions** | **AOF** |
| 1 | 2.3286 | 2.1093 | -0.1508 | -0.8368 |
| 2 | 0.3061 | 2.0275 | 1.5634 | 3.9370 |
| 3 | -4.0930 | -0.2281 | 2.7878 | -14.6597 |
| 4 | -0.7024 | -0.1698 | -0.9965 | -4.1237 |
| 5 | -16.4073 | -0.8605 | 6.1609 | -24.6575 |
| **Average Change** | **-3.7136** | **0.5757** | **1.873** | **-8.0681** |

**Table 6-22: The results of comparing the individual PHEVs design to the family solution for 3 sub-platforms of motor size**

| Variant | Difference (%) | | | |
|---|---|---|---|---|
| | **Fuel Efficiency** | **Cost** | **Emissions** | **AOF** |
| 1 | -0.2167 | 0.7055 | -1.2753 | 2.2222 |
| 2 | -1.4061 | -0.6537 | -0.0449 | 0.7874 |
| 3 | -1.6244 | -0.0885 | -2.1929 | -1.0363 |
| 4 | 1.3696 | -0.2954 | -2.4605 | 3.2086 |
| 5 | -2.6590 | -0.3109 | -4.2028 | -10.3448 |
| **Average Change** | **-0.9073** | **-0.1286** | **-2.0353** | **-1.0326** |

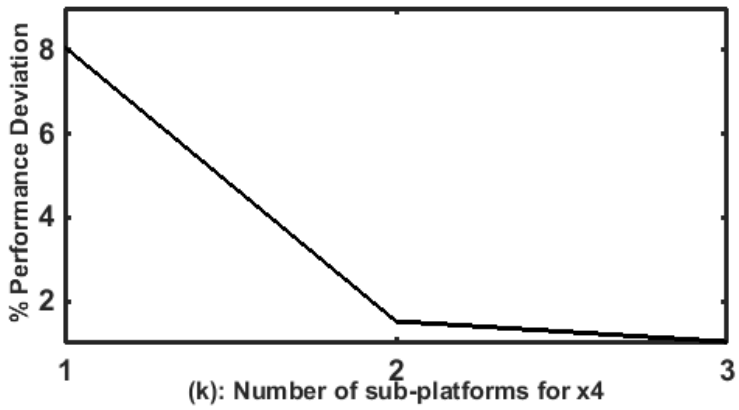


**Figure 6-16: Performance deviation per *k* for $X_4$**

## 6.7. Summary

The family design for a family of 5 PHEV variants was obtained in this chapter, by applying the strategy proposed in Chapter 3 of this study. Among the considered design variables, the upper and lower SOC bounds were excluded from consideration toward commonality, due to their different nature as compared to the rest of design variables. The commonalization and partitioning strategies suggested a single platform for the power-split device ratio, while multiple sub-platforms were suggested for the engine size and motor size. The number of battery modules was also kept as a non-platform variable, and the family design stage was implemented with three design variables for each PHEV at Step 4 of this chapter. The percentage of change in performance of fuel efficiency, costs, and emissions, as well as the AOF value was less than 2% in average for the entire family, while a few improvements were also obtained on some variants for some individual objectives.

Two observations are made; one is that since the variants are of differences in desired objective values, some might lose performance through a commonalization scheme, while some others can benefit from the new shared value which can positively

affect their performance. The other observation is that there are more than one objective to affect the optimization algorithm behaviour, and improvement on one objective or some of the objectives of interest is a possible circumstance in presence of more objectives or effective parameters on the overall performance of the product. Both observations are in line with the benefits resulting from the family design, which is the reduced cost of producing more variants through commonalization. Though the cost modeling for manufacturing the powertrain is not included into this study, however, it is clear that the manufacturing set-up costs, the inventory costs, and the delivery time for products obtained through family design methodologies will be less than those of non-shared production specifications.

In addition, the obtained family design shows acceptable loss in average over the entire family for all the objectives of interest, and can be used as a solution to obtain cost savings in shared powertrain component sizes, while meeting the expectations on performance for the target market segments. In case of the strong preferences to reduce the performance loss to below 10%, the first action recommended based on the last step of our family design algorithm is to exclude the motor size from the commonalization scheme for this vehicle, and repeat the optimization with four design variables (i.e., SOC window bounds, motor size, and NBM). The resulting design can have a larger motor size, which increases the utilization of electric energy, but at the same time imposes some additional cost to the design, and the trade-off between these objectives determines the level of improvement in the AOF value.

# Chapter 7. Conclusion, contributions, limitations, and future directions

The motivation for this study comes from the unaddressed need for a design framework for the PHEV that integrates both the market side and the manufacturing side concerns and provides design solutions for this complex product within reasonable time and computational cost. The main objective to pursue was to develop an approach to support product family design for PHEV powertrains that can cover a wide range of customers' needs in different market segments.

## 7.1. Summary of contributions

This thesis provides answers to three fundamental questions related to PHEV family design as summarized below:

**1.** ***How to ensure both the manufacturing efficiency and the customer satisfaction for PHEVs in various market segments?***

This question was addressed through the concept of product family design, where the best trade-off between the benefits of manufacturers and customers can be obtained. Product family design is an attempt to find the right level of sharing among various parts, components, and/or functionalities of members of a family of products, so that reasonable saving can be obtained through shared parts, while the new design solutions can still meet the diverse expectations of customers in various market groups or segments.

A thorough review of the existing developments in the family design research area was implemented to facilitate the recognition of available methods, through which the gap between specific needs for a PHEV family design optimization study and the current developments was identified. The main unaddressed need was a method with sufficient efficiency to provide supporting information for a complex problem like the PHEV design,

within reasonable computational cost and desired reliability. Since the selected family was a scale-based family, the review of the literature was narrowed down to scale-based family design methods in Chapter 2, and more detailed review of the existing approaches created the idea of leveraging sensitivity analysis to decide on proper candidates for platform configuration.

The main gap that this dissertation addressed in using sensitivity analysis for family design includes the high dependency of conventional sensitivity analyses on several function evaluations. This issue is a challenge for simulation-based problems such as our PHEV problem, since for assessing performance of the vehicle even for small distances such as 7 miles, a few minutes was needed to obtain the simulation output. For longer distances such as the 60 miles, this number turned into order of hundreds of minutes, making it significantly slow and inefficient to apply the conventional sensitivity analysis-based method.

The proposed method in this dissertation was shown to use significantly less number of function evaluations toward facilitating platform configuration decisions. For example, in Chapter 4 it was shown that the required samples for the universal electric motors family design problem through the proposed method is by *65+140n* samples less than that of the method proposed by Dai and Scott , where n is the average number of optimization iterations.

**2. *Which PHEV can be the best for each market segment?***

There are several studies in the literature which have addressed the following issue: a) Assessment of various market penetration scenario; b) Surveys to analyze customer behavior/preferences and to identify their perceived benefits in regard to PHEVs; and c) Assessment of customer data from resources such as National Household Transportation Survey (NHTS) for finding the level of fitness of available vehicle designs for various segments. Through review of such studies, a set of five PHEVs were selected as our reference for family design.

By assessing all the existing suggestions and findings from such studies, in Chapter 6, five variants were selected as the proper representatives of customers' needs in the PHEV market. The main criterion for differentiation of the variants is the distance to be traveled on the electric energy, known as AER, and the selected values included 7, 20, 30,

40, and 60 miles for such parameter. Other typical performance constraints such as the maximum time to achieve specific speed and acceleration, as well as gradeability constraint was applied to all the vehicle designs at the optimization stage, so that the obtained solutions are assured to meet other requirements on top of AER for each segment.

The following assumptions, considerations and measurements apply to the selected variants:

- The general configuration settings follow the design of Toyota MY04 Prius as modeled in PSAT, with power-split powertrain configuration which is consistent with the intended configuration of this study.
- The studied battery is Saft Li-Ion which is widely used and evaluated in different studies for their great potential as energy storage devices for PHEV due to higher energy density and specific energy.
- A thorough simulation-based study is done for finding the optimal PHEV specifications for meeting different ranges of AER through an extended-range charge-depleting control strategy (which is a modification to the power split hybrid control strategy in PSAT).

**3. What methodology can be the most efficient for facilitating the design of such a complex family?**

In Chapter 3 an approach was proposed to enable identifying the platform configuration based on sensitivity analysis and evaluation of all the design variables.

The specific contribution of this part is that the proposed family design and platform configuration approach in this dissertation has the capability of handling expensive black-box design problems such as PHEV design which is simulation-based. The performance of the proposed method was first tested in Chapter 4, on a well-known test problem in the family design research area, i.e., a family of ten universal electric motors with eight design variables each. The reason for such application was to compare the results of the obtained family design with the existing contributions in the literature, as well as to make sure that the information provided through this method is reliable to be applied to real black-box

design problems for which no benchmark exists. The results of application to the test problem showed efficiency of the proposed method in identifying the appropriate candidates for commonalization, as well as its efficiency in providing desired solution for the shared value of each platform and sub-platform.

The proposed method was then further improved based on detailed assessments and comparisons, and enabled obtaining family design solutions with more commonality as compared to the family designs in the literature for the electric motors family problem, while the number of needed function evaluations for making platform configuration decisions are significantly reduced through the proposed approach.

The required model for facilitating this family design was developed in SimDriveline, as presented in Chapter 5 of this study, and was validated according to the existing data from well-known test labs such as the Argonne National Laboratory. The validated model was then used in Chapter 6 though connection to an efficient optimization algorithm called TR-MPS 2.0, and the proposed meta-model based family design strategy was applied to the problem.

The accuracy of the metamodel provided assurance on the reliability of information provided about impact of various design variables. Further assessment of the impact of each design variable was also studied through a small conventional sensitivity analysis study, which provided consistent results about relative impact of variables on the fuel efficiency, emissions, and cost, as well as on the aggregated objective function.

The platform configuration was determined in section 6.5 and 6.6, and the family design was obtained afterwards for 3 design variables in each variant design problem.

The results of the family design indicated reasonable level of loss on performance, with an average of less than 2% on all the objectives for the entire family. The level of commonality obtained was also measured through the Commonality Index (CI), as 78% increase in sharing, compared to the no-family design case.

In terms of PHEV product family design, following benefits have been obtained:

- The needs of a vast part of the market are covered in our study, through a thorough review of the market penetration scenarios, current market, features and utility factor of different specifications of PHEVs for users, and the detailed information such as cost models developed for such studies in the literature

- The proposed family design method suits for the expensive simulation-based design optimization problem for the PHEVs and results in computational cost savings
- Desired information toward making commonalization decisions are conveniently provided by this approach, through merging two important phases of family design for black-box problems, i.e., the structure of the objective function for the problem under study, and the relative impact of each variable on the overall vehicle performance.
- The design framework is flexible and can be updated for providing optimum design options based on market changes and any future modifications in the effective parameters such as the unit costs.
- The design approach is applicable to other powertrain configurations as well as other variations of the unconventional vehicles, such EV and HEVs.

The contributions of this research are as follows:

1. Review of the market-related studies and research on market penetration scenarios for PHEVs, and identification of the variants in demand by various market segments
2. Development of a generic simulation model for the power-split PHEVs with full parametric modeling capability for design optimization purposes.
3. Formulation of the powertrain family design problem for optimizing multiple objectives including the fuel efficiency, GHG emissions, and the operating and powertrain costs
4. Development of an efficient platform configuration and product family design strategy for problems involving expensive and unknown functions.

Analysis and comparison of various parameters on the PHEV performance and discussion on the implications for obtaining savings in the manufacturing costs while increasing the market share through mass customization.

## 7.2. Limitations and open questions

The performance of the obtained solution for the PHEV family can be compared with more results upon availability, both in terms of alternate optimization algorithms, and

alternate family design strategies. Since this problem is entirely designed in this research with no previous assessments at this level, there is no clue on whether other optimization algorithms would improve the solutions obtained. The only evidence in this dissertation is the convergence plots used to monitor the behaviour of the algorithm. Use of alternate algorithms which might be able to handle the constraints in a more efficient way, can be a future contribution for this research. Also, similar to the universal electric motors family design problem, if other existing methods in the literature are applied to the same design problem, a better understanding of strengths and weaknesses of both methods can be obtained.

One interesting parameter to include in potential future research is developing more customer-oriented objectives, upon availability of more data in future. Techniques such as choice modeling will enable ranking the customer preferences in regard with PHEVs, and the entire objective setting can become more intuitive, emphasizing more on the real parameters of importance based on customers' input.

In regard to the PHEVs, evaluation of the resulting family solutions coupled with various types of control strategies can be also an interesting direction for further research. One of the observations in this study was that using larger engine results in more fuel consumption and more reliance of the vehicle on the engine as main source of propulsion. This behaviour can be controlled through playing around the chosen thresholds for the control strategy, and an interesting area of study can be optimization of more parameters related to the control strategy. The only chosen parameters for optimization in this study were the SOC window bounds, which appeared helpful in allowing commonalization of the non-control parameters such as the engine size and the power-split device ratio. However, the design of the vehicles can be improved further, if an optimal strategy for power control is first obtained, and then the component sizes are optimized within such strategy. This approach however can be challenging too, in the sense that the optimality of control parameters and component sizes are not fully independent from each other. A simultaneous optimization of all the design and control strategy parameters in an integrated formulation can prevent sub-optimality. However, such approach will have remarkable computational complexities and the entire decision making in this regard comes to the

trade-off between the level of sacrificed performance versus the level of cost savings in computations for optimization.

Another consideration to discuss is the impact of distance between charges, and the distance the vehicle would be driven over. As per Shiau [112], the minimum operation cost in terms of $/mile would happen when the AER is almost the same as the distance between charges. For AERs higher than that specific value, if the vehicle is not charged, this operating cost increases rapidly. As such, taking the distance between the charges into account can be a worthwhile factor to be integrated into future studies as well.

Another observation is the higher impact of the fuel efficiency on the AOF value, in the sense that the AOF to a great extent moves in the same way as the fuel efficiency has moved after commonalization. Examination of other weights rather than 0.33 for each objective can reveal interesting facts about the nature of this specific deign problem, and can provide guidelines in regard to the appropriate directions for focus in design.

Another area for more research is the integration of detailed life cycle cost models for the powertrain and specifically the battery with the performance optimization and vehicle family design. Such formulation can provide a thorough assessment of the effective parameters on the ultimate performance of the product, and the optimization results to be obtained from such a comprehensive formulation can be a more solid solution for the manufacturers.

Using SimDriveline and other toolboxes in Simscape requires all the components to be correctly constrained, and the debugging process can be quite challenging otherwise. Another drawback is that the models in SimDriveline and SimElectronics may not generate the most accurate results as mathematical models do since most of these models are ideal. Different power losses need to be additionally modeled as well in the physical context.

In summary, it is worth to note that the effect of the control strategy and modeling specifications can be different in reality. Depending on the chosen control strategy, the correlations or sensitivities of the various available variables on the PHEV's objective

function might accordingly take different values. As such, it may not be far from expectation to observe differences in the GSI vector order for a different set of control strategy and driving conditions.

In the end, only a small portion from the myriad of possible explorations was investigated in this dissertation. The trade-off between the complexities resulting from increased degrees of freedom and integrated parameters into the modeling resulted in limitations and the need to set a scope for the level of assessments. However, the hope is that by future developments of the research in the family design area, as well as the high-dimensional back-box expensive problems optimization area, more capable methodologies to handle such family design challenges will be developed. The author hopes this study can facilitate the required knowledge for future research in this regard.

# References


[1] Shiau, C.-S. N. and Michalek, J. J., 2009, "Optimal Product Design Under Price Competition," Journal of Mechanical Design, 131(7), pp. 071003-10.

[2] Simpson, T. W., Maier, J. R., and Mistree, F., 2001, "Product platform design: method and application," Research in Engineering Design, 13(1), pp. 2-22.

[3] Pirmoradi, Z., Hajikolaei, K. H., and Wang, G. G., 2014, "Designing Scalable Product Families for Black-Box Function," proceedings of the IDETC/CIE 014, Buffalo, NY, USA, DETC2014-35334. p. V02BT03A040.

[4] Khire, R. A., Messac, A., and Simpson, T. W., 2006, "Optimal design of product families using Selection-Integrated Optimization (SIO) Methodology," proceedings of the 11th AIAA/ISSMO Symposium on Multidisciplinary Analysis and Optimization, AIAA 2006.

[5] Blanco, S., 2011 "2012 Toyota Prius Plug-In Hybrid now offers 111 MPGe", 2011 Sept 14 2011 [cited 2015 June 12], Available from: http://www.autoblog.com/2011/09/14/2012-toyota-prius-plug-in-hybrid-mpge-mpg/.

[6] Heffner, R. 2007, "Semiotics and Advanced Vehicles: What Hybrid Electric Vehicles (HEVs) Mean and Why it Matters to Consumers," University of California, Davis, PhD Dissertation, Davis, CA.

[7] Karbowski, D., Haliburton, C., and Rousseau, A., 2007, "Impact of component size on plug-in hybrid vehicles energy consumption using global optimization," proceedings of the 23rd International Electric Vehicle Symposium, Anaheim, CA. p. 520-534.

[8] Banvait, H. 2009, "Optimal energy management system of Plug-in Hybrid Electric Vehicle," Purdue University Master of Science Indianapolis, Indiana.

[9] Sikes, K., Gross, T., Lin, Z., Sullivan, J., Cleary, T., and Ward, J., 2010 "Plug-in hybrid electric vehicle market introduction study: final report",Oak Ridge National Laboratory (ORNL), http://www.osti.gov/bridge, ORNL/TM-2009/019.

[10] Bradley, T. H. and Frank, A. A., 2009, "Design, demonstrations and sustainability impact assessments for plug-in hybrid electric vehicles," Renewable and Sustainable Energy Reviews, 13(1), pp. 115-128.

[11] Johnston, B., McGoldrick, T., Funston, D., Kwan, H., Alexander, M., Alioto, F., Culaud, N., Lang, O., Mergen, H., and Carlson, R., 1998, "The Continued Design and Development of the University of California, Davis FutureCar," SAE SPEC PUBL, SAE, WARRENDALE, PA,(USA), Feb 1998, 1359, pp. 53-66.

[12] Nemry, F., Leduc, G., and Munoz, A., 2009 "Plug-in Hybrid and Battery-Electric Vehicles: State of the research and development and comparative analysis of energy and cost efficiency",Institute for Prospective and Technological Studies, J.R.C. No. JRC54699.

[13] Kelly, K. J., Mihalic, M., and Zolot, M., 2002, "Battery usage and thermal performance of the Toyota Prius and Honda Insight during chassis dynamometer testing," proceedings of the Battery Conference on Applications and Advances, 2002. The Seventeenth Annual, IEEE. p. 247-252.

[14] Alizon, F., Shooter, S. B., and Simpson, T. W., 2010, "Recommending a platform leveraging strategy based on the homogeneous or heterogeneous nature of a product line," Journal of Engineering Design, 21(1), pp. 93 - 110.

[15] "First Drive: 2012 Toyota Prius PHEV", 17 Nov. 2011], Available from: http://www.motortrend.com/roadtests/alternative/112_0912_2012_toyota_prius_phev_review/viewall.html.

[16] Wikipedia, 2015 "History of plug-in hybrids", 2015 [cited 2015 7 Dec. 2015], Available from: https://en.wikipedia.org/wiki/History_of_plug-in_hybrids.

[17] Meyer, M. and Lehnerd, A. P., *The power of product platform– building value and cost leadship*. 1997, New york, Free Press.

[18] Simpson, T., Siddique, Z., and Jiao, J., *Platform-Based Product Family Development*, in *Product Platform and Product Family Design*, Simpson, T.W., Siddique, Z., and Jiao, J.R. 2006, Springer US. pp. 1-15.

[19] Moon, S. K. 2008, "A strategic module-based platform design method for developing customized families of products and services," The Pennsylvania State University, Doctor of Philosophy Dissertation, Pennsylvania.

[20] Jiao, J., Simpson, T., and Siddique, Z., 2007, "Product family design and platform-based product development: a state-of-the-art review," Journal of Intelligent Manufacturing, 18(1), pp. 5-29.

[21] Pirmoradi, Z., Wang, G. G., and Simpson, T. W., *A Review of Recent Literature in Product Family Design and Platform-Based Product Development*, in *Advances in Product Family and Product Platform Design*. 2014, Springer. pp. 1-46.

[22] Pirmoradi, Z. and Wang, G. G., 2011, "Recent Advancements in Product Family Design and Platform-based Product Development: A Literature Review," proceedings of the IDETC/CIE 011, Washington DC., USA. p. 1041-1055.

[23] Li, L., Huang, G. Q., and Newman, S. T., 2007, "Interweaving genetic programming and genetic algorithm for structural and parametric optimization in adaptive platform product customization," Robotics and Computer-Integrated Manufacturing, 23(6), pp. 650-658.

[24] Kumar, D., Chen, W., and Simpson, T. W., 2006, "A Market-Driven Approach to the Design of Platform-Based Product Families," 11th AIAA/ISSMO Multidisciplinary Analysis and Optimization Conference, Portsmouth, VA., AIAA 2006-6919.

[25] Meyer, M. H. and Lehnerd, A. P., "The power of product platforms: building value and cost leadership. 1997," New York, NY, 10020: 39.

[26] Khire, R., Messac, A., and Simpson, T. W., 2006, "Optimal design of product families using Selection-Integrated Optimization (SIO) Methodology," 11th AIAA/ISSMO symposium on multidisciplinary analysis and optimization, Portsmouth, VA, AIAA-2006-6924.

[27] Dai, Z. and Scott, M., 2007, "Product platform design through sensitivity analysis and cluster analysis," Journal of Intelligent Manufacturing, 18(1), pp. 97-113.

[28] Simpson, T., *Methods for Optimizing Product Platforms and Product Families*, in *Product Platform and Product Family Design*, Simpson, T.W., Siddique, Z., and Jiao, J.R. 2006, Springer US. pp. 133-156.

[29] Fujita, K., 2002, "Product variety optimization under modular architecture," Computer-Aided Design, 34(12), pp. 953-965.
[30] Simpson, T. W., Maier, J. R. A., and Mistree, F., 2001, "Product platform design: method and application," Research in engineering Design, 13(1), pp. 2-22.
[31] Messac, A., Martinez, M. P., and Simpson, T. W., 2002, "Effective product family design using physical programming," Engineering Optimization, 34(3), pp. 245-261.
[32] Fellini, R., Kokkolaras, M., Papalambros, P., and Perez-Duarte, A., 2005, "Platform Selection Under Performance Bounds in Optimal Design of Product Families," Journal of Mechanical Design, 127(4), pp. 524-535.
[33] Nayak, R. U., Chen, W., and Simpson, T. W., 2002, "A variation-based method for product family design," Engineering Optimization, 34(1), pp. 65-81.
[34] Messac, A., Martinez, M. P., and Simpson, T. W., 2002, "Introduction of a product family penalty function using physical programming," Journal of Mechanical Design, 124(2), pp. 164-172.
[35] Chowdhury, S., Messac, A., and Khire, R., 2010, "Developing a non-gradient based mixed-discrete optimization approach for comprehensive product platform planning (cp3)," proceedings of the 13th AIAA/ISSMO Multidisciplinary Analysis Optimization Conference, AIAA, AIAA 2010-9174.
[36] Chowdhury, S., Messac, A., and Khire, R. A., 2011, "Comprehensive Product Platform Planning (CP3) Framework," Journal of Mechanical Design, 133(10), pp. 101004-15.
[37] Messac, A., Chowdhury, S., and Khire, R., *One-Step Continuous Product Platform Planning: Methods and Applications*, in *Advances in Product Family and Product Platform Design*. 2014, Springer. pp. 295-321.
[38] Khajavirad, A. and Michalek, J. J., 2008, "A Decomposed Gradient-Based Approach for Generalized Platform Selection and Variant Design in Product Family Optimization," Journal of Mechanical Design, 130(7), pp. 071101-8.
[39] Fellini, R., Kokkolaras, M., Michelena, N., Papalambros, P., Perez-Duarte, A., Saitou, K., and Fenyes, P., 2004, "A sensitivity-based commonality strategy for family products of mild variation, with application to automotive body structures," Structural and Multidisciplinary Optimization, 27(1), pp. 89-96.
[40] Wei, W., Feng, Y., Tan, J., and Li, Z., 2009, "Product platform two-stage quality optimization design based on multiobjective genetic algorithm," Computers & Mathematics with Applications, 57(11), pp. 1929-1937.
[41] Ninan, J. A. and Siddique, Z., *Cascading Platforms for Product Family Design*, in *Advances in Product Family and Product Platform Design*. 2014, Springer. pp. 367-390.
[42] Marion, T. and Simpson, T., *Platform Leveraging Strategies and Market Segmentation*, in *Product Platform and Product Family Design*, Simpson, T.W., Siddique, Z., and Jiao, J.R. 2006, Springer US. pp. 73-90.
[43] Simpson, T. W., Seepersad, C. C., and Mistree, F., 2001, "Balancing commonality and performance within the concurrent design of multiple products in a product family," Concurrent Engineering, 9(3), pp. 177-190.
[44] de Weck, O. L., Suh, E. S., and Chang, D., 2003, "Product family and platform portfolio optimization," ASME 2003 International Design Engineering Technical Conferences and Computers and Information in Engineering Conference, American Society of Mechanical Engineers. pp. 175-185.

[45] Fellini, R., Papalambros, P., and Weber, T., 2000, "Application of a product platform design process to automotive powertrains," proceedings of the 8th AIAA/USAF/NASA/ISSMO Symposium on Multidisciplinary Analysis and Optimization AIAA 2000-4849.

[46] Nelson, S. A., Parkinson, M. B., and Papalambros, P. Y., 2001, "Multicriteria optimization in product platform design," Transactions-American Society Of Mechanical Engineers Journal Of Mechanical Design, 123(2), pp. 199-204.

[47] Siddique, Z., Rosen, D. W., and Wang, N., 1998, "On the applicability of product variety design concepts to automotive platform commonality," proceedings of the ASME Design Engineering Technical Conferences, Atlanta, Georgia, USA, DTM-5661 (1998).

[48] Fisher, M., Ramdas, K., and Ulrich, K., 1999, "Component sharing in the management of product variety: A study of automotive braking systems," Management Science, pp. 297-315.

[49] Sako, M. and Murray, F., 1999, "Modules in design, production and use: implications for the global auto industry," IMVP Annual Sponsors Meeting, Citeseer.

[50] Kokkolaras, M., Fellini, R., Kim, H., Michelena, N., and Papalambros, P., 2002, "Extension of the target cascading formulation to the design of product families," Structural and Multidisciplinary Optimization, 24(4), pp. 293-301.

[51] Fellini, R., Kokkolaras, M., Papalambros, P., and Perez-Duarte, A., 2005, "Platform selection under performance bounds in optimal design of product families," Journal of Mechanical Design, 127, pp. 524.

[52] Shahi, S. K., Wang, G. G., An, L., Bibeau, E., and Pirmoradi, Z., 2012, "Using the Pareto set pursuing multiobjective optimization approach for hybridization of a plug-in hybrid electric vehicle," Journal of Mechanical Design, 134(9), 094503.

[53] Turlapati, V. V. K. 2010, "Modeling and Optimization of A Plug-In Hybrid Electric Vehicle," Clemson University, Masters Thesis, Clemson, SC.

[54] Liu, J. 2007, "Modeling, configuration and control optimization of power-split hybrid vehicles," The University of Michigan, Doctor of Philosophy Dissertation, Ann Arbor, MI.

[55] Liu, J. and Peng, H., 2008, "Configuration, Sizing and Control of Power-Split Hybrid Vehicle," 9th International Symposium on Advanced Vehicle Control, Kobe, Japan.

[56] Moura, S. J., Fathy, H. K., Callaway, D. S., and Stein, J. L., 2011, "A Stochastic Optimal Control Approach for Power Management in Plug-In Hybrid Electric Vehicles," Control Systems Technology, IEEE Transactions on, 19(3), pp. 545-555.

[57] Eshani, M., Gao, Y., Gay, S. E., and Emadi, A., 2005, "Modern electric, hybrid electric and fuel cell vehicles," Fundamentals, Theory, and Design. Boca Raton, FL: CRC.

[58] Syed, S. A., Lhomme, W., and Bouscayrol, A., 2009, "Modelling comparison of planetary gear using EMR and Simdriveline for Hybrid Electric Vehicles," proceedings of the Vehicle Power and Propulsion Conference, 2009. VPPC '09. IEEE. p. 1835-1841.

[59] EmrahTolgaYildiz 2010, "Nonlinear Constrained Component Optimization Of A Plug-In Hybrid Electric Vehicle," Purdue University, Master of Science Indianapolis, Indiana.

[60] Galdi, V., Ippolito, L., Piccolo, A., and Vaccaro, A., 2001, "A genetic-based methodology for hybrid electric vehicles sizing," Soft Computing - A Fusion of Foundations, Methodologies and Applications, 5(6), pp. 451-457.
[61] MathWorks, 2015 "Diesel Engine", Vehicle Components 2015 [cited 2014 Sept 7 2014], Available from: http://www.mathworks.com/help/physmod/sdl/drive/dieselengine.html.
[62] Fellini, R., Michelena, N., Papalambros, P., and Sasena, M., 1999, "Optimal design of automotive hybrid powertrain systems," proceedings of the First International Symposium On Environmentally Conscious Design and Inverse Manufacturing, EcoDesign '99. p. 400-405.
[63] Zhang, X. and Mi, C., *Vehicle Power Management: Modeling, Control and Optimization*. 2011, Springer Science & Business Media.
[64] Wang, Q. 2008, "Concurrent multi-objective optimization of plug-in parallel HEV by a hybrid evolution algorithm," University of California, Davis, Doctoral degree Dissertation, Davis, CA, USA.
[65] Gonder, J. and Markel, T., 2007, "Energy management strategies for plug-in hybrid electric vehicles," SAE Technical Paper, 1, pp. 0290.
[66] Gao, Y. and Ehsani, M., 2010, "Design and Control Methodology of Plug-in Hybrid Electric Vehicles," IEEE Transactions on Industrial Electronics, 57(2), pp. 633-640.
[67] Haji Hajikolaei, K., Pirmoradi, Z., and Wang, G., 2014, "Decomposition for Large-Scale Global Optimization Based on Quantified Variable Correlations Uncovered by Metamodeling," Journal of Engineering Optimization.
[68] Pirmoradi, Z., Haji Hajikolaei, K., and Wang, G. G., 2014, "Designing scalable product families by the radial basis function–high-dimensional model representation metamodelling technique," Journal of Engineering Optimization, pp. 1-17.
[69] Simpson, T. W., 2004, "Product platform design and customization: Status and promise," Ai Edam-Artificial Intelligence for Engineering Design Analysis and Manufacturing, 18(1), WOS:000226587100002 pp. 3-20.
[70] Fellini, R., Kokkolaras, M., and Papalambros, P. Y., 2006, "Quantitative platform selection in optimal design of product families, with application to automotive engine design," Journal of Engineering Design, 17(5), pp. 429 - 446.
[71] Simpson, T. W., Chen, W., Allen, J. K., and Mistree, F., 1996, "Conceptual design of a family of products through the use of the robust concept exploration method," proceedings of the 6th. AIAA/USAF/NASA/ISSMO Symposium on Multidisciplinary Analysis and Optimization. p. 1535-1545.
[72] Li, G., Wang, S.-W., and Rabitz, H., 2002, "Practical approaches to construct RS-HDMR component functions," The Journal of Physical Chemistry A, 106(37), pp. 8721-8733.
[73] Shan, S. and Wang, G. G., 2010, "Metamodeling for high dimensional simulation-based design problems," Journal of Mechanical Design, 132(5), 051009.
[74] Sobol, I. M., 1993, "Sensitivity estimates for nonlinear mathematical models," Mathematical modeling and computational experiment journal, 1(4), pp. 407-414.
[75] Alış, Ö. F. and Rabitz, H., 2001, "Efficient implementation of high dimensional model representations," Journal of Mathematical Chemistry, 29(2), pp. 127-142.
[76] Shan, S. and Wang, G. G., 2009, "Development of adaptive rbf-hdmr model for approximating high dimensional problems," proceedings of the ASME 2009 International Design Engineering Technical Conferences and Computers and

Information in Engineering Conference, American Society of Mechanical Engineers. p. 727-740.
[77] Li, G., Hu, J., Wang, S.-W., Georgopoulos, P. G., Schoendorf, J., and Rabitz, H., 2006, "Random sampling-high dimensional model representation (RS-HDMR) and orthogonality of its different order component functions," The Journal of Physical Chemistry A, 110(7), pp. 2474-2485.
[78] Seber, G. A., *Multivariate observations*. Vol. 252. 2009, John Wiley & Sons.
[79] Thevenot, H. J. and Simpson, T. W., 2006, "Commonality indices for product family design: a detailed comparison," Journal of Engineering Design, 17(2), 19328371 pp. 99-119.
[80] Martin, M. and Ishii, K., 1996, "Design for variety: a methodology for understanding the costs of product proliferation," proceedings of the Design Theory and Methodology – DTM'96 (Wood, K., ed.), ASME, Sacramento, CA, DETC1996/DTM-1610.
[81] Khajavirad, A., Michalek, J., and Simpson, T., 2009, "An efficient decomposed multiobjective genetic algorithm for solving the joint product platform selection and product family design problem with generalized commonality," Structural and Multidisciplinary Optimization, 39(2), pp. 187-201.
[82] Simpson, T. W., Siddique, Z., and Jiao, J., *Product platform and product family design: methods and applications*. 2006, Springer Verlag.
[83] Amjad, S., Neelakrishnan, S., and Rudramoorthy, R., 2010, "Review of design considerations and technological challenges for successful development and deployment of plug-in hybrid electric vehicles," Renewable and Sustainable Energy Reviews, 14(3), pp. 1104-1110.
[84] Heywood, J. B., *Internal combustion engine fundamentals*. Vol. 930. 1988, Mcgraw-hill New York.
[85] Graham, R., 2001, "Comparing the benefits and impacts of hybrid electric vehicle options," Electric Power Research Institute (EPRI), Palo Alto, CA, Report, 1000349.
[86] Lin, Z. and Greene, D., 2010 "Who Will More Likely Buy PHEV: A Detailed Market Segmentation Analysis",Oak Ridge National Laboratory (ORNL), Center, N.T.R.
[87] Abe, S., 2010, "Development of Toyota Plug-in Hybrid Vehicle," Journal of Asian Electric Vehicles, 8(2), pp. 1399-1404.
[88] 2007 "Global Market Analysis of Plug in Hybrid Electric Vehicles",Frost & Sullivan Research services, No. M12D–18.
[89] Skerlos, S. J. and Winebrake, J. J., 2010, "Targeting plug-in hybrid electric vehicle policies to increase social benefits," Energy Policy, 38(2), pp. 705-708.
[90] Kurani, K. S., Heffner, R. R., and Turrentine, T., 2008, "Driving plug-in hybrid electric vehicles: Reports from US drivers of HEVs converted to PHEVs," circa 2006-07, Institute of Transportation Studies.
[91] Simpson, A., *Cost-benefit analysis of plug-in hybrid electric vehicle technology*. 2006, National Renewable Energy Laboratory.
[92] Santini, D. and Vyas, A., 2008 "How to Use Life-cycle Analysis Comparisons of PHEVs to Competing Powertrains",Argonne National Lab., Univ. of Chicago, US Dept. of Energy, Illinois, Chicago, Illinois
[93] Rousseau, A., Shidore, N., Carlson, R., and Freyermuth, V., 2007, "Research on PHEV Battery Requirements and Evaluation of Early Prototypes," Advanced Automotive Battery Conference, May 16-18, 2007, Long Beach, CA.

[94] Shiau, C. S. N., Samaras, C., Hauffe, R., and Michalek, J. J., 2009, "Impact of battery weight and charging patterns on the economic and environmental benefits of plug-in hybrid vehicles," Energy Policy, 37(7), pp. 2653-2663.
[95] Egbue, O. and Long, S., 2012, "Barriers to widespread adoption of electric vehicles: An analysis of consumer attitudes and perceptions," Energy Policy, 48, pp. 717-729.
[96] Axsen, J. and Kurani, K. S., 2010, "Anticipating plug-in hybrid vehicle energy impacts in California: constructing consumer-informed recharge profiles," Transportation Research Part D: Transport and Environment, 15(4), pp. 212-219.
[97] Duvall, M., Knipping, E., Alexander, M., Tonachel, L., and Clark, C., 2007, "Environmental assessment of plug-in hybrid electric vehicles. Volume 1: Nationwide greenhouse gas emissions," Electric Power Research Institute, Palo Alto, CA, 1015325.
[98] Investments, J.-C., 2009, "The American Recovery and Reinvestment Act of 2009."
[99] Santini, D. and Vyas, A., 2008, "How to use life cycle analysis comparisons of PHEVs to competing powertrains," Argonne National Lab., Univ. of Chicago, US Dept. of Energy, Chicago, Illinois.
[100] Laboratory, A. N., 2010 "GREET Model", 2010 [cited 2012 12 September], Available from: http://greet.es.anl.gov/.
[101] Gonder, J. and Simpson, A., *Measuring and reporting fuel economy of plug-in hybrid electric vehicles*. 2006, National Renewable Energy Laboratory.
[102] Hauffe, R., Samaras, C., and Michalek Jeremy, J., 2008, "Plug-in hybrid vehicle simulation: how battery weight and charging patterns impact cost, fuel consumption and CO2 emissions," proceedings of the ASME 2008 International Design Engineering Technical Conferences and Computers and Information in Engineering Conference, American Society of Mechanical Engineers, DETC2008-50027. p. 969-976.
[103] Winkel, R., Mieghem, R. V., Santini, D., Duvall, M., Conte, V., Alakula, M., Badin, F., Bleis, R., Brouwer, A., and Debal, P., 2006, "Global Prospects of Plug-in Hybrids," 22nd International Battery, Hybrid, and Fuel Cell Electric Vehicle Symposium and Exhibition, Yokohama, Japan.
[104] Shiau, C.-S. N., Samaras, C., Hauffe, R., and Michalek, J. J., 2009, "Impact of battery weight and charging patterns on the economic and environmental benefits of plug-in hybrid vehicles," Energy Policy, 37(7), pp. 2653-2663.
[105] Dai, Z. and Scott, M. J., 2006, "Effective Product Family Design Using Preference Aggregation," Journal of Mechanical Design, 128(4), pp. 659-667.
[106] Markel, T., Brooker, A., Gonder, J., O'Keefe, M., Simpson, A., and Thornton, M., 2006 "Plug-In Hybrid Vehicle Analysis",National Renewable Energy Laboratory (NREL), Golden, CO., NREL-MP-540-40609.
[107] Wu, X., Cao, B., Li, X., Xu, J., and Ren, X., 2011, "Component sizing optimization of plug-in hybrid electric vehicles," Applied Energy, 88(3), pp. 799-804.
[108] Li, Y. and Kar, N., 2011, "Advanced design approach of power split device of plug-in hybrid electric vehicles using Dynamic Programming," proceedings of the Vehicle Power and Propulsion Conference (VPPC), 2011 IEEE, IEEE. p. 1-6.
[109] Sobol, I. M., 1993, "Sensitivity estimates for nonlinear mathematical models," Math. Mod. Comp., 1(4), pp. 407-414.

[110] Wang, L., Shan, S., and Wang, G. G., 2004, "Mode-pursuing sampling method for global optimization on expensive black-box functions," Engineering Optimization, 36(4), pp. 419-438.
[111] Cheng George H., Y. A., Haji Hajikolaei Kambiz, G. Gary Wang, 2015, "Trust Region Based Mode Pursuing Sampling Method for Global Optimization of High Dimensional Design Problems," Journal of Mechanical Desesign, 137 (2- 021407), pp. 1-9.
[112] Shiau, C.-S. 2010, "Design Decision Making for Market Systems and Environmental Policy with Vehicle Design Applications," Carnegie Mellon University, Doctor of Philosophy Pittsburgh, Pennsylvania.
[113] Moawad, A., Singh, G., Hagspiel, S., Fellah, M., and Rousseau, A., 2009, "Impact of Real World Drive Cycles on PHEV Fuel Efficiency and Cost for Different Powertrain and Battery Characteristics," EVS24 International Battery, Hybrid and Fuel Cell Electric Vehicle Symposium 1 EVS24, Stavanger, Norway.
[114] Sharer, P., Rousseau, A., Nelson, P., and Pagerit, S., 2006, "Vehicle Simulation Results for Plug-in HEV Battery Requirements," Argonne National Laboratory, EVS22.

# Appendix A.

# The Universal Electrics Motor Design Problem Specifications

The universal electric motors family design problem formulation is presented in this section, taken from Simpson et al. [30]. The nomenclature is presented in Table A-1. **Error! Reference source not found.** shows the value of the fixed parameters for this problem.

**Table A-1: The nomenclature for the universal electric family design problem**

| Symbol | Definition | Symbol | Definition |
|---|---|---|---|
| $a$ | Number of current paths on the armature | $N_c$ | Number of turns of wire on the armature |
| $A_a$ | Area between a pole and the armature [mm2] | $N_s$ | Number of turns of wire on the field, per pole |
| $A_{wa}$ | Cross-sectional area of wires on armature | $\rho$ | Resistivity of copper [Ohms/m] |
| $A_{wf}$ | Cross-sectional area of wires on field [mm2] | $\rho_{copper}$ | Density of copper [kg/m3] |
| $I$ | Magnetomotive force [Ampere×turns] | $\rho_{steel}$ | Density of steel [kg/m3] |
| $K$ | Magnetic flux [Webers, Wb] | $P_{armature}$ | Number of poles on the armature |
| $B$ | Magnetic field strength (generated by the current in the field windings) [Tesla, T] | $\Re$ | Total reluctance of the magnetic circuit [Ampere×turns/m] |
| H | Magnetizing intensity [Ampere×turns/m] | $P_{field}$ | Number of poles on the field |
| $I$ | Electric current [Amperes] | $P$ | Gross Power Output [W] |
| $K$ | Motor constant [n.m.u.] | $r_o$ | Outer radius of the stator [m] |
| $I_r$ | Diameter of armature [m] | $R_a$ | Resistance of armature windings [Ohms] |

**Table A-1 (Continued)**

| Symbol | Definition | Symbol | Definition |
|---|---|---|---|
| $l_g$ | Length of air gap [m] | $R_s$ | Resistance in the field windings [Ohms] |
| $l_c$ | Mean path length within the stator [m] | $\Re_a$ | Reluctance of one air gap [Ampere×turns/m] |
| $L$ | Stack length [m] | $\Re_s$ | Reluctance of the stator [Ampere×turns/m] |
| $\mu_{steel}$ | Relative permeability of steel [n.m.u.] | $\Re_r$ | Reluctance of the armature [Ampere×turns/m] |
| $\mu_o$ | Permeability of free space [Henrys/m] | $t$ | Thickness of the stator [m] |
| $\mu_{air}$ | Relative permeability of air [n.m.u.] | $T$ | Torque [Nm] |
| $m$ | Plex of the armature winding [n.m.u.] | $V_t$ | Terminal voltage [Volts] |
| $\Omega$ | Rotational speed [rad/sec] | $Z$ | Number of conductors on the armature |
| $M$ | Mass [kg] | $\eta$ | Efficiency |

## Details of the design problem

The equations for the performance of the electric motors are presented as follows:

### *Power (P)*

$$P = P_{in} - P_{losses} \quad \text{(A-1)}$$

$$P_{in} = V_t I \quad \text{(A-2)}$$

$$P_{losses} = P_{Copper} + P_{Brush} \quad \text{(A-3)}$$

$$P_{Copper} = I^2(R_a + R_s) \quad \text{(A-4)}$$

$$P_{Brush} = \alpha I \quad \text{(A-5)}$$

$\alpha = 2$ volts. So, by substitution:

$$P = V_t I - I^2(R_a + R_s) - 2I \quad \text{(A-6)}$$

Resistance of the armature and field windings can be written in terms of the design variables:

$$Resistance = \frac{(Resistivity)(Length)}{Area_{cross-section}} \quad \text{(A-7)}$$

$$R_a = \frac{\rho(2L+4(r_0-t-l_{gap}))N_c}{A_{armature-wire}} \quad \text{(A-8)}$$

$$R_s = \frac{\rho(2)(2L+4(r_0-t))N_s}{A_{field-wire}} \quad \text{(A-9)}$$

**Table A-2: Fixed parameters for the test problem**

| Parameter | Value |
|---|---|
| a | 2 |
| $l_r$ | 0.7 mm |
| $\mu_0$ | $4\pi 10^{-7}$ |
| $\mu_{air}$ | 1 |
| m | 1 |
| $\rho$ | $1.68 * 10^{-8}$ Ohms/m |
| $\rho_{copper}$ | 8940 Kg/$m^3$ |
| $\rho_{steel}$ | 7850 Kg/ $m^3$ |
| $P_{armature}$ | 2 |
| $P_{field}$ | 2 |
| $V_t$ | 115 volts |

***Efficiency (η)***

$$\eta = \frac{P}{P_{in}} \tag{A-10}$$

***Mass (M)***

$$Mass = M_{stator} + M_{armature} + M_{windings} \tag{A-11}$$

$$M_{stator} = \pi(r_0^2 - (r_0 - t)^2)(L)(\rho_{steel}) \tag{A-12}$$

$$M_{Armature} = \pi\left(r_0 - t - l_{gap}\right)^2(L)(\rho_{steel}) \tag{A-13}$$

$$M_{windings} = \left(N_c\left(2L + 4\left(r_0 - t - l_{gap}\right)\right)A_{wa} + 2N_s\left(2L + 4(r_0 - t)\right)A_{wf}\right)\rho_{copper} \tag{A-14}$$

***Torque***

$$T = K\phi I \tag{A-15}$$

$$K = \frac{(Z)(\mathrm{P}_{armature})}{2\pi a} \tag{A-16}$$

$$Z = 2N_c \tag{A-17}$$

$a = 2m = 2$, $a$ is the number of current paths on the armature.

$$\mathrm{P}_{armature} = 2 \Rightarrow K = \frac{N_c}{\pi} \tag{A-18}$$

$$\phi = \frac{\Im}{\Re} \tag{A-19}$$

$$\Im = N_s I \tag{A-20}$$

$$\Re = \Re_s + \Re_r + 2\Re_a \tag{A-21}$$

Reluctance $\mathfrak{R}$ in genral is:

$$\mathfrak{R} = \frac{Length}{(Permeability)(Area_{cross-section})} \tag{A-22}$$

$$\mathfrak{R}_s = \frac{l_c}{2\mu_{steel}\mu_0 A_s}\ ,\ l_c = \pi(2r_0 + t)/2 \tag{A-23}$$

$$\mathfrak{R}_r = \frac{l_r}{\mu_{steel}\mu_0 A_r} \tag{A-24}$$

$$\mathfrak{R}_a = \frac{l_a}{\mu_{air}\mu_0 A_a} \tag{A-25}$$

Cross-section area of the stator: $A_s = tL$

Cross-section area of the armature: $A_r = l_r L$

Cross-section area of the air-gap: $A_a = l_{gap} L$

Following the main references for the universal motor family design problem, the two cross-section areas of armature and the air-gap are assumed to take the same value.

$$A_r = A_a = l_r L \tag{A-26}$$

$$\begin{cases} \mu_{steel} = -0.2279H^2 + 52.411H + 3115.8 & H \le 220 \\ \mu_{steel} = -1486.33\ln(H) + 11633.5 & 220 < H \le 1000 \\ \mu_{steel} = 1000 & 1000 < H \end{cases} \tag{A-27}$$

$$H = \frac{N_c I}{l_c + l_r + 2l_{gap}} \tag{A-28}$$

Mass and efficiency are the objectives of design to achieve the minimum possible mass as well as the maximum possible efficiency, subject to satisfying the design constraints and performance requirements. The design constraints are described below, and are summarized in Table A-3. Each motor has eight design variables, whose description and design range are as follows:

1. Number of turns of wires on the armature ($100 \le N_c \le 1500$) turns

2. Number of turns of wire on each field pole ($1 \leq N_s \leq 500$) turns
3. Cross-sectional area of the wire used on the armature ($0.01 \leq A_{wa} \leq 1.0$) $mm^2$
4. Cross-sectional area of the wire used on the field poles ($0.01 \leq A_{wf} \leq 1.0$) $mm^2$
5. Radius of the motor ($10 \leq r_0 \leq 100\ mm$)
6. Thickness of the stator ($0.5 \leq t \leq 10\ mm$)
7. Current drawn by the motor ($0.1 \leq I \leq 6.0\ Amp$)
8. Stack Length ($1 \leq L \leq 100\ mm$)

Efficiency (η): The target efficiency is 70% for all the motors, but it shall never fall below 15% (note that other published works have used the same values [1, 3, 21]).

Mass (M): There are different mass targets due to the variation of the torque expected from each variant. The maximum allowable mass varies between 1.75 kg for variant one which shall give less torque, and 2.2 kg for motor number ten with the highest torque requirement. The desired or target mass varies between 0.25 and 0.7 kg accordingly.

Magnetizing intensity (H): A magnetizing intensity below 5,000 is required for assuring that the magnetizing flux within the motor will not exceed the physical flux carrying capacity of the steel.

Power (P): The desired power is 300W for each motor in the family, imposing an equality constraint to the design problem.

**Table A-3: The system constraints for the universal electric motor problem**

| | |
|---|---|
| Magnetizing intensity, H | $H_{max} \leq 5000$ |
| Feasible geometry | $t < r_0$ |
| Power output, P | $P = 300\ W$ |
| Motor efficiency, h: | $\eta \geq 0.15$ |
| Mass, M | $M \leq 2.0\ Kg$ |
| Torque, T | *T* = 0.05, 0.1, 0.125, 0.15, 0.2, 0.25, 0.3, 0.35, 0.4, 0.5 *Nm* |

# Appendix B.

# Validation of the simulation model

For the simulation-based design and optimization studies, the validation process is done by comparing the simulation results with the previously validated results obtained from or published by test labs, research labs, or automotive makers. Since the test data for the MY 2004 Prius model is available, the simulation results are compared with the test data. The number of data points is different between the simulation results and the test data, and only the trend can be compared as well as some sample points. The time scale is the same in both simulation and test. Besides, the output of each component is verified and is found to be highly similar to realistic components in term of maximum or rated performance.

## B-1. Engine Validation

The simulation results for engine are not smooth curves, and the comparison with the test data is not very straight forward at the sample points. However, the trends in engine torque and efficiency are very similar to the test data, as shown in Figure B-1.

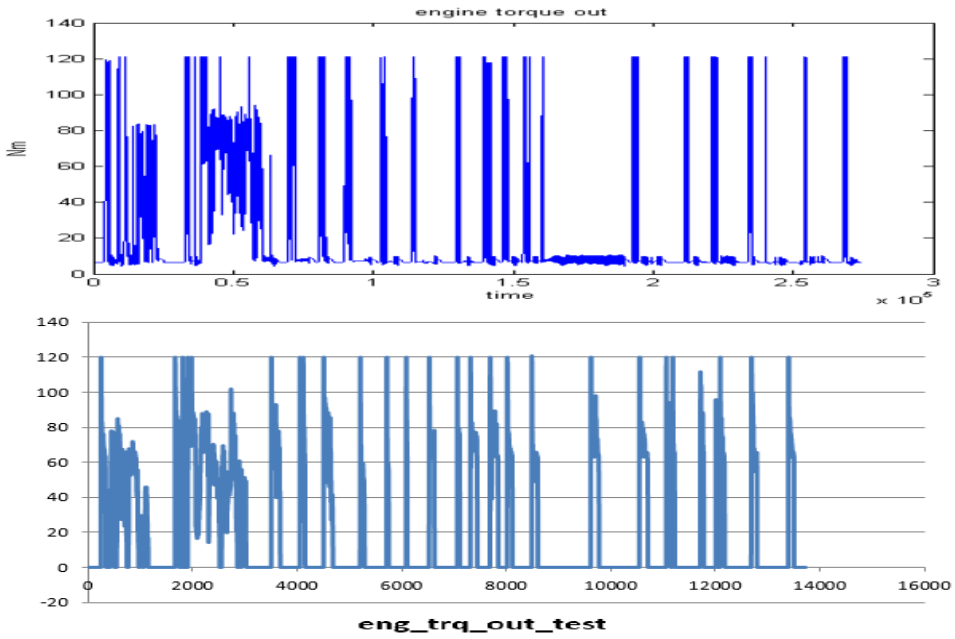


**Figure B-1: Engine Torque Comparison**

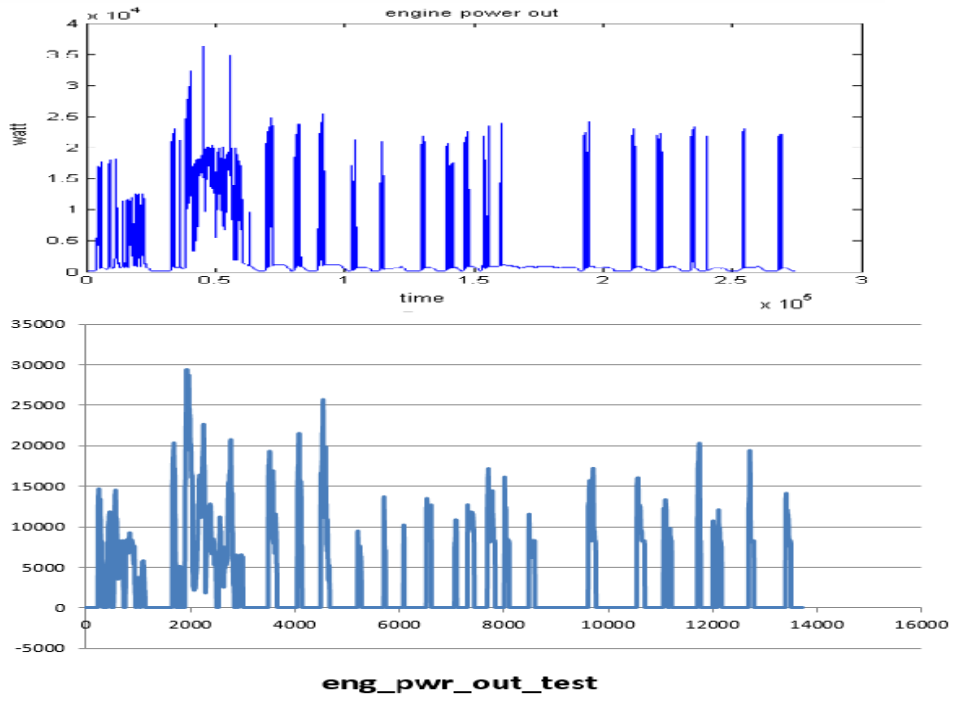


**Figure B-2 Engine Power Comparison**

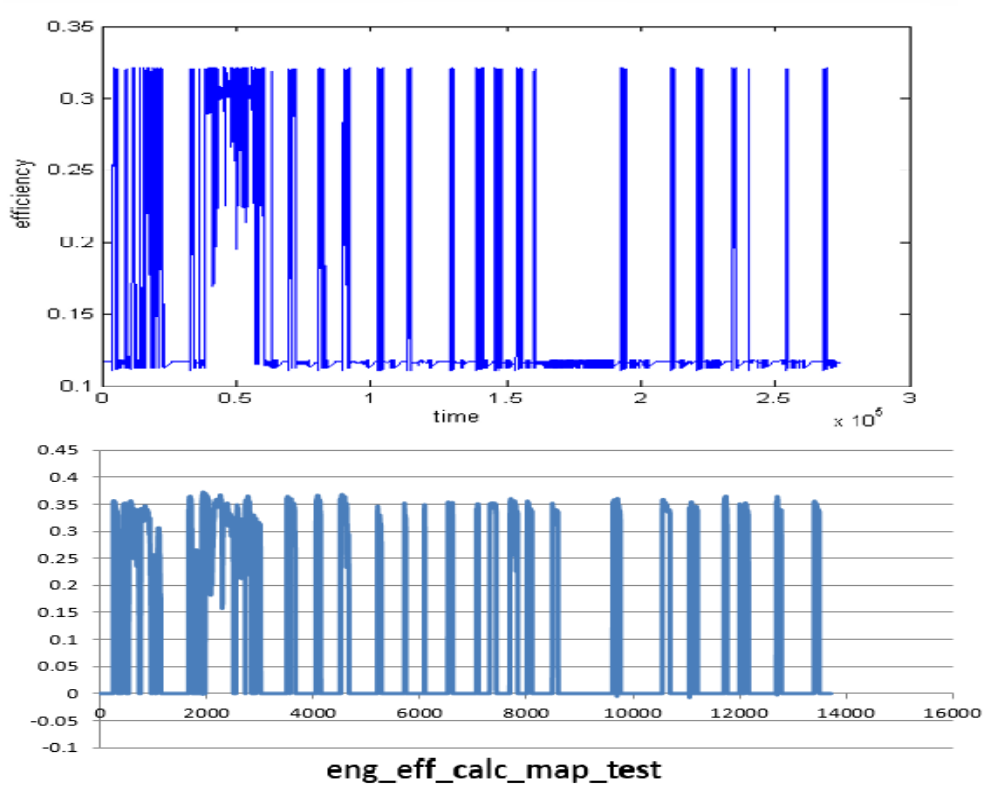


**Figure B-3 Engine Efficiency Comparison**

## B-2. Motor Validation

As seen in the plots of Figure B-4, the trend in the simulation generally matches the test data. The regenerative torque in the simulation, however, is slightly less than the test data. This is because the regenerative torque in the simulation is scaled down by the transmission efficiency, regenerative range, and battery charging efficiency. The motor torque plot illustrates that the motor only assists the engine since the motor only generates a portion of its available torque. As seen in the plot, the torque of the motor generally stays below its maximum continuous torque, 200 Nm. Negative torque in the plot reflects the regenerative braking of the vehicle. The reason for the spikes in the plot looks like to be caused by the clutch engaging and disengaging.

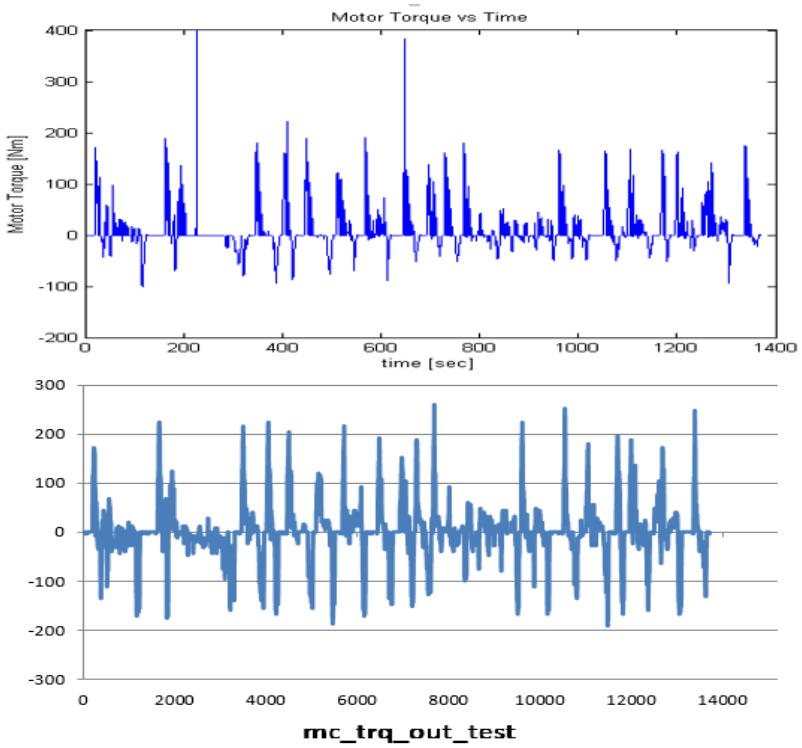


**Figure B-4 Motor Torque Comparison**

## B-3. Battery Validation

The SOC in simulation follows the test data as shown in Figure B-5, except that it decays slower. This difference is resulted from the inherent differences between the triggers in the control strategies of the simulation model and the test data, but the overall trend of having charge-depletion and dominance of the motor and the battery as the propulsion source, are all in line with the test data, implying the model is reliable for future simulation and design purposes.

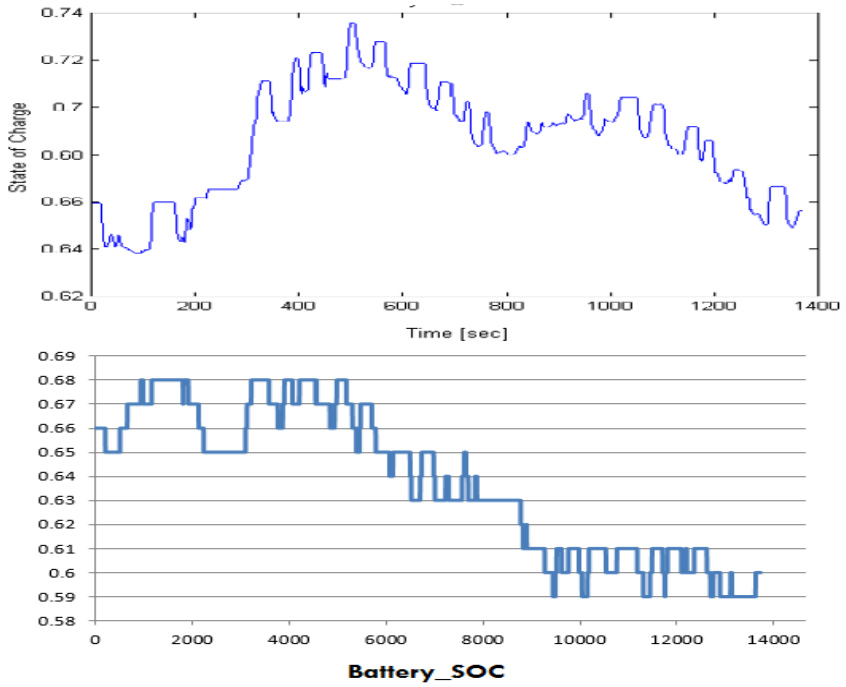


**Figure B-5 Battery SOC Comparison**

The results of comparing the battery current per simulation run for the test data and the simulation model of our study are also shown in Figure B-6, again showing identical trends in peaks and valley of the current over time, which is depending on the power-split portfolio, where zero current occurs when the engine is the only source of propulsion, and negative current shows the moments during which the battery has been charged either by the engine, or through regenerative breaking.

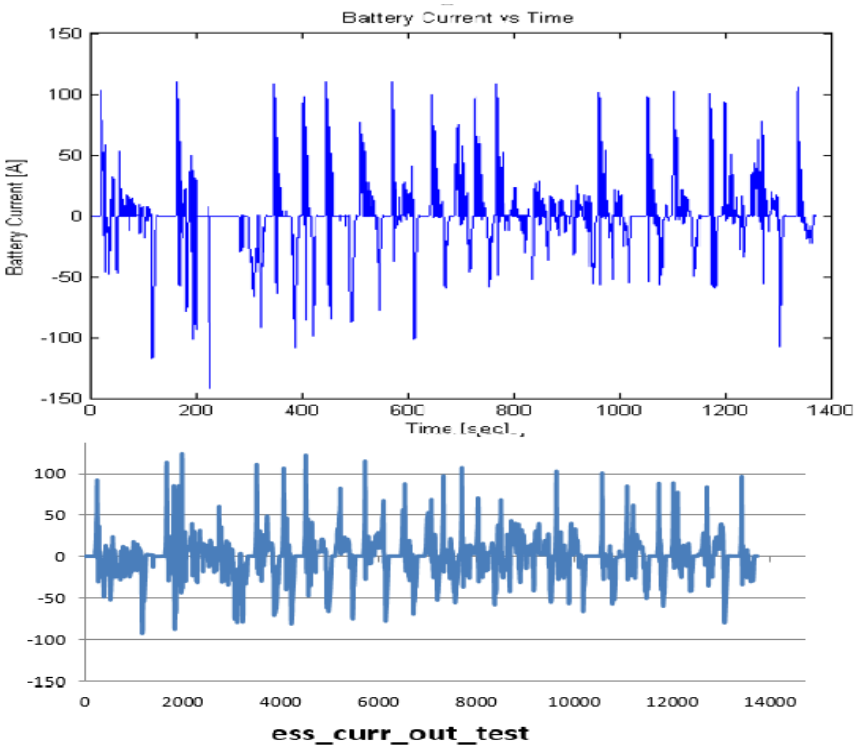


**Figure B-6: Battery Current Comparison**

## B-4. Vehicle Validation

The validation of the vehicle model is obtained through comparing the actual torque on wheels per time (taken from test data in the literature), versus the simulation output for the same parameter. The results are shown in Figure B-7.

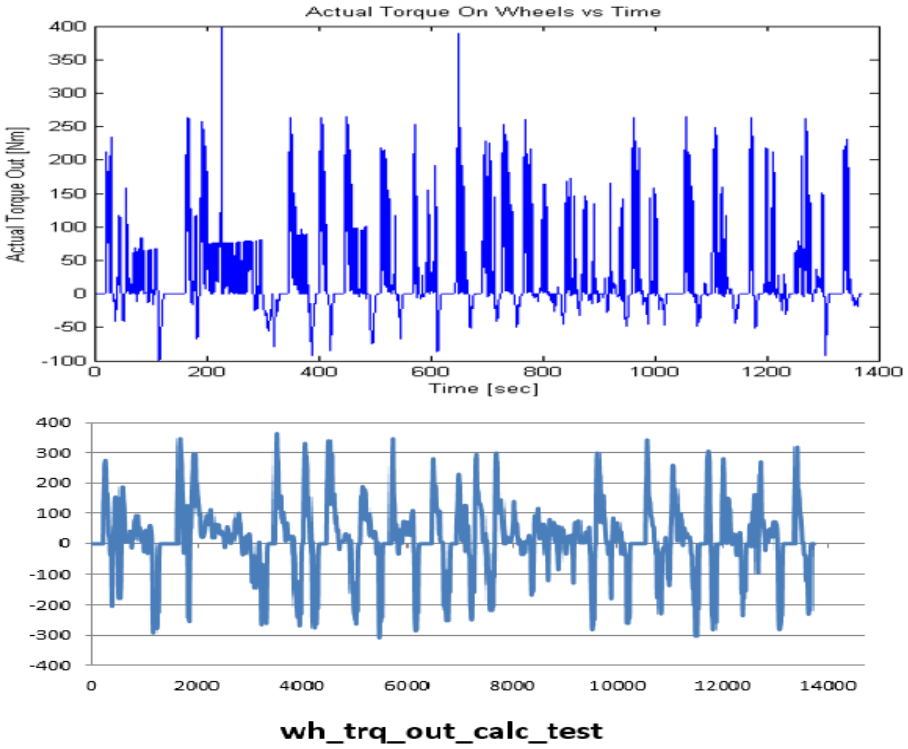


**Figure B-7: Torque on Wheel Comparison**

The comparison points out that the actual torque on the wheel matches the test data although the negative torque in the simulation are smaller. The negative torque is scaled down by the regenerative range and transmission efficiency so they are less than the test data.

# Appendix C.

# List of the publications

1. Shahi S. K., Wang G. G., An L., Bibeau E. and Pirmoradi Z. 2012. “Using the Pareto Set Pursuing Multiobjective Optimization Approach for Hybridization of a Plug-In Hybrid Electric Vehicle”, *Journal of Mechanical Design*, vol. 134, pp. 094503
2. Pirmoradi, Z., Wang, GG, Simpson TW, “Recent advancements in Product Family Design and platform-based product development: a literature review”, *International Journal of Product Development (IJPD)*, Under revision (submitted in Dec. 2014)
3. Hajikolaei, K. H., Pirmoradi, Z., Cheng, G. H. and Wang, G. G. 2014. “Decomposition for large-scale global optimization based on quantified variable correlations uncovered by metamodelling.” *Engineering Optimization*, doi:10.1080/0305215X.2014.895338.
4. Pirmoradi, Z., Hajikolaei, K. H., and Wang, G. G. 2014.”Designing Scalable Product Families for Black-Box Functions”, *Engineering Optimization*, Oct. 2014, DOI**:** 10.1080/0305215X.2014.971776.
5. Pirmoradi, Zhila, G. Gary Wang, and Timothy W. Simpson. "A Review of Recent Literature in Product Family Design and Platform-Based Product Development." Advances in Product Family and Product Platform Design. Springer New York, 2014. 1-46.
6. Pirmoradi, Z. and Wang, G. G., “Recent Advancements in Product Family Design and Platform-Based Product Development: A Literature Review,” *Proceedings of IDETC/CIE 011,* Vol. 2011, NO. 54822, pp. 1041-1055, 2011.
7. Z. Pirmoradi, K. Haji Hajikolaei, G. Wang, “Design Optimization on the basis of “white-box” uncovered via meta-modeling”, 8th AIAA Multidisciplinary Design Optimization Specialist Conference, 23–26 April 2012, Honolulu, Hawaii, USA
8. Pirmoradi, Z., Hajikolaei, K. H., and Wang, G. G. 2014.”Designing Scalable Product Families for Black-Box Functions”, *Proceedings of the IDETC/CIE 014*, 17-20 August 2014, Buffalo, NY, USA.
9. Pirmoradi, Z., and Wang, G. G. 2015.”Sensitivity and correlation analysis and implications in scalable product family design for Plug-in Hybrid Eclectic Vehicles”, *Proceedings of the IDETC/CIE 015*, 2-5 August 2015, Boston, Massachusetts, USA.
10. Pirmoradi, Z., and Wang, G. G., “Metamodeling-Based Product Family Design of Plug-in Hybrid Electric Vehicles”, Submitted to the Journal of Vehicular technology, Feb. 2016.